1996

Active Tectonics of the Northeastern Mojave Desert, California.

David F. Macconnell
Louisiana State University and Agricultural & Mechanical College

ACTIVE TECTONICS OF THE NORTHEASTERN MOJAVE DESERT, CALIFORNIA

A Dissertation

Submitted to the Graduate Faculty of the
Louisiana State University and
Agricultural and Mechanical College
in partial fulfillment of the
requirements for the degree of
Doctor of Philosophy

in

The Department of Geology and Geophysics

by
David F. MacConnell
B.S., San Diego State University, 1988
May 1996

ACKNOWLEDGMENTS

No project as large and encompassing as that of a dissertation is performed by an individual acting alone. This project has cost me many years in its achievement; some, now behind me, and some, I'm quite sure, have been paid for off the tail end of my life. However, the cost surely would have been much dearer had I not had the help of my friends, family and associates.

My advisor, Roy Dokka, has been a most valued and demanding critic, a loyal working associate, and a close friend. Thank you, Roy, for providing an environment rich in technologies, ideas and quality student associates--an academic climate which has stimulated my growth as a geologist. I thank Chad McCabe for the use of the LSU paleomagnetism laboratory and for his considerable time and effort spent on this project, both in the field and in the lab. Ajoy Baksi conducted geochronological studies on rocks from my field area. This manuscript has benefited greatly from the reviews and suggestions of Darrell Henry and Oscar Huh.

I have always enjoyed geological field research especially when the days are bright and the air is cool; however, when the weather gets rough, as it often does in the Mojave Desert, one truly develops an understanding of how misery is far less painful when shared. I especially thank Minji Chu, Rob Lewis, Molly Malone, Chad McCabe, Mike McCurry, Tim Ross, and Hodge Walker for the arduous work performed, the camaraderie shared and the valuable discussions held in "the field." My family has been a great source of inspiration to me; for my every achievement they have given fanfare far out of proportion, and for every disappointment they were ready with thoughtful words. Regardless of the distance separating us, their love and support have helped to keep my spirits high and motivation strong.

I thank the Department of Geology and Geophysics for providing financial as well as logistical support. I am grateful for the monetary contributions I have received from

Amoco Oil Co., Arco Oil and Gas, Shell Oil Co., Exxon Exploration Co., and the Houston Geological Society. This work was also supported by the Geodynamics Branch of NASA under contract awarded to M.Miller (P.I.) and R. K.Dokka (Co-I.), a NSF grant (EAR9219191), and a contract with the U.S. Army (#959353). Much appreciated help with the logistics of field operations and living accommodations were provided by W. McNutt and L. Sturgis (Bendix Corp.) and R. Quinones and Lt. Col. Schnable (U.S. Army, NTC). I also thank Exxon Exploration Company for providing me with the greatest incentive to knuckle down and finish this dissertation--a job.

Finally I thank my beloved Elizabeth Keller for coloring life rich and vibrant with love and adventure, for making every hour away from work a chance to remember how sweet life can be...nothing has had more of an impact on my sense of purpose.

TABLE OF CONTENTS

LIST OF TABLES

LIST OF FIGURES

LIST OF PLATES

ABSTRACT

This study has led to an improved understanding of the active tectonics and seismic hazards of the northeastern Mojave Desert region and has provided a means with which to assess regional strain models proposed by previous workers. Primary data sets include published and unpublished geologic maps, Landsat Thematic Mapper multi-spectral imagery, SPOT panchromatic imagery as well as hand-held ground and aerial photographs (panchromatic, color and color-infrared), color video, digital topography, gravity, seismicity and paleomagnetic data. Prior to analysis, data sets were organized into a geographic information system implemented on a UNIX workstation. This allowed for the simultaneous visualization of combinations of data sets in order to gain new perspectives on spatial and temporal relationships.

Most faults of the northeastern Mojave Desert region have moved in late Quaternary time with many currently active and seismogenic. The most prominent zone of seismicity is along the Goldstone Lake fault zone. It is proposed that the net right slip across the Goldstone Lake fault zone is ~10 km. This amount of displacement represents ~18% of the total right-shear, ~57 km, likely to have occurred across the northeastern Mojave Desert since ~6-10 Ma.

Paleomagnetism studies confirm that there has been little to no regional vertical-axis rotation of the Goldstone Lake region since ~22 Ma. This result constrains the northern limit of early Miocene, regional crustal rotations which formed as a consequence of right shear along the Trans Mojave-Sierran shear zone. Furthermore, geometric/kinematic models of the late Cenozoic tectonic evolution of the northeastern Mojave Desert which require regional vertical-axis rotations of this region are refuted by this result.

The Goldstone Lake fault zone is likely more significant than previously recognized; the location, orientation, length and seismicity of the Goldstone Lake fault zone give

cause to conclude that it may be capable of producing earthquakes similar in magnitude to that of the Landers earthquake (M=7.3, June 28, 1992).

CHAPTER 1: INTRODUCTION

OVERVIEW

Purpose

The purpose of this study is to develop an improved understanding of the active tectonics of the northeastern Mojave Desert region. In order to realize this goal an integrative study was launched to define the spatial and temporal distribution of Neogene strata as well as to establish the geometry, timing and kinematics of late Cenozoic faults and associated fault blocks. Field studies, coupled with analyses of earthquake data, satellite imagery, and paleomagnetic data have resulted in an improved understanding of the active tectonics and seismic hazards of the northeastern Mojave Desert region and have provided a means with which to assess regional strain models proposed by previous workers (Garfunkel, 1974; Luyendyk et al., 1980,1985; Carter et al., 1987; Dokka and Travis, 1990; Dokka, 1993; Ross, 1994, Dokka and Ross, 1995). The area of study corresponds to the region delimited by the Coyote Lake fault to the south, the Garlock fault to the north, the Goldstone Lake fault zone to the west, and the southern extension of the Death Valley fault zone to the east (Fig. 1.1). Historically, access into this region has been limited because much of this region falls within the boundaries of the U.S. Army's National Training Center (NTC), Naval Air Weapons Station (NAWS), and the Goldstone Deep Space Communication Complex. Thus, the geology of this region has been understudied in comparison to surrounding areas.

The structural architecture of this region is dominated by five E-W striking faults: the Garlock, Fort Irwin, Coyote Canyon and its likely eastward extension north of the Tiefort Mountains, Bicycle Lake, and the Quinones Creek-Coyote Lake faults (Plate 1). The Garlock fault is a ~260 km long, E-W striking sinistral fault that spans the northern Mojave Desert (Davis and Burchfiel, 1973). The Garlock fault terminates

Figure 1.1. Fault and seismicity map of the Mojave Desert.

to the west and to the east at the San Andreas fault and at the southern extension of the Death Valley fault zone, respectively (Brady and Verosub, 1984). The Fort Irwin, Coyote Canyon, Bicycle Lake, and Quinones Creek-Coyote Lake faults apparently terminate to the west along the NNW striking Goldstone Lake fault zone and its southern extension the Paradise fault. These E-W striking faults apparently terminate to the east at the southern extension of the Death Valley fault zone and into the structures of Mesquite Valley disturbed zone (Dokka and Travis, 1990a). The nature of the eastern terminations of these faults is unclear.

Preliminary analysis reveals that the Goldstone Lake region is a key study area for two reasons: 1) the Goldstone Lake region contains the thickest and most complete Neogene volcanic section (~1100 m) and, 2) it is the location of the intersection between the Goldstone Lake fault zone (east branch) and the Coyote Canyon fault (Plates 1 and 2). Both of these faults are elements of regionally extensive fault systems; therefore, an understanding of their geometry and kinematics is crucial in the development of a regional tectonic model. These faults intersect in the vicinity of Pink Canyon in the Goldstone Lake region where fault plane features are well exposed and rocks adjacent to the faults are appropriate for paleomagnetic studies of vertical-axis rotation. The apparent similarity of fault geometries and fault-block interactions in the Pink Canyon area with other fault intersections of regional importance (e.g., the Fort Irwin fault zone / Goldstone Lake fault zone, and the Quinones Creek-Coyote Lake fault / Paradise fault) further emphasize the value of a thorough analysis of geologic relations in the Pink Canyon area. For these reasons, detailed field investigations and paleomagnetic studies were conducted in the Goldstone Lake region.

The results of this study suggest that most faults of the region have been active in late Quaternary time with many currently active and seismogenic. Presently, the most prominent zone of seismicity is a NNW trending belt that extends from Yermo north

through the Goldstone area (Fig.1.1). This zone is dominated by the Goldstone Lake fault zone. Although our efforts are not expressly directed at geologic hazards analysis, the data compiled in this study provide a first order assessment of potential seismic activity.

The newly recognized Goldstone Lake fault zone represents the easternmost of three major, NW striking, active fault systems that currently cut the northern Mojave; the others include the Gravel Hills and Blackwater faults (Fig. 1.1). Collectively, these systems likely accommodate the bulk of current right-shear across the Eastern California shear zone (ECSZ) through the northern Mojave Desert (Dokka and Travis, 1990a).

Significance

The June 28, 1992, M7.3 Landers, California, earthquake dramatically emphasized the role that the Eastern California shear zone of the Mojave Desert-Death Valley region has played and continues to play in accommodating the dextral shear between the Pacific and North American plates in late Cenozoic time (Fig. 1.2). Comparison of integrated net slip along the shear zone with motion values across the entire transform boundary indicates that between 9% and 23% of the total relative plate motion has occurred along the ECSZ since its probable inception ~10-6 Ma (Dokka and Travis, 1990b). Dokka and Travis (1990a) also demonstrated that strain in the Mojave Desert Block is inhomogeneous and is partitioned into domains that are separated by major strike-slip faults and extensional zones; they presented a geometric-kinematic model for the Mojave Desert block portion of the ECSZ that explained observed geological and geophysical data. Dokka (1993) offered an updated and areally more extensive geometric-kinematic model for the ECSZ that included all of southeastern California.

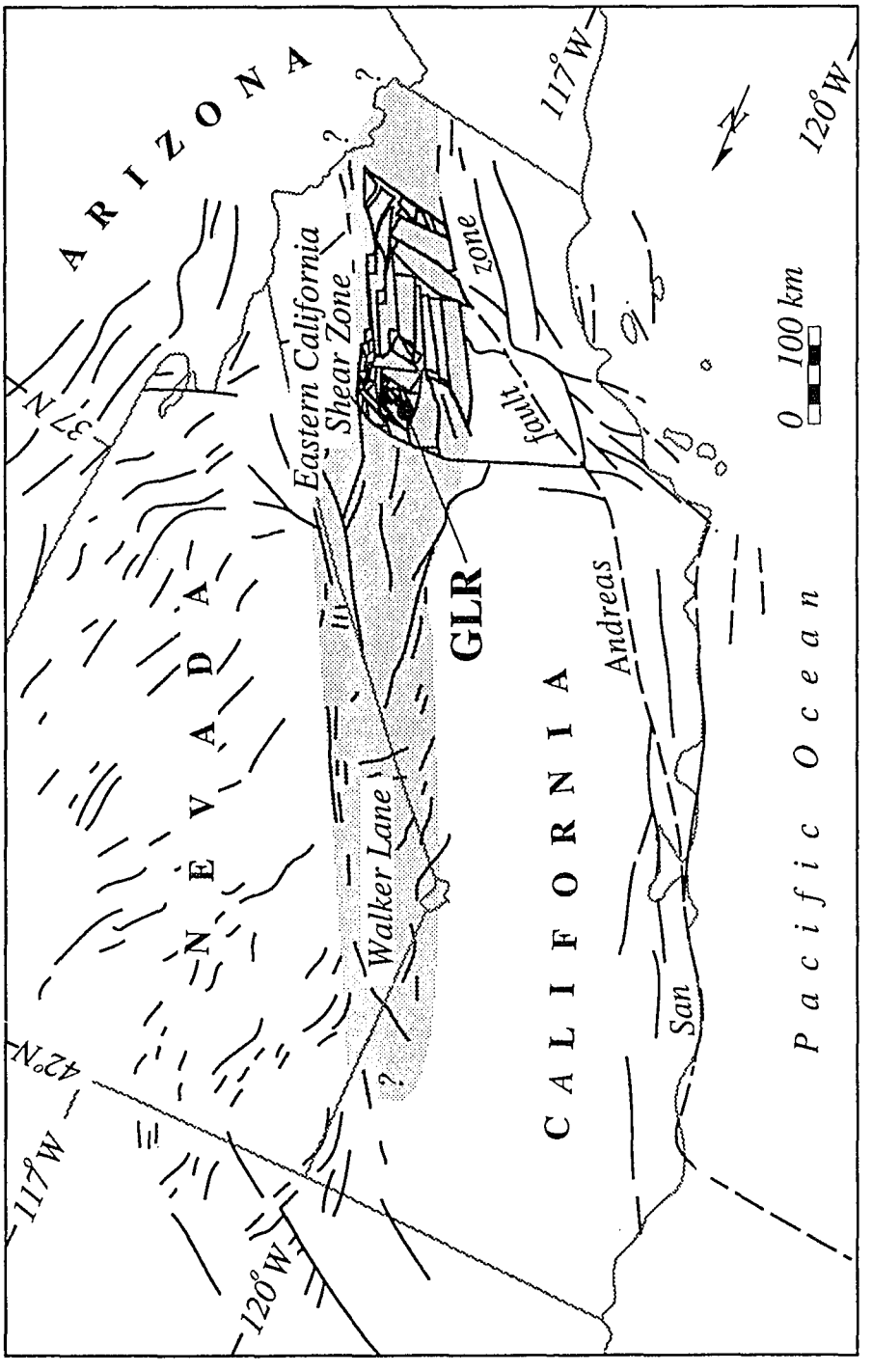

Figure 1.2 Schematic map of the Pacific-North American transform boundary in the western USA highlighting the Eastern California shear zone and Goldstone Lake region (GLR). Modified from Dokka and Travis (1990a).

Both of these models consider that deformation within the ECSZ has been largely accomplished by strike-slip translation along dominantly NW striking shears, along with clockwise tectonic rotations of blocks bounded by ~E-W, left-slip faults.

The study of Dokka and Travis (1990a) also pointed out that uncertainties regarding the structure of the largely unstudied northeastern Mojave Desert represented a major obstacle to a more complete understanding of the kinematic development of the ECSZ. The lack of information on the northeastern Mojave Desert has precluded the development of a tectonic model based on well constrained, local relations.

Objectives

This study of active tectonics is designed to investigate several aspects of late Cenozoic tectonics in the northeastern Mojave Desert . The major questions to be resolved include: 1) What is the structural architecture of the northeastern Mojave Desert? 2) What is the late Cenozoic tectonic history of the northeastern Mojave Desert region and how does it relate tectonically to the rest of the Mojave Desert Block? 3) Which faults have been active in the Quaternary and what is the likelihood of future activity?

Approach and Methods

Faults of the northeastern Mojave Desert were detected, mapped, and studied using a combination of field mapping, image analysis of satellite imagery and digital elevation models, and seismicity studies. Primary data sets include published and unpublished geologic maps, Landsat Thematic Mapper (TM) multi-spectral imagery, SPOT panchromatic imagery, digital topography, gravity, and seismicity. These data sets were augmented by hand-held ground and aerial photographs (panchromatic, color and color-infrared), and color video.

Field Methods

Field mapping efforts in ancient volcanic centers can incur difficulties due to the complex nature of facies relationships common to volcanic settings as well as the obscuring effects of post-depositional weathering, erosion and deformation. Syn-volcanism erosional rates are often relatively high and may have nothing to do with local or regional tectonism (Cas and Wright, 1988). On the other hand, local basins can form in response to rifting or caldera collapse and lead to the preservation of relatively thick and complete sections of volcanic and volcaniclastic deposits. However, these relatively well preserved sections are often proximal to source vents and exhibit rapid facies changes both in a lateral and vertical sense (Hildreth and Mahood, 1986). Relatively resistant units (i.e., lava flows, domes, dikes, etc) are often preferentially preserved, leading to their disproportionate abundance in the rock record (Cas and Wright, 1988). Resistant units often have steep linear or sinuous margins upon which other units may onlap or be abruptly juxtaposed. Thus, outcrop patterns and contacts in volcanic rocks can be difficult to interpret, especially if rocks are deformed and poorly exposed. Given the complex nature of geologic relations in ancient volcanic centers, lateral and vertical facies changes need to be well understood in areas of good exposure where the stratigraphic section is more or less complete in order to make reasonable inferences regarding the nature of contacts in areas of poor exposure. Most faults in the northeastern Mojave Desert disrupt late Quaternary alluvium and therefore can be mapped into bedrock with some confidence even where these rocks are poorly exposed and the nature of the contacts is difficult to discern. In such areas the multi-disciplinary approach employed in this study is especially beneficial. Remote sensing data, seismicity data, and paleomagnetic studies can test field based interpretations as well as to guide field research efforts to the most promising localities.

Access into certain areas on the Fort Irwin Military Reservation is limited or restricted either by base authorities or by cautious field geologists. Interruptions of live-fire M1 tank maneuvers were avoided. Land-mine fields that had yet to be cleaned were generally skirted even where they crossed fault contacts. Demolition sites were also given adequate respect. In areas such as these, where field mapping could lead to loss of life or limb, remote sensing techniques were employed with enthusiasm.

Remote Sensing Studies

Remote sensing is the art and science of observing objects without making direct physical contact. In this paper, the term remote sensing refers to the use of reflected and emitted electromagnetic radiation in order to discern the nature of the materials and phenomena exposed at the Earth's surface. Digital satellite remote sensing data were used extensively in this study because the data: 1) provide a synoptic view of the Earth allowing the observer to see regional geology at a glance, while also offering the opportunity to change scale readily, adapting to the needs of the problem under study; 2) enhance an interpreters' ability to identify and discriminate between materials by using a portion of the electromagnetic spectrum that is outside the range of detection of the unaided eye; 3) facilitate geological mapping in areas where access is limited or totally restricted such as firing or bombing ranges; 4) can be combined easily and displayed simultaneously with other types of data (i.e., geological maps, seismic data, potential fields data, digital topography, etc) for multi-disciplinary analysis; and, 5) facilitate pre-mission planning, locating promising target areas for detailed field studies, as well as post-mission re-evaluation.

Landsat TM, SPOT panchromatic, and high altitude color-infrared photographs were particularly useful in this study. A full description of the nature of these data sets and the method of acquisition, processing and interpretation is beyond the scope of

this paper but a brief description of a few important characteristics and methods follows.

Landsat Thematic Mapper

For optimum utilization, Landsat TM data were manipulated and analyzed in digital form, usually in the band combinations 7, 4,and 2 allocated to the red, green and blue color guns, respectively. The following are some notably important uses of these bands; however, there are many more influences on the spectral reflection characteristics of desert materials than those described below. Band 7 is acquired from the mid-infrared portion of the spectrum (2.08-2.35 μm), it is useful for discriminating between rock types mostly on the basis of iron oxide and moisture content; band 4 is acquired from the near-infrared portion of the spectrum (0.76-0.90 μm) and is useful as a measure of the relative density and health of vegetation; band 2 is acquired from the green portion of the visible spectrum (0.52-0.60 μm) and is designed to measure the green reflectance peak for vegetation. This combination of bands is pleasing to the eye and generally provides good discrimination between various types of surface materials found in desert environments. Landsat TM data have a spatial resolution of ~30 m though objects smaller than this can be detected if the reflectance of the object contrasts sharply with that of the surrounding materials (Lillesand and Kiefer, 1987).

SPOT-Landsat TM Merge

SPOT panchromatic (gray-scale) data was co-registered with digitally resampled Landsat TM data (bands 7,4,2) producing a four-component image using a variation of the mutiplicative method of Crippen (1989). This method causes less distortion of color than other image merging techniques (i.e., addition, subtraction, and division) (Crippen, 1989). Crippen (1989) first removed the image intensity component (albedo) by band ratioing, and then replaced it by merging with band-average data or SPOT data. Our variation of this method does not remove the intensity component

contained in the Landsat TM data, but only enhances it with the higher spatial resolution (10 m) SPOT panchromatic data. The resulting three bands were then stretched into the original 8-bit digital number format. SPOT data were also merged with Landsat TM band-ratio data using the multiplicative method of Crippen (1989). The band-ratio data (bands 3/1, 5/4, 5/7) were used to emphasize the compositional differences of the rocks (e.g., Ford et al., 1990). Further processing steps included edge enhancement and contrast stretching, both designed to limit image degradation and maximize interpretability. These data were georeferenced and used for on-screen digitizing and analysis.

High Altitude Color-Infrared Aerial Photographs

High altitude color-infrared aerial photographs were obtained from the Directorate of Public Works at the Fort Irwin NTC. These images were used simultaneously with the satellite data by displaying large-format slides produced from photograph positives onto a projection screen directly above the computer monitor. Photographs were of high quality, and had superior spatial resolution to the Landsat TM data. Used in this manner, problems related to the complex spatial distortion often associated with aerial photographs were eliminated.

Interpretation

The association of rock types with specific features in an image was based on field investigations and previous geologic maps of the area. Faults were detected and mapped using visual image analysis. Lineaments resulting from abrupt spectral and textural contrasts that coincided with aligned physiographic features were mapped as faults (e.g. Ford et al, 1990). However, where alternative interpretations were considered likely (e.g., anthropogenic features, drainage lineaments formed by coalescing alluvial fans, parallel bedding of lithologic units, ridge-lines defined by

shadows, etc) faults were not mapped unless unequivocal evidence was obtained in the field (i.e. ground truth). All major faults were confirmed by field observations.

Seismicity Data

Seismicity data of the northeastern Mojave Desert were obtained from the Southern California Seismographic Network (SCSN) data catalog, an Internet accessible data base hosted by the California Institute of Technology and the U.S.G.S. These data include surface location (latitude and longitude), magnitude, depth, date, and an estimation of the quality of the location accuracy for seismic events occurring during the period January 1, 1990-Sept., 30, 1995. Only data having location qualities of A and B were used. The estimated accuracy of these data is reported to be ±1 km and ±2 km horizontal, and ±2 km and ±5 km vertical for A and B quality events, respectively. Data include 107,587 seismic events (Fig. 1.1), 634 in the northeastern Mojave Desert (Plate 1), and range in magnitude from <1.0 to 4.2. Earthquake hypocenters generally range from 0 to 12 km depth. All data were reviewed to avoid seismic events that were anthropogenic in nature, such as explosions related to mining or military activity. Epicentral data were used to determine the activity of faults and to identify faults not exposed at the ground surface. In order to ensure that the location quality estimates were reliable, no events prior to the year of 1990 were used as suggested by the SCSN. Shocks and aftershocks of the Landers event of June 28th 1992 account for the majority of recorded events in the northeastern Mojave Desert region.

Paleomagnetism Data

Paleomagnetism studies were carried out in the Goldstone Lake region to test several competing tectonic models of the late Cenozoic tectonic movements of major fault blocks in the northeastern Mojave Desert. One of the main differences in these models is the magnitude and geographic extent of vertical-axis tectonic rotations. Samples were taken from three fault blocks bounded by two major faults of the region,

the Goldstone Lake fault zone (east branch) and the Fort Irwin fault. Samples from these fault blocks were initially analyzed separately to generate site means. From these data, fault-block means were generated, and finally all data were grouped together to obtain a regional mean. Sample sites were chosen where the structural and stratigraphic relations were well known. Stratigraphic sections were sampled as thoroughly as possible in order to adequately average secular variation of the paleofield.

Geographic Information System

Prior to analysis, all data sets (geological maps, satellite images, digital terrane data, earthquake data, gravity models, and paleomagnetic data) were organized into a Geographical Information System, the Mojave GIS (Dokka et al., 1993, 1994) and implemented on a UNIX workstation using Arc/Info and ERDAS Imagine software. The Mojave GIS is an analytical environment for the simultaneous visualization and analysis of combinations of data sets. This environment provides a powerful means of gaining new perspectives on spatial and temporal relationships, testing tectonic models, and developing new ideas.

CHAPTER 2: GEOLOGY OF THE NORTHEASTERN MOJAVE DESERT

INTRODUCTION

To unravel the puzzle of present-day tectonic regimes it is necessary to have a knowledge of the effects and features of previous geologic events. Conversely, in order to successfully reconstruct the paleogeography of a region, we must be able to accurately remove the effects of more recent geologic events. This chapter documents the regional stratigraphy and structure of the northeastern Mojave Desert. For the purpose of obtaining the perspective required to understand modern structural relations, the discussion begins with a general overview of the regional geologic history of the Mojave Desert with emphasis on the northeastern Mojave Desert; we then present a stratigraphic description of the Goldstone Lake region and discuss the style of volcanism represented by Neogene rocks in this area. The final section of this chapter is a review of all the major faults of the northeastern Mojave Desert region.

OVERVIEW OF THE GEOLOGICAL HISTORY

Pre-Tertiary Geology

The geologic history of the northeastern Mojave Desert is recorded by rocks dating back to Ordovician time (Carr et al., 1981). The northeastern Mojave Desert occupied a position near the miogeoclinal-cratonal hingeline throughout much of the Paleozoic (Martin and Walker, 1991, 1992). Crustal shortening during Permo-Triassic time (Miller and Sutter, 1982; Martin and Walker, 1991; Snow, 1992) put Paleozoic eugeoclinal rocks over coeval miogeoclinal strata and produced southwest verging structures (Miller and Sutter, 1982). Snow (1992) named this thrust system the Last Chance thrust system and proposed that the fault cut through the Goldstone Lake region, striking approximately northwest and continuing north to the Garlock fault. Martin and Walker (1991) proposed that a regional zone of contractional deformation,

dated as Middle to Late Jurassic, affected rocks of the Mojave Desert from the Soda Mountains westward to the Shadow Mountains resulting in 30 km of southeast-vergent structural overlap, as implied by paleogeographic reconstruction models. Henry and Dokka (1992) studied the mineral assemblages and textures of regionally metamorphosed metasedimentary rocks in the Waterman Metamorphic Complex, north and northwest of Barstow, CA. Henry and Dokka (1992) proposed that a major Mesozoic tectonometamorphic event resulted in the tectonic burial of supracrustal rocks to a depth of 25-30 km in the Middle Jurassic to Early Cretaceous. During the Mesozoic, at least two major phases of plutonic activity were widespread throughout the region, the first occurred in the Late Jurassic, the second in Late Cretaceous time (Miller and Sutter, 1982). Voluminous Mesozoic plutonism greatly obscured the pre-Tertiary rock record such that major structures have largely been defined by inference (Silver and Anderson, 1974; Burchfiel and Davis, 1981; Glazner et al., 1989; Miller and Sutter, 1982; Snow, 1992; Walker et al., 1990; Martin and Walker, 1991).

Late Cretaceous to Early Cenozoic Erosional Epoch

From Late Cretaceous to latest Oligocene time the Mojave Desert region apparently stood relatively high (Hewett, 1954), was dominated by erosional processes, and shed detritus to the south and west (Nilsen and Clark, 1975). The dacite tuff, tuff breccia, basalt, and conglomerate of the Jackhammer Formation may represent the oldest Tertiary rocks in the Mojave Desert region (McCulloh, 1952). These rocks are inferred to be late Oligocene age (Dokka and Woodburne, 1986). Regional studies conducted by Armstrong and Higgins (1973) and Armstrong and Suppe (1973) found no primary volcanic or plutonic rocks of Eocene or Oligocene age in the Mojave Desert region. This period of tectonic and magmatic quiescence ended in the early Miocene.

Early Miocene Extensional Tectonics

In early Miocene time the central Mojave Desert underwent a profound change in physiography, tectonics, magmatism, and sedimentation patterns as a result of detachment-style extensional tectonics (~24-20 Ma)(Dokka, 1986, 1989ab; Dokka and Woodburne, 1986; Glazner et al., 1989; Walker et al., 1995). This detachment-dominated extensional orogen was a locus of pre-, syn- and post-kinematic volcanic activity from ~24 to 18 Ma (Dokka et al., 1988, 1991; Walker et al., 1995). The northeast Mojave Desert region lies to the north and east of the Mojave Extensional Belt (Dokka, 1989) in the unextended "highlands." There are no known occurrences of Tertiary age "deep-rooted" detachment-faults in the study area, nor is there a regular pattern of normal faulting and tilting of Tertiary strata that would suggest that the northeastern Mojave Desert was the site of early Miocene detachment-dominated extensional tectonics. The above discussion suggests that the mechanism responsible for early Miocene (~22 - 18 Ma, a probable minimum range, MacConnell et al, 1994) volcanism in the northeastern Mojave Desert was not directly related to detachment-dominated regional extension.

Early Miocene Regional Dextral Shear

Dokka and Ross (1995) present structural and paleomagnetic evidence for a major ~E-W striking zone of deformation, the Trans Mojave-Sierran shear zone (TMSSZ), that transferred strain from extensional terranes in southeastern California and Arizona to the North American plate margin in southern California. A key element in this model is the interpretation of early Miocene regional rotations from paleomagnetic studies (Ross et al., 1989; Ross, 1994, 1995). Paleomagnetism studies (Chapter 3; MacConnell et al., 1994) confirm the notion that the northeastern Mojave Desert lies beyond the zone affected by the TMSSZ. Furthermore, there is no evidence of

significant early Miocene ~E-W striking dextral faults or related structures in the study area.

Early Miocene Volcanism in the Northeastern Mojave Desert

In the northeastern Mojave Desert the first products of silicic volcanism were deposited directly over plutonic and metamorphic basement rocks at the beginning of the Miocene time (~22.3 ± 1.5 Ma) (MacConnell et al., 1994). Neogene volcanic rocks are best exposed in the Goldstone Lake, Myrick Spring, and Eagle Crags areas (Plate 1). Volcanism produced a bimodal suite of rocks; large-volume silicic domes, lava flows and pyroclastic rocks with subordinate basaltic flows were followed by lava flows and pyroclastic rocks of predominantly basaltic affinities. Based on regional gravity data, physiography, and the spatial and temporal distribution of rock types, the early to middle Miocene volcanic rocks of the northeastern Mojave Desert likely represent an ancient caldera system (MacConnell, this paper; Sabin et al., 1994). Volcanic activity continued through mid-Miocene time (~12 Ma)(Sabin et al, 1994). Where exposed, these rocks exhibit little evidence of syn-depositional tectonic activity characteristic of other parts of the Mojave Desert during early and middle Miocene (e.g. Dokka and Ross, 1995); major Tertiary bedding contacts are conformable and all late Cenozoic faults cut the entire Tertiary section. However, Miocene volcanic rocks of the study area are intimately related to a caldera ring fracture system (e.g., Eagle Crags, Sabin et al, 1994; and Pink Canyon, MacConnell, this paper). Although wide-spread volcanism appears to have ceased by late Miocene time, minor eruptions of small volume basalts continued until at least ~5.6 Ma in the vicinity of Bicycle Lake (Yount et al., 1994)(Plate 1). This deposit as well as other apparently young basalt flows (i.e. "the Whale", UTM: 550500E 3895238N)(Plate 1) may be the result of local crustal extension associated with post-10 Ma strike-slip faults (e.g., Dokka, 1993).

Late Cenozoic Tectonics

Modern physiography of the Mojave Desert strongly reflects the underlying structural architecture that is a direct result of late Miocene to recent wrench tectonics (Dokka, 1993). Dibblee (1961) documented the dominant NW striking faults of the Mojave Desert and proposed that they were related to the San Andreas fault system. Since the early 1980's several geometric-kinematic tectonic models have been proposed that relate late Cenozoic faulting in the Mojave Desert to dextral movement between the North American and Pacific plates (Luyendyk et al., 1980; Luyendyk et al., 1985; Carter et al., 1987; Dokka and Travis, 1990ab; Dokka, 1993)(Please refer to Chapter 3 for a more thorough discussion of these models). Dokka and Travis (1990a) defined the Eastern California shear zone as a major thoroughgoing zone of right shear accommodating at least 9 to 18% of the total right-shear motion between the Pacific and North American plates since 13 Ma. Dokka and Travis (1990a) and Dokka (1993) demonstrated that strain in the Mojave Desert Block is inhomogeneous and is partitioned into domains that are separated by major strike-slip faults and extensional zones (Fig. 2.1). Dokka and Travis (1990a) and Dokka (1993) proposed that deformation of the northeastern Mojave Desert region was facilitated by a combination of NW striking, right-slip faults as well as E-W striking, left-slip faults; this resulted in an overall strain pattern of ~N-S shortening and ~E-W extension. It was reasoned that oblique extension along the Mesquite Valley disturbed zone created new space that has now been partially filled by fault blocks translated from the north and west (Fig. 2.2). Motions along generally east striking faults such as the Fort Irwin and Coyote Canyon fault zones are thought to be associated with fault blocks that "escaped" eastward towards the extensional Mesquite Valley disturbed zone.

Most faults of the northeastern Mojave Desert region have been active in late Quaternary time with many currently active and seismogenic. Faults of the area are

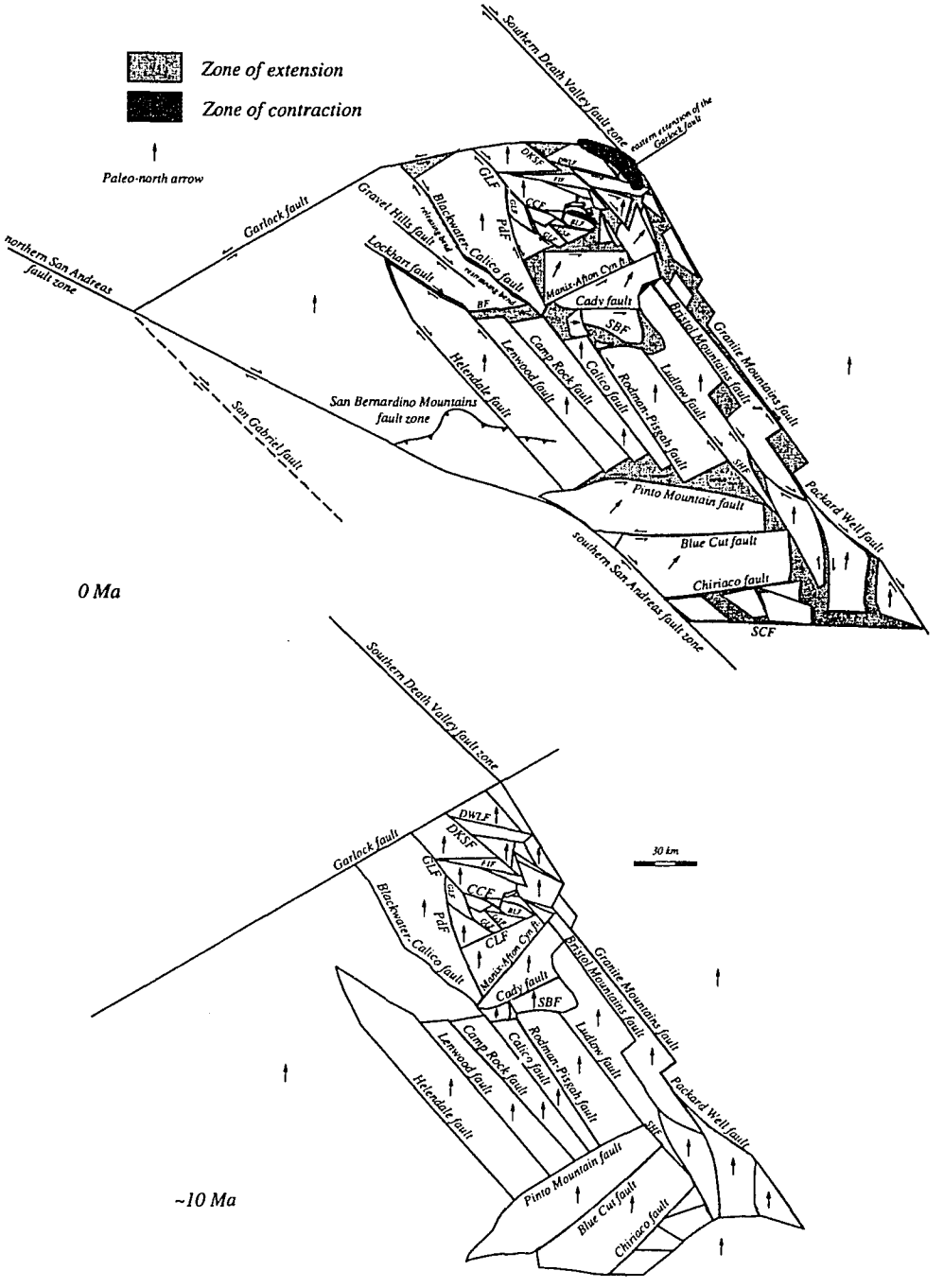

Figure 2.1. Geometric-kinematic model for the late Cenozoic evolution of the Eastern California shear zone. (A) Present-day. (B) Pre-faulting, ca. 10 Ma. BLF, Bicycle Lake fault; CCF, Coyote Canyon fault; CLF, Coyote Lake fault; DKSF, Desert King Spring fault; DWLF, Drinkwater Lake fault; FIF, Fort Irwin fault; GSF, Garlic Spring fault; GLF, Goldstone Lake fault zone; PdF, Paradise fault; SBF, Sleeping Beauty fault; SCF, Salton Creek fault; SHF, Sheep Hole fault. After Dokka, 1993.

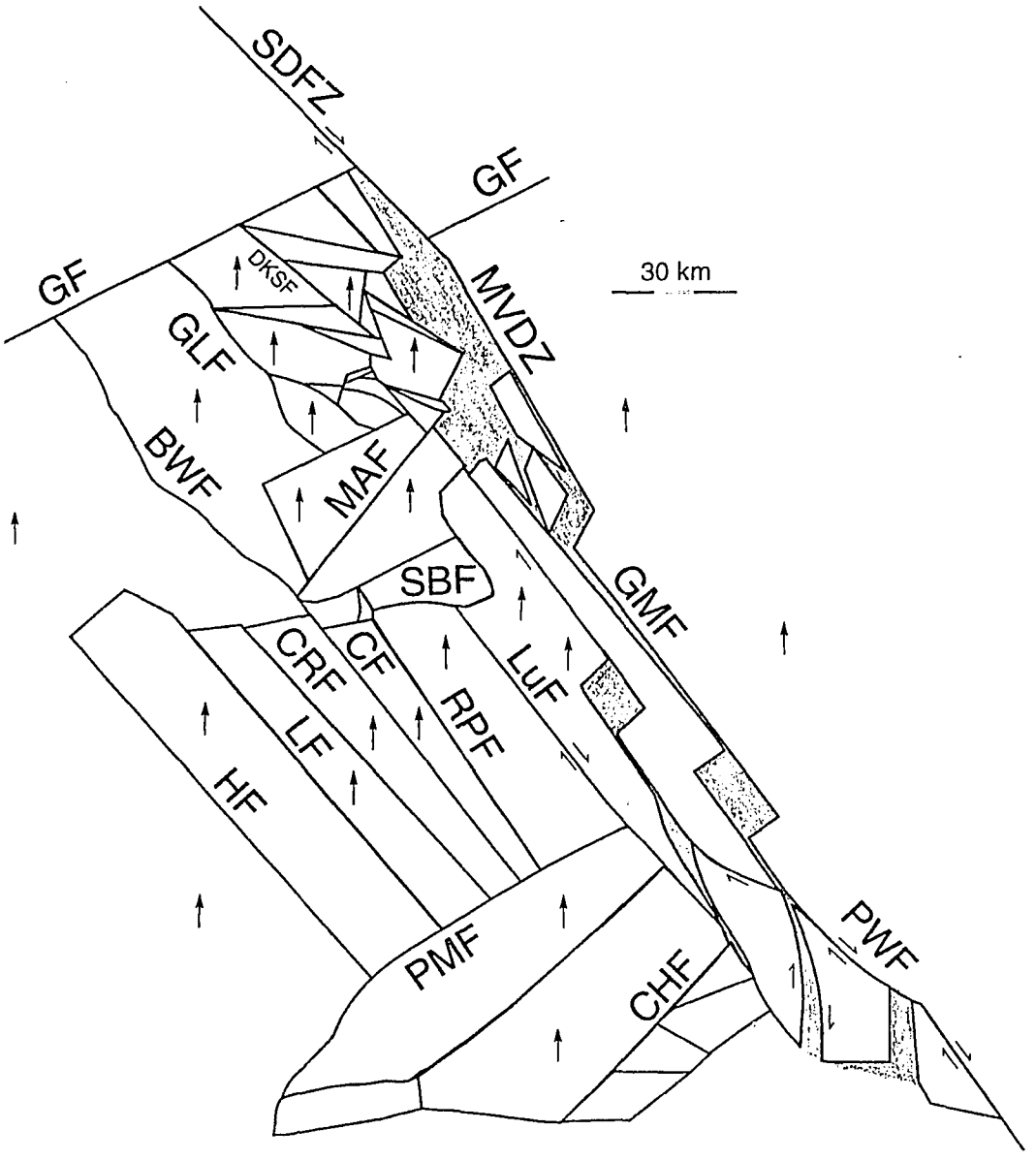

Figure 2.2. Model showing inferred location and amount of crustal extension along the Mesquite Valley disturbed zone due to early motions within the Eastern California shear zone. See Figure 2.1 for key to abbreviations. After Dokka, 1993.

mainly strike-slip, including both dextral and sinistral types, with many fault segments characterized by significant dip slip. Presently, the most prominent zone of seismicity is a NNW trending belt that extends from Yermo north through the Goldstone area and continuing to near the Garlock fault (Fig. 1.1). This zone is dominated by the Goldstone Lake fault zone. Other active faults include the Coyote Lake, Quinones Creek, and Schnable Canyon faults (Plate 1). Several faults lying east of the Goldstone Lake fault zone are also suspected of recent activity based on their youthful geomorphic expression and, in some cases, spatial association with small earthquakes; these include the West McLean Lake fault, Fort Irwin fault zone, Tiefort Mountain fault, Bicycle Lake fault, Coyote Canyon fault, Garlic Springs fault (Plate 1). The topographic expression of the Desert King Spring fault zone and nearby East McLean Lake fault have been subdued by erosion; they do not cut active stream deposits, and are historically aseismic (Plate 1). On this basis, both of these faults are considered inactive. Throughout the northeastern Mojave Desert, minor amounts of crustal extension associated with Quaternary strike-slip faulting have led to the development of internally drained inter-range basins. These isolated, local basins are filled with alluvial and pluvial sediments (Plates 1 and 3).

STRATIGRAPHY OF THE GOLDSTONE LAKE REGION

Introduction

Detailed stratigraphic studies were conducted in the Goldstone Lake region in support of paleomagnetism work (Chapter 3) as well as to gain an understanding of cross-fault lithologic associations. Volcaniclastic rock units are herein described and interpreted as sedimentary rocks where definitive criteria supporting pyroclastic origin could not be met (as per Cas and Wright, 1988). Criteria used in the determination of primary pyroclastic deposits include welded glass shards, carbonized wood fragments, flattened pumice, and gas escape pipes. In a few cases the use of the term

"sedimentary" is likely a misnomer; suspect rock units will require further analysis (e.g. paleomagnetism "conglomerate test") in order to infer their emplacement mechanism. The rock record reaches back to Ordovician time in the Goldstone Lake region and includes: Paleozoic metasedimentary and Mesozoic granitoid basement rocks, Neogene volcanic and volcaniclastic rocks, and basin-filling Quaternary fanglomerate and pluvial sediments.

Basement Rocks of the Goldstone Lake Region

The geology and physiography of the Goldstone Lake region are illustrated in Plate 2. The record of Paleozoic and Mesozoic sedimentation and tectonics in the northeastern Mojave Desert is almost entirely represented by isolated roof pendants of greenschist to amphibolite grade metasedimentary rocks of Paleozoic eugeoclinal and basinal origins (Carr et al., 1981; Miller and Sutter, 1982). These rocks underwent metamorphism and deformation which produced southwest-vergent structures in pre-Early Triassic time (Miller and Sutter, 1982). Ordovician and Permian age metasedimentary rocks have been dated by correlation based on one reported Ordovician graptolite fossil (Carr et al., 1981), lithologic resemblances, and similar structural style to rocks observed in the El Paso Mountains (Miller and Sutter, 1982). Plutonic rocks consisting of gabbro, quartz diorite, and tonalite were intruded during Late Jurassic time (~148 Ma), followed by the emplacement of voluminous granitic plutons in Late Cretaceous time (85-90 Ma) (Miller and Sutter, 1982).

Early Miocene Volcanic and Volcaniclastic Rocks of the Goldstone Lake Region

Previous studies have shown that there is no record of primary volcanic or plutonic activity in the Mojave Desert from Late Cretaceous to at least late Oligocene time (Armstrong and Higgins, 1973; Armstrong and Suppe, 1973; Cross and Pilger, 1978; Glazner and Loomis, 1984; Dokka and Woodburne, 1986; Armstrong and Ward,

1991). Ar^{40}/Ar^{39} dating of volcanic rocks of the Goldstone Lake region yield an oldest age on rhyolite pumice clasts of 22.3 ± 1.5 Ma (hornblende, total fusion) and a youngest age on a formation capping basalt of 18.4 ± 0.2 Ma (whole-rock, stepwise) (A.K. Baksi, reported by MacConnell et al., 1994). Studies by Sabin et al. (1994) yield ages as young as 12.4 Ma based on Ar^{40}/Ar^{39} plateaus from volcanic rocks of the Eagle Crags area. Some of the best exposed and thickest sections of early Miocene age rocks in the northeastern Mojave Desert crop out in the Goldstone Lake region (Plate 3). These volcanic and volcaniclastic strata are herein informally named the formation of Pink Canyon.

Stratigraphy of the Formation of Pink Canyon: Pink Canyon Section

The Pink Canyon area is located near the intersection of the Coyote Canyon and Goldstone Lake faults (Plate 2). A generalized stratigraphic column is illustrated in Plate 3. Figure 2.3 is an interpreted oblique-view aerial video image of the Pink Canyon area. The basal unconformity is a topographically irregular paleo-erosion surface above a basement complex consisting of dioritic plutonic rocks intruded by granitic garnet-muscovite pegmatite dikes. Clast supported, boulder breccias derived locally from the basement complex, are exposed in paleo-depressions and exhibit little lateral continuity. Volcaniclastic deposits containing significant proportions of basement derived clasts overlie the basement and basal breccias on a somewhat irregular surface. These sediments consist of ~30 m of gray, tuffaceous siltstone, sandstone and matrix supported conglomerates. Cobble-size, angular to subangular clasts of gneiss, diorite, garnet-muscovite pegmatite, rhyolite and sub-rounded pumice are common in conglomeratic beds. The ratio of pre-Tertiary basement clasts to volcanic clasts decreases upward in the section. Most beds are massive, although some beds exhibit plane-parallel bedding. These strata are interpreted to be interbedded lahars and fluvial deposits. Cross-cutting these deposits near the mouth of

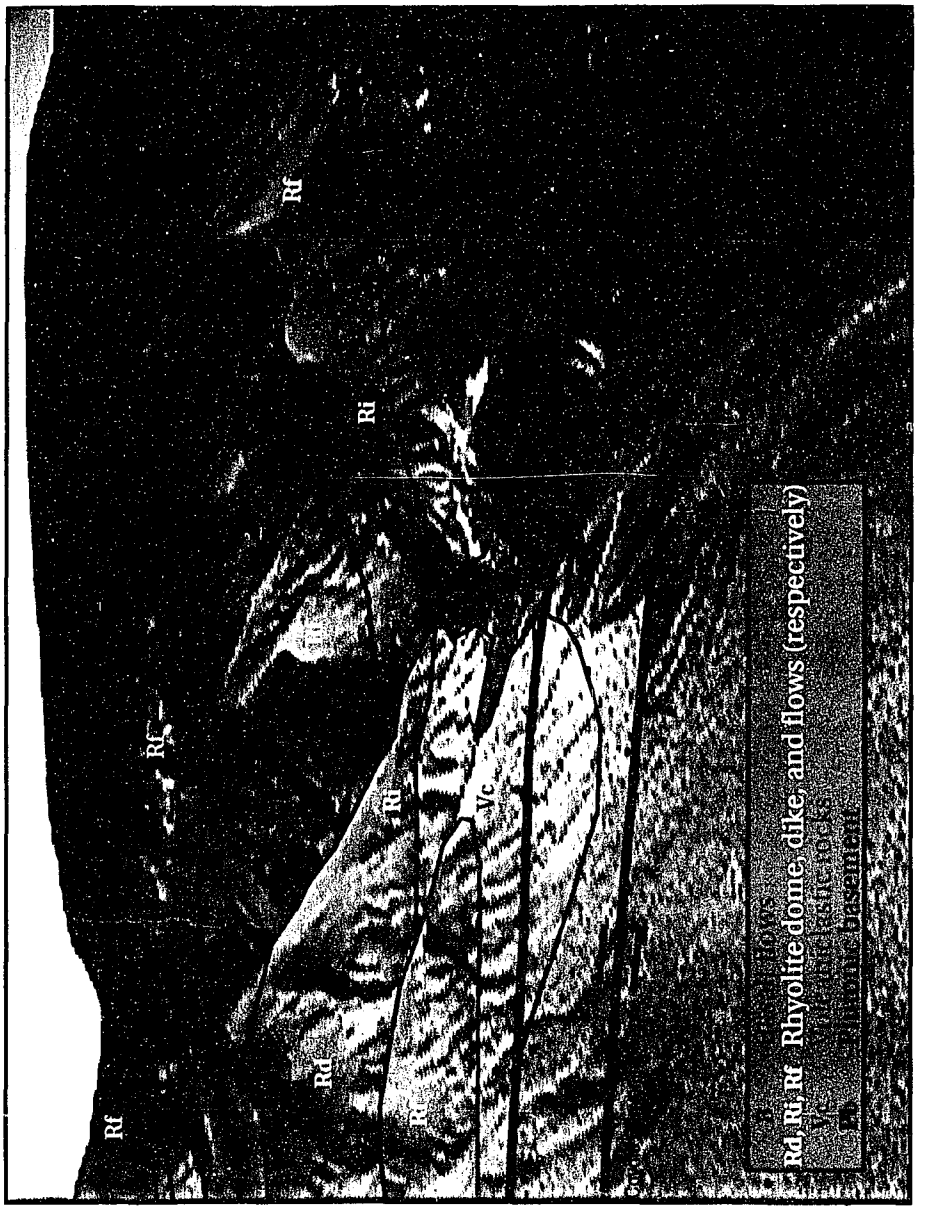

Figure 2.3. Interpreted oblique-view aerial video image of Pink Canyon. View is to the northeast. Top of ridge is ~1480 m elevation. Coyote Canyon fault zone is at ~1135 m elevation. Total relief is ~345 m. Width of view across background is ~1.5 km.

Pink Canyon at an angle ~90° to bedding is a vertically flow-banded rhyolite dike approximately 75 m thick (Fig. 2.4). Sediments show a gradual change in color from gray to salmon to brick red as they approach the dike. The stratigraphic sequence exposed on the north side of the dike begins with ~25 m of tuffaceous sedimentary rocks. The first deposit is a matrix supported massive tuff breccia (~8m thick) containing angular to sub-angular clasts (up to ~2 cm diameter) of gneiss, gabbro, flow-banded rhyolite, perlitic obsidian, and pumice. This deposit is overlain by a ~3.5 m thick, gray, plane-parallel thin-bedded sandstone to matrix supported pebble conglomerate. Above this deposit is a medium to thick bedded conglomerate containing boulders as large as 50 cm (Fig.2.5, Fig. 2.6). Clast lithologies include garnet-muscovite pegmatite, gneiss, rhyolite, and perlitic obsidian. Finer deposits are pumice rich, whereas, coarse deposits contain as much as 80% angular to sub-angular basement derived clasts. This unit is interpreted to be a fanglomerate. A red volcaniclastic sandstone unit (~6.0 m thick) overlies this deposit (Fig. 2.6). Sedimentary structures include low angle truncation surfaces and trough cross-beds. The average grain size is a medium sand with occasional pebble-size lag deposits. This unit is interpreted to be a braided stream deposit. The last sedimentary deposit in this section is a light brown plane-parallel bedded sandstone that grades into an angular pebble conglomerate (Fig. 2.6). Deposited conformably over these epiclastic units is a ~475 m thick aphyric rhyolite flow (Fig. 2.3). Although this unit is thicker than average it contains no evidence of internal layering or other characteristics that would be inconsistent with an interpretation of a single flow unit. This rhyolite is proximal to the source vent which is located adjacent to, and directly west of, the mouth of Pink Canyon. The flow is composed of a basal, central, and upper zone (e.g., Bonnichsen and Kauffman, 1987). Above a locally scoured but generally flat lower contact lies a perlitic vitrophere of basal crumble breccia ~5-10 m thick (Fig. 2.7). This unit

Figure 2.4. Rhyolite dike at the mouth of Pink Canyon: Note subvertical flow banding, tire tracks for scale.

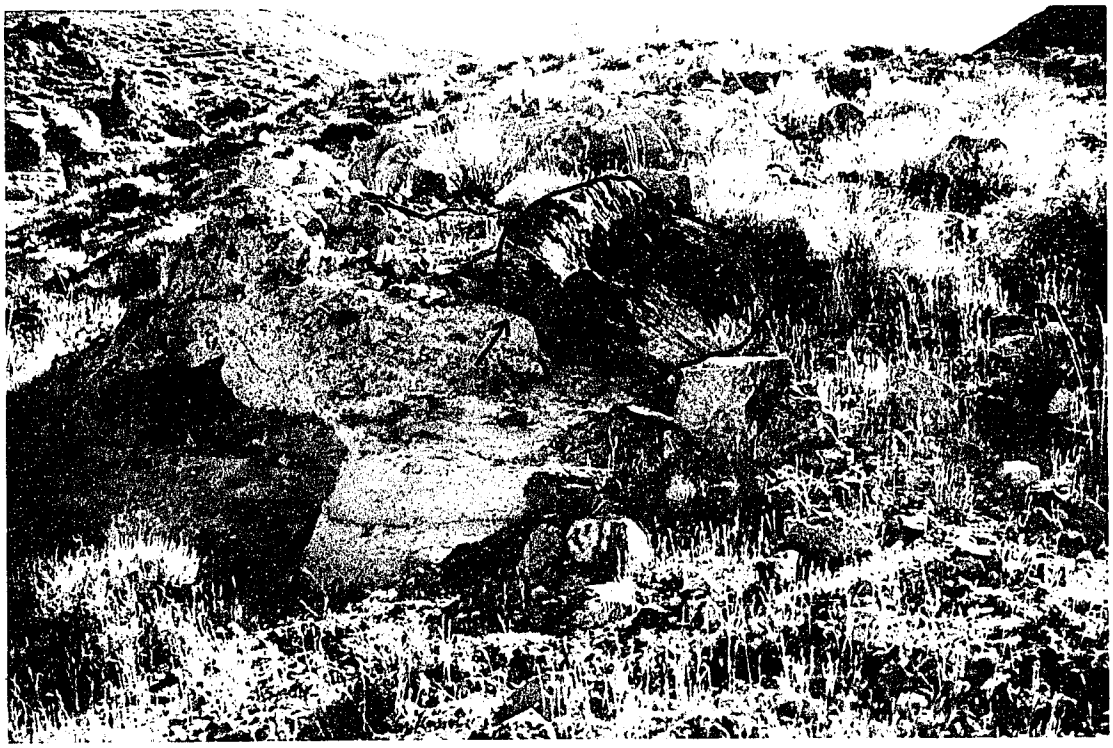

Figure 2.5. Gneissic megaclast in lower volcaniclastic section of the formation of Pink Canyon. Megaclast partially outlined in black. Arrow points to camera lens cover (~50 mm in diameter).

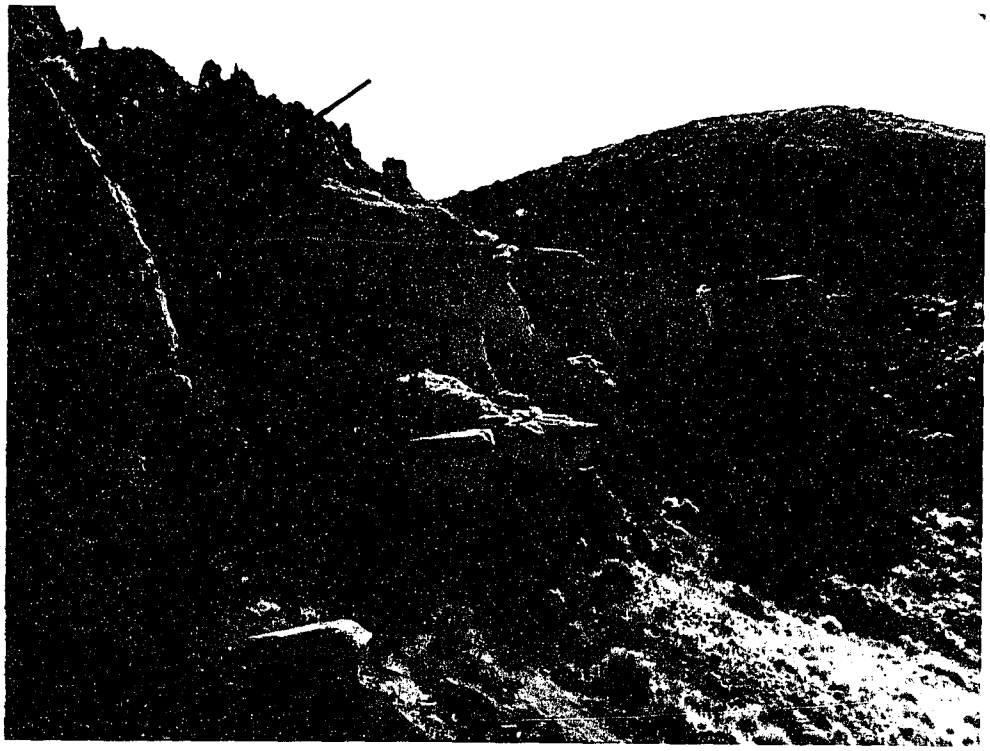

Figure 2.6. Top of the lower volcaniclastic section of the formation of Pink Canyon. Arrows point to bedding contacts discussed in text. The pale red sandstone (center of image) overlying the conglomerate is ~6 m thick.

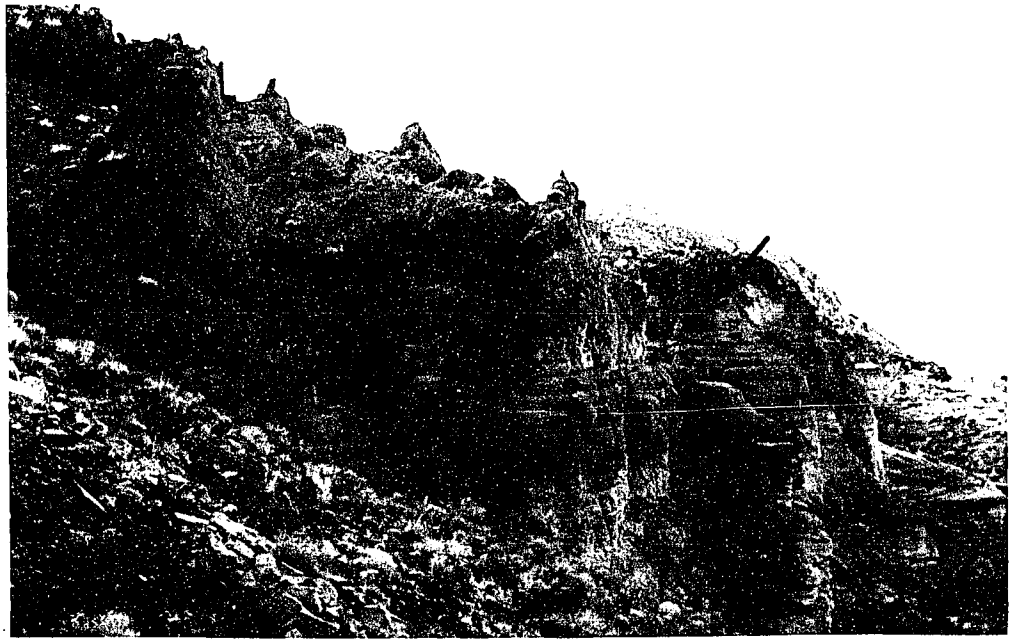

a)

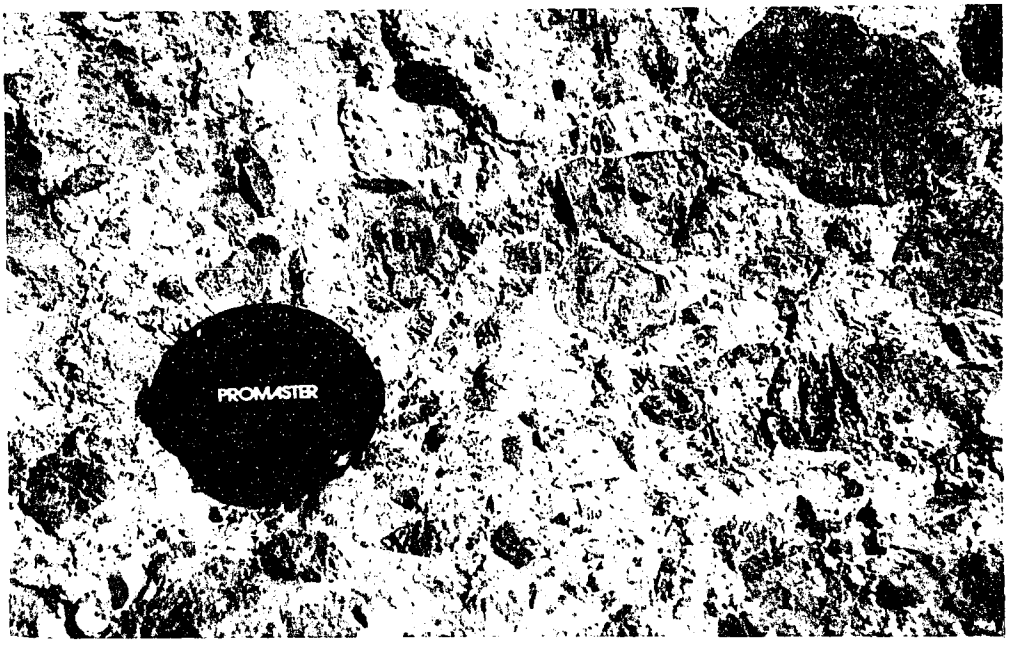

b)

Figure 2.7. Basal rhyolite breccia. a) Contact between lower volcaniclastic sequence and overlying rhyolite flow, arrow points to bedding contact, light brown unit below contact is ~2 m thick; and b) perlitic breccia, camera lens cover is ~50 mm diameter.

contains glassy rounded to angular boulders up to several meters in diameter. The basal zone likely represents the accumulation of blocks that fell from the advancing flow front and were subsequently buried by the lava flow itself (e.g., Hausback, 1987). The central zone is a massive aphyric rhyolite flow with white and light reddish gray flow-banding. The contact between these two units is irregular and deformed. This flow lacks internal bedding or layering, and is essentially devoid of lithic fragments and pumice. "Shrinkage joints" form weakly defined six-sided column structures (~1 m per side)(Fig. 2.8). These joints are especially prevalent in the lower half of the central zone; they do not occur in the basal zone. All of these features suggest that this flow is a primary lava rather than a remobilized welded tuff (Bonnichsen and Kauffman, 1987). The upper zone contains glassy and devitrified rhyolite, is reddish-orange in color and strongly brecciated (Fig. 2.9).

A second sequence of volcaniclastic rocks overlie the irregular flow-top breccia. The first deposit in this section of rocks is a ~1.7 m thick, gray, trough cross-bedded, matrix supported pebble to cobble conglomerate with occasional clast supported pebble horizons. Clasts lithologies include angular flow-banded rhyolites and rare granitoid basement and sub-rounded pumice. Above this unit lies a ~8 m thick laterally extensive series of brown, white, orange, and olive-green colored, well sorted, normal and reverse graded, non-welded, lapilli air-fall beds (~5-30 cm thick)(Fig. 2.10). Clast lithologies include ~80% pumice, with subordinate obsidian and angular rhyolite; no basement derived clasts are present. Interbed contacts are often razor sharp. This unit is overlain by ~25 m of trough cross-bedded sandstones and conglomerates and plane-parallel bedded sandstones. Individual beds are up to ~1.0 m thick and are rich in granitoids, diorite, flow-banded rhyolite, and pumice clasts. Low-angle truncation features are common. Clasts are subangular to subrounded and are as large as 20 cm. This unit contains sandwave bedforms (e.g., antidunes, symmetrical dunes with

Figure 2.8. Central rhyolite zone: Arrows point to base of vertically oriented shrinkage joints.

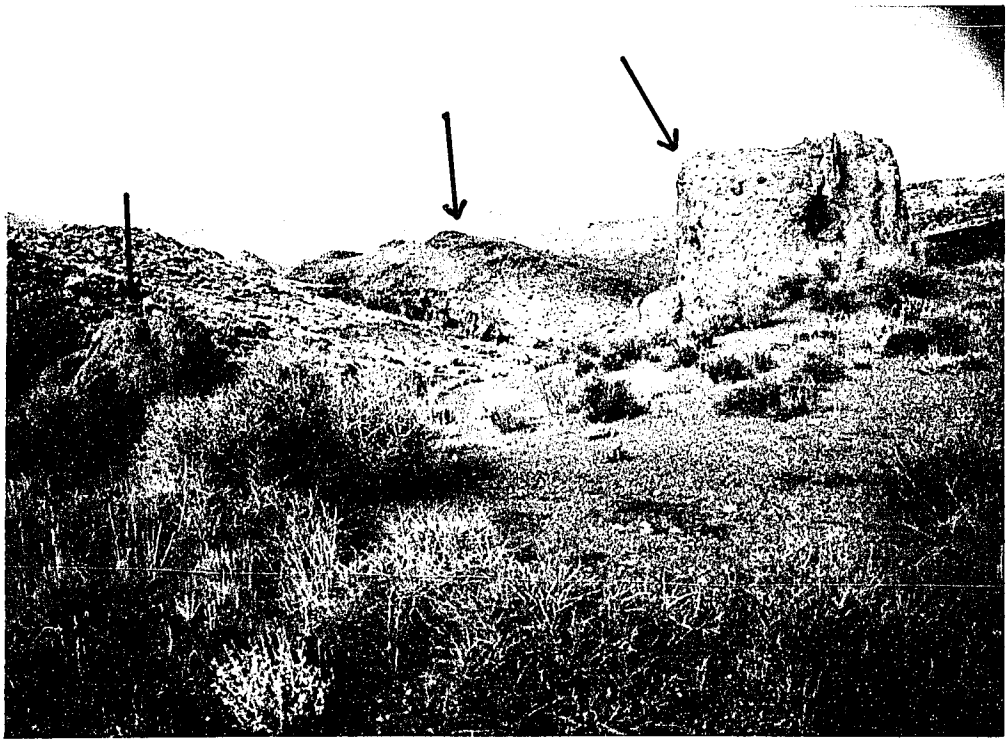

Figure 2.9. Upper rhyolite zone. Arrows point to erosional remnants of flow surface. Outcrop at right is ~5 m wide.

Figure 2.10. Air-fall tuffs in the formation of Pink Canyon. Distinctive white tuff bed above black beds is ~40 cm thick.

leeward accumulations of coarse-grained deposits) and ballistic impact structures that are suggestive of primary pyroclastic surge deposits (Fig. 2.11)(e.g., Wohletz and Sheridan, 1979). However, no welded fabrics, gas escape pipes, or other key criteria were identified. The emplacement mechanism of this deposit is therefore uncertain.

A second rhyolite flow, ~107 m thick, superposes the volcaniclastic rocks (Fig. 2.3). This flow is layered and consists of a middle section composed of highly distorted, glassy, flow-banded, buff to light reddish-gray and black, porphyritic rhyolite that pinches out to both the east and west. The middle section is encased in a plastically deformed, welded, white to light gray, rhyolite flow breccia that pinches out to the south in the Pink Canyon vicinity (Fig. 2.3, Fig. 2.12a,b) and is truncated by the Goldstone Lake fault zone (east branch) to the west (Plate 3). The exposures in the Pink Canyon area are thought to represent a distal flow margin. Rare rounded cobbles of granitoid basement are entrained in the middle section of the flow (Fig. 2.13). The rounded nature of these clasts may be caused by abrasion during transport from depth or thermal spalling rather than the result of fluvial processes (Williams and McBirney, 1979). Plutonic xenoliths are most common during the late stages of catastrophic eruptions that lead to the formation of calderas (Williams and McBirney, 1979).

Above this second rhyolite flow, a third section of volcaniclastic rocks is present (Fig.2.3). The first unit in this section is a massive, ~4.5 m thick, matrix supported boulder conglomerate fining upward to sandstone. Large clasts are flow-banded rhyolite, matrix is pumice rich. Above this unit is a ~4 m thick series of well sorted, laterally extensive in the Pink Canyon area, non-welded, basaltic scoria lapilli beds; individual beds range in thickness from ~1-20 cm (Fig. 2.14). Some beds exhibit normal grading. This unit is interpreted as a sub-plinian air-fall deposit. These volcaniclastic deposits are overlain by a porphyritic, sanidine dacite (?) flow in exposures north of Pink Canyon and by an areally extensive ~330 m thick pile of

Figure 2.11. Possible ballistic impact structure: Note sandwave bed forms. Camera lens cover is ~50 mm in diameter.

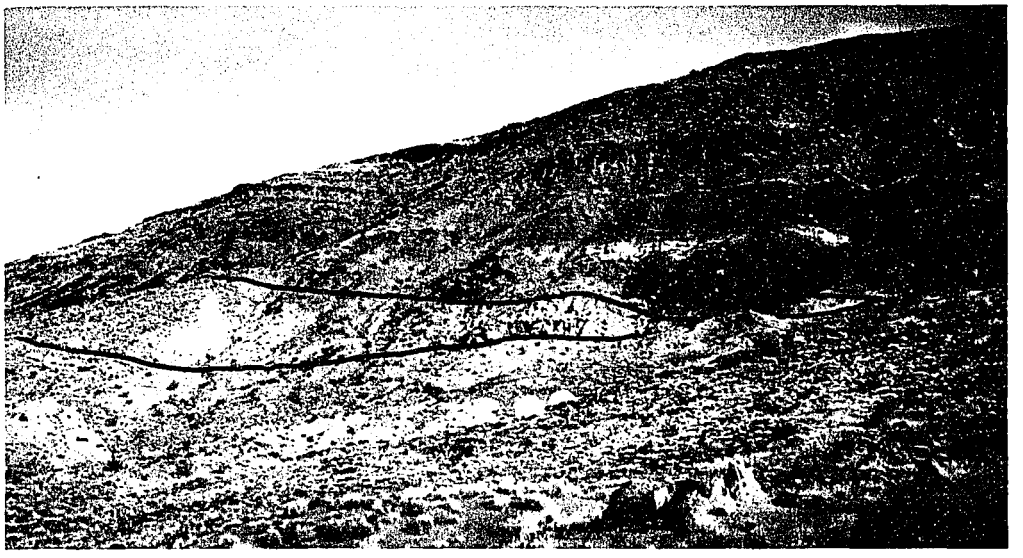

a)

b)

Figure 2.12. Second rhyolite flow in the Pink Canyon area: a) pinching out of second rhyolite flow to the south, outlined in black; and b) plastically deformed flow breccia. Line above arrow is ~30 cm long. Sinuous line through center of photograph follows curvature of fold.

Figure 2.13. Granite cobble in second rhyolite flow in the Pink Canyon area. Cobble marked by arrow is ~10 cm in diameter.

Figure 2.14. Basaltic scoria lapilli beds. Clasts are 1-2 cm in diameter.

"capping" basalt flows to the northeast and east (Plates 2 and 3, Fig. 2.3). Basalts are interpreted to have been rapidly and episodically deposited based on the following observations. First, paleomagnetic studies suggest that although the 65 m thick basalt in the Central Mesa, consisting of at least 16 consecutive flows, the rocks do not adequately sample secular variation (similar to the findings of Calderone, 1990). Second, basalt sequences show very little interflow sedimentation. Third, basalt sequences show no evidence of significant internal erosion. Although some of these basalts have been previously mapped as Quaternary volcanics (Jennings et al. 1962, 1992), our studies suggest that these are lower Miocene in age.

Stratigraphy of the Formation of Pink Canyon: Coyote Hills Section

The Coyote Hills are located south of the Coyote Canyon fault and northwest of Fort Irwin (Plate 2). Tertiary strata of the Coyote Hills lie nonconformably above a topographically irregular granitoid basement contact exhibiting local relief of >40 m. The first major stratigraphic unit is a volcaniclastic sequence ~25 m thick (Plate 3). Within it, the first well exposed unit occurs several meters above the basement contact. It is a clast supported pebble to cobble conglomerate, at least 2 m thick, consisting of granitoid, diorite, and rhyolite lithics, as well as pumice clasts. The next higher unit is a white to buff colored, thin, plane-parallel bedded, coarse-grained volcaniclastic sandstone to siltstone. Some beds exhibit normal grading. Very fine bedded (~1 mm) fine ash layers occur within this section and are laterally continuous at outcrop scale. Occasional pebble conglomerate beds (~20 cm thick) occur in the lower section. A laterally discontinuous pebble conglomerate containing granitoid and diorite lithic fragments and an erosional lower contact occurs high in this section. A ~25 m thick basalt flow overlies the volcaniclastic rocks along a reddish-orange baked contact. The basalt flow is overlain by a ~25 m thick volcaniclastic sandstone unit. A ~440 m thick series of rhyolite lavas, containing a basal vitrophere and at least two flows, overlies

the lower sequence. These rocks are commonly flow-banded and contain abundant sanidine in the lower section. A final section of volcaniclastic sandstones and siltstones (~20 m thick) occur above the rhyolites and, in turn, are capped by ~25 m of basalt flows (Plate 3).

Stratigraphy of the Formation of Pink Canyon: Corral Hills Section

The Corral Hills are located just west of Fort Irwin (Plate 2). Tertiary strata are relatively thin in the Corral Hills (~110 m thick) and contain a lower volcaniclastic unit (~40 m thick) and an overlying capping basalt (Plate 3). The volcaniclastic section begins with ~15 m of white to buff colored, plane-parallel bedded, pumice rich siltstones and sandstones. A matrix supported, basement rich conglomerate overlies these sediments, and locally shows evidence of soft-sediment load deformation along the contact. Basement clasts are as large as 1.5 m. Above this coarse-grained conglomerate are thin to medium bedded, buff colored pumice-rich sandstones, containing occasional erosional scours (~1.0 m deep) with basement-derived pebble to cobble sized lag deposits. A chert deposit lies ~7 m below the basalt/volcaniclastic contact. A ~70 m pile of basalt flows overlies a reddish-brown oxidized baked contact (~2-3 m thick). Basalts are commonly vesicular and exhibit oxidized flow tops.

Stratigraphy of the Formation of Pink Canyon: Central Mesa Section

The Central Mesa area is located southeast of Goldstone Lake (Plate 2). Basement rocks in this area were characterized and dated by Miller and Sutter (1982). Tertiary strata lie nonconformably on an irregular paleosurface above crystalline basement of both Cretaceous felsic and Jurassic mafic affinities and metamorphic roof pendants that occur as isolated pods in Jurassic plutonic rocks (Miller and Sutter, 1982). Epiclastic pumice-rich volcaniclastic rocks were the first Tertiary units deposited (Plate 3). These units consist of ~25 meters of white to buff interbedded sandstones and matrix supported breccias and conglomerates. Sedimentary rocks onlap basement in the

southern Central Mesa area, and are deposited along a buttress unconformity over felsic (rhyolitic ?) volcanic flows and breccias in the central Central Mesa area (Plate 3). Basalts overlie both sedimentary rocks and felsic volcanic flows and range in thickness from ~1 to 10 m. Basalts are commonly massive from the lower contact to the middle of the flow; vesicularity increases upward rapidly to highly vesiculated, reddish-orange oxidized flow tops. A paleomagnetism "conglomerate test" was conducted on a pumice conglomerate unit near the base of the sedimentary section. The Watson (1956) test for randomness of directions was applied to the specimen mean data. Samples passed the test for randomness at the 95% confidence level. This suggests that these pumice clasts were deposited as a matrix-supported volcaniclastic conglomerate (possibly of laharic origin).

Geographic Distribution of Volcanic Centers

Neogene age volcanic vents of both rhyolitic and basaltic types occur in the Goldstone Lake region. The southeasternmost vent is located at the mouth of Pink Canyon and consists of a large rhyolite dome and a co-intruded, 75 m thick dike (Fig. 2.3, Fig. 2.4). Both of these features contain vertical flow-banding and have no discernable discrete contact, but rather merge together seemlessly. Erosional remnants of basaltic scoria cones occur north of Pink Canyon on the east side of Hidden Valley (Plates 1 and 2, Fig. 2.15). These deposits were formed during Strombolian eruptions and contain agglutinate, spindle bombs, and cored bombs containing xenoliths of angular aphyric rhyolite fragments (Fig. 2.16ab). Ejecta such as these represent diagnostic facies of volcanic terranes that suggest a near vent environment (within hundreds of meters)(Cas and Wright, 1989). These vents were subsequently partially buried by aphyric rhyolite lava flows. On the west side of Hidden Valley, just north of the main stream course, a small ~N-S striking, vertically flow-banded, rhyolite dike

Figure 2.15. Ancient eroded remnant of a basaltic scoria cone in Hidden Valley. View toward southwest. Arrow points to inferred center of vent. Black line follows bedding around cone. Dashed line indicates the approximate location of the Goldstone Lake fault (east branch) which truncates the western flank of the scoria cone.

a)

b)

Figure 2.16. Basaltic bombs: a) spindle bombs and, b) cored bomb.

crops out. It is ~10m thick on its northern end and pinches out rapidly to the south. An E-W trending series of four massive dacite-andesite domes occur north of Goldstone Lake and south of MARS (Plates 1 and 2). An erosional lag deposit of sub-round blocks, consisting of a rock type similar to that of the domes south of MARS, is strewn across a north dipping slope in the northernmost Central Mesa area. Some of these blocks exceed 1 m in diameter and exhibit shrinkage cracks protruding radially out from the center of the block, which suggests that they were emplaced ballistically. The size of these blocks suggests that they were deposited within a few kilometers of the source vent (Williams and McBirney, 1979). No other source vents have been identified in the Goldstone Lake region.

Summary of Volcanism in the Goldstone Lake Region

Many aspects of the nature of Neogene volcanism (e.g., geochemistry, petrogenesis, volumetrics) were beyond the scope of this study. However, this study has led to the compilation and interpretation of volcanological data that is noteworthy as well as useful in the development of a regional tectonic model. The following is a brief discussion of the most pertinent findings.

Caldera Related Volcanism in the Northeastern Mojave Desert

It is proposed that Neogene volcanic deposits of the northeastern Mojave Desert region were likely deposited in a caldera environment. Preliminary composition analysis as well as the areal and stratigraphic distribution of volcanic rocks in the Goldstone Lake region suggest that they represent a genetically related "bimodal" mafic and silicic volcanic suite (McCurry, 1992, personal communication). The facies types and geographic distribution described in this study are similar to those predicted by models for continental silicic volcanoes (e.g., Cas and Wright, 1988). According to the Cas and Wright model, the focal element of continental silicic volcanism is the caldera structure, around the margins of which rhyolitic lavas and domes as well as

basaltic scoria cones occur (Cas and Wright, 1988). Epiclastic sediments are also common caldera-fill deposits. Ignimbrite deposits are the one common volcanic rock that is predicted by the continental silicic volcano model that has yet to be identified in our studies. It is possible that some of the rocks that have been classified as epiclastic in this study are actually pyroclastic in nature. Whatever their mode of emplacement, these pumice-rich deposits represent voluminous eruptions of tephra. Locally, caldera subsidence may have been facilitated by the evacuation of the magma chamber through the eruption of lava flows, domes and air-fall deposits rather than large-volume pyroclastic flows.

Thickness Variations of the Volcanic Section in the Goldstone Lake Region

The Pink Canyon section contains multiple rhyolite flows and is adjacent to a large rhyolite dome and a co-intruded dike (Plate 3, Fig. 2.3). Rocks here are ~1100 m thick and comprise the thickest section of Neogene volcanic deposits in the northeastern Mojave Desert region (Plate 3). The Coyote Hills section, located directly southeast of the Pink Canyon section, is relatively thick (~600 m) and contains multiple rhyolite flows (Plate 3). South of the Coyote Hills, the formation of Pink Canyon is substantially thinner (~100 m thick) and contains only epiclastic deposits and capping basalt flows. The rapid change in thickness to the south suggests that the basin margin (caldera rim) was nearby. The ring-fracture system along the caldera rim likely served as a conduit up through which the rhyolites of Pink Canyon were extruded (e.g. Bailey et al., 1976). The westward extension of the proposed caldera rim is likely truncated by the late Miocene (?) to recent Goldstone Lake fault (east branch)(Fig. 2.17). On the west side of the Goldstone Lake fault, the closest volcanic vent complex occurs north of Goldstone Lake and south of Mars (Plates 1 and 2). The domes in this area are on the edge of a regional gravity low that stretches from the Eagle Crags area to the Granite Mountains (Fig. 2.17).

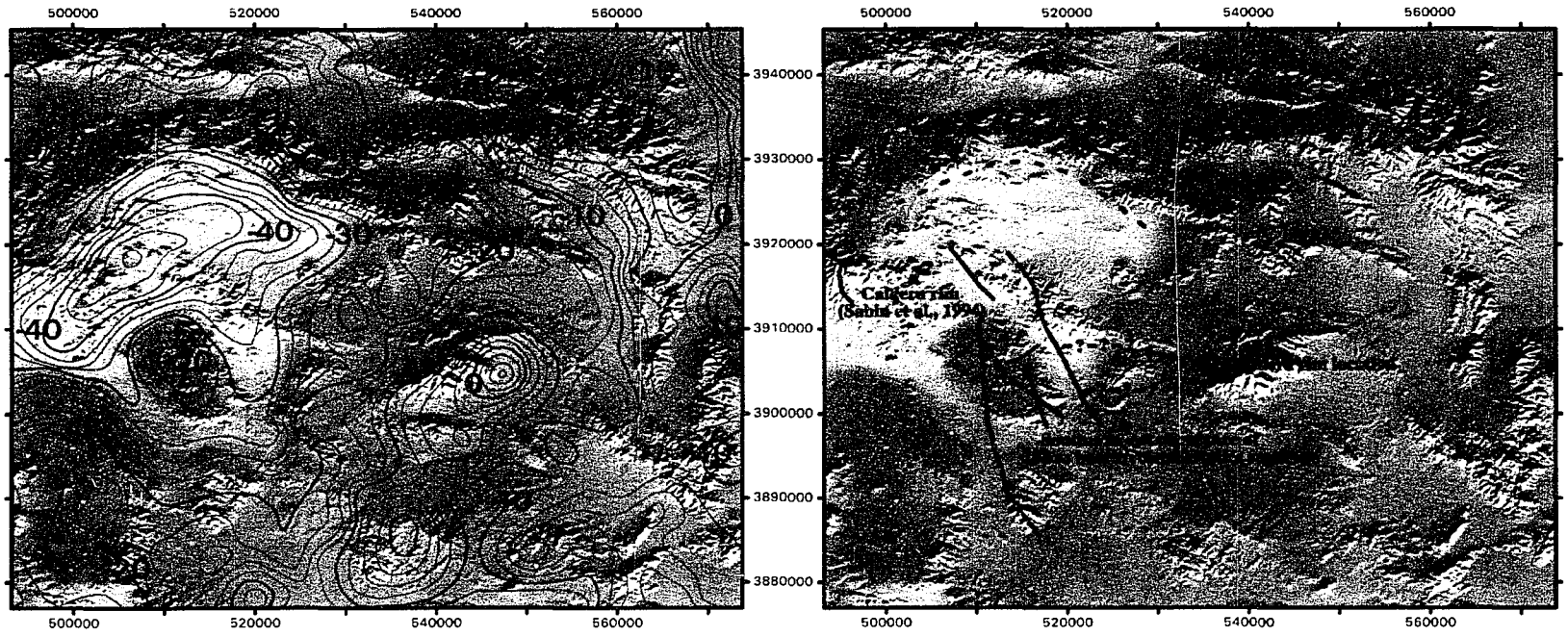

Figure 2.17. Isostatic Gravity Map: Gravity data draped over topography. Color fades from blue (high) to orange (low). Contour interval = 10 mgal. Approximate locations of inferred caldera rim shown as dashed lines. "Offset caldera rim location" based primarily on stratigraphic relations. Coordinate System: UTM.

Gravity Models

Gravity data have been used in previous studies in order to characterize modern and ancient caldera systems (Yokoyama, 1963; Pakiser et al.,1964; Kane et al., 1976; Williams and McBirney, 1979). Almost all calderas associated with voluminous eruptions of pumice show negative gravity anomalies, usually between 10 and 30 mgal (Yokoyama, 1963). Pakiser et al. (1964) and Kane et al. (1976) observed a major gravity low spatially associated with the Long Valley caldera. The gravity low has a relative amplitude of more than 50 mgal. Kane et al. (1976) proposed that the gravity anomaly at Long Valley is caused by relatively porous caldera fill deposits which vary in density and type considerably across the caldera. Kane et al. (1976) estimated the average thickness of fill deposits to be ~2 to 3 km. Gravity data from the northeastern Mojave Desert are consistent with a caldera interpretation and provide an approximation of the regional extent of the structure. A regional gravity low that generally coincides with the geographic distribution of Neogene volcanic rocks and reflects regional physiography can be observed in Figure 2.17 (original gravity map provided by W. Hamilton of the U.S.G.S.). A 47.5 mgal gravity low is located at 506476E 3918516N UTM.

Results of a gravity survey conducted by the Geothermal Program Office, Department of Navy, yield details about the regional gravity anomaly not observed in the regional data described above. This data set contains over 1000 measurement stations from the Eagle Crags area to Tiefort Mountain. A 25 mgal gravity low is centrally located just north and west of MARS near the boarder of the NTC and the NAWS (Sabin et al., 1994). Sabin et al. (1994) identified an east-west trending density ridge depicted in gravity contours that traversed the region from Tiefort Mountain to Pink Canyon. Here, the lineament is apparently offset in a right-lateral sense to the north and continues toward the west, this offset may be the result of

dextral slip along the Goldstone Lake fault zone. Sabin et al. (1994) also recognized a curvilinear anomaly that is coincident with the geographic distribution of volcanic rocks as well as an arcuate shaped topographic ridge in the Eagle Crags area. Sabin et al. (1994) proposed that this arcuate feature reflects the presence of a relatively small caldera centered on the Eagle Crags area.

On the basis of the above discussion, it is proposed that the Neogene volcanic rocks of the northeastern Mojave Desert were erupted in association with caldera formation. The areal extent of this caldera, as suggested by gravity data, is comparable to that of the Long Valley caldera which is ~17 x 32 km in diameter (Bailey et al., 1976). The Goldstone Lake fault zone apparently truncates the rim of this feature in the vicinity of Pink Canyon and displaces it ~10 km in a dextral sense. This amount of offset is compatible with the geographic distribution and thickness trends of the Neogene volcanic sequence and provides our best estimate of the magnitude of slip along the Goldstone Lake fault zone (Fig. 2.17).

FAULTS OF THE NORTHEASTERN MOJAVE DESERT

Introduction

Previous Work

The most up-to-date compilation of previous studies of late Cenozoic faulting in the northeastern Mojave Desert was presented in Jennings (1992). Conspicuously absent from this compilation, however, is reference to the unpublished but widely circulated mapping performed by the Southern Pacific Co. in the late 1950's. These maps cover mainly the area along and south of the National Training Center and were constructed at a scale of 1:24,000. These maps provided us with a generally reliable source of local mapping that facilitated mission planning and field studies. Other studies include Byers (1960) and Yount et al. (1994); these are government sponsored, general

geological mapping projects in the vicinity of Alvord Mountain and Fort Irwin basin, respectively.

Approach and Methods

With a clearer understanding of the active tectonics of the northeastern Mojave Desert being our goal, a study was designed to locate, map, and determine the age and kinematics of young faults of the area. These data have resulted in an improved understanding of the active tectonics and seismic hazards of the northeastern Mojave Desert region and have provided a means with which to assess regional strain models proposed by previous workers (Garfunkel, 1974; Luyendyk et al., 1980,1985; Carter et al., 1987; Dokka and Travis, 1990; Dokka, 1993; Ross, 1994, Dokka and Ross, 1995).

Faults of the northeastern Mojave Desert were detected and mapped by a combination of field mapping, image analysis of satellite imagery and digital elevation models, and gravity and seismicity studies. All major faults were confirmed in the field. Prior to analysis, data sets were organized into a geographical information system (GIS) implemented on a UNIX workstation. This allowed for the simultaneous visualization of combinations of data sets in order to gain new perspectives on spatial and temporal relationships. Primary data sets include published and unpublished geologic maps, Landsat TM multispectral imagery, SPOT panchromatic imagery, digital topography, gravity, and seismicity. These data sets were augmented by hand-held ground and aerial photographs (panchromatic, color and color-infrared), and color video. See Chapter 1 for a review of the pertinent data sets and methodologies.

Late Cenozoic faults mapped during the course of this study are shown on Plate 1; localities referred to in the text are also shown in this figure. To aid the reader, our discussion of faults is organized according to geographical area. For discussion

purposes, the northeastern Mojave is informally subdivided into the following subregions: Goldstone Lake-Superior Valley-Paradise Range; Coyote Lake-Alvord Mountain-Cronese Mountain; Granite Mountains-Drinkwater Lake; Central Fort Irwin; Avawatz-Mesquite Valley disturbed zone. These divisions are somewhat arbitrary; no direct relation to the genetic nature of structures is intended. Naturally, some structures extend through more than one subregion; however, each structure is discussed only in the region within which it is a dominant feature.

Goldstone Lake-Superior Valley-Paradise Range

Goldstone Lake Fault Zone

The Goldstone Lake fault zone is a NNW-trending zone of dominantly right-slip faults that extends from Coyote Lake north to near the Garlock fault (Plate 1, Table 2.1). As illustrated on Plate 1, the Goldstone Lake fault zone and its southern extensions, the Paradise and the East Paradise faults, is associated with more seismic events than any other fault system in the northeastern Mojave Desert. Beginning near the Garlock fault zone, the Goldstone Lake fault zone passes south-southeast through the Myrick Spring area (Plate 1). At the north end of Goldstone Lake, the Goldstone Lake fault zone apparently splits into two main branches (designated as west and east branches). The east branch of the Goldstone Lake fault apparently steps to the east (left-step) following the high range of volcanic rocks that trend SSE toward Fort Irwin basin (Plate 2). The width of the fault zone at this latitude is 4-6 km. This overstep occurs at the intersection of the western end of the Fort Irwin fault zone and the Goldstone Lake fault zone in the vicinity of MARS (UTM: 508400E 3920100N). Analysis of satellite images and digital topography suggests the occurrence of a large-scale antiform to the north of this overstep in the valley between MARS and the Granite Mountains (~2.5 km north of MARS)(Plate 1). The axial trace on this fold has a bearing of 300°; the fold plunges gently to the northwest. The location and geometry

Table 2.1. Faults of the Northeastern Mojave Desert

Faults	Strike	Sense (dominant direction)	Length (km)	Offset/ Net Slip^	Seismicity (number of events)	Active
NW TO NNW STRIKING FAULTS						
Goldstone Lake fault zone	**NNW**	**Right O, FM**	**65+**	**? / 10+**	**>100**	**Y**
Goldstone Lake fault (east branch)	330°	Right O	34	? / 10	13	Y
Goldstone Lake fault (west branch)	315°	Right inferred	13	? / <5	13	Y
Paradise fault	345°	Right O, FM	40	2 / <5	>50	Y
East Paradise fault	305°	Right inferred	7	? / <5	>50	Y
Schnable Canyon fault	345°	Norm inferred	6	? / ?	8	Y
Garlic Spring fault	310°	Right inferred	6	? / ?	0	Y
Desert King Spring fault	305°	Right inferred	13	? / 24*	0	N
E-W STRIKING FAULTS						
Coyote Lake-Quinones Creek fault zone	**270°**	**Left O, FM**	**40**	**5 / 13***	**>25**	**Y**
Coyote Lake fault	270°	Left O	36	5 / ?	3	Y
Quinones Creek fault	250° to 270°	Left O, FM	22	? / ?	>20	Y
Bicycle Lake fault	**270°**	**Left O**	**24**	**3.5 / <5**	**1**	**Y**
Coyote Canyon fault zone	**270°**	**Left O**	**40**	**1 / <5**	**2**	**Y**
Coyote Canyon fault	270°	Left O	20	1 / <5	1	Y
Tiefort Mountain fault (north branch)	270°	Left, Rev O	20	? / <5	0	Y
Tiefort Mountain fault (south branch)	305°	Rev O	6	? / <5	1	Y
Fort Irwin fault zone	**270°**	**Left O**	**53**	**3.5 / <5**	**0**	**Y**
East McLean Lake fault	265°	Left O	11	? / ?	0	N
West McLean Lake fault	270°	Left inferred	10	? / ?	0	Y
Garlock fault zone	**270**	**Left O**	**260**	**65 / 65**	**1**	**Y**

EXPLANATION: Faults in bold face font are major active faults, faults in plain font are individual faults; Seismicity data include dates 1-1-90 to 9-30-95, data were obtained from the SCSN, the number of events on the Garlock fault reflects only the activity of the fault segment that lies within the northeastern Mojave Desert. Right = right lateral; Left = left lateral; Norm = normal slip; Rev = reverse slip; O = known from field observations; FM = inferred from focal mechanisms (Hafner and Hauksson, 1994); ^ net slip is inferred, units = meters; * from Dokka and Travis (1990a).

of this antiform as well as the presence of up-to-the-north, E-W striking shears near MARS suggest that contraction may have occurred in this area across the left-step in the Goldstone Lake fault zone. Exposures of segments of the Goldstone Lake fault zone (east branch) can be seen at various places along the range from northeast of Goldstone Lake to west of Fort Irwin (Plate 1). These include the region between Pink Canyon and Hidden Valley where fault slivers can be observed in the field to step north along right-stepping en echelon faults (UTM: 516690E 3910930N), and at (UTM: 517640E 3908440N) where late Quaternary alluvium has been uplifted and tilted to the northeast (Fig. 2.18). The second largest seismic event (M=4.1) in the northeastern Mojave Desert during the past 15 years occurred at 518170E 3912970N UTM in association with this fault (Plate 1). Right separation of volcanic vent facies (dikes and domes) across the Goldstone Lake fault (east branch) as well as a deflection of gravity contours along the Goldstone Lake fault (east branch) from Pink Canyon to near MARS suggests that the caldera rim has been displaced ~10 km in a right lateral sense (Fig. 2.17). This restoration is also consistent with the geographic distribution and thickness variations of the Neogene volcanic sequence (Plate 3).

Evidence for the Goldstone Lake fault (west branch) includes: 1) the alignment of physiographic lineaments seen on the ground, Landsat TM imagery, and topographic maps; 2) abrupt changes in structural attitude across the inferred fault trace; and 3) the alignment of earthquake epicenters (Plate 1). Because the main strand of the Goldstone Lake fault (west branch) occupies major active drainages, direct observation of outcrop scale fault plane features was not possible; secondary faults that are subparallel and/or merge with this trend are well exposed in the Central Mesa area south of Goldstone Lake (Plates 1 and 2). Here, splays of the Goldstone Lake fault (west branch) are identifiable as abrupt lithologic contacts exposed on canyon walls that juxtapose basalt flows against rhyolites along a near vertical surface. At a locality

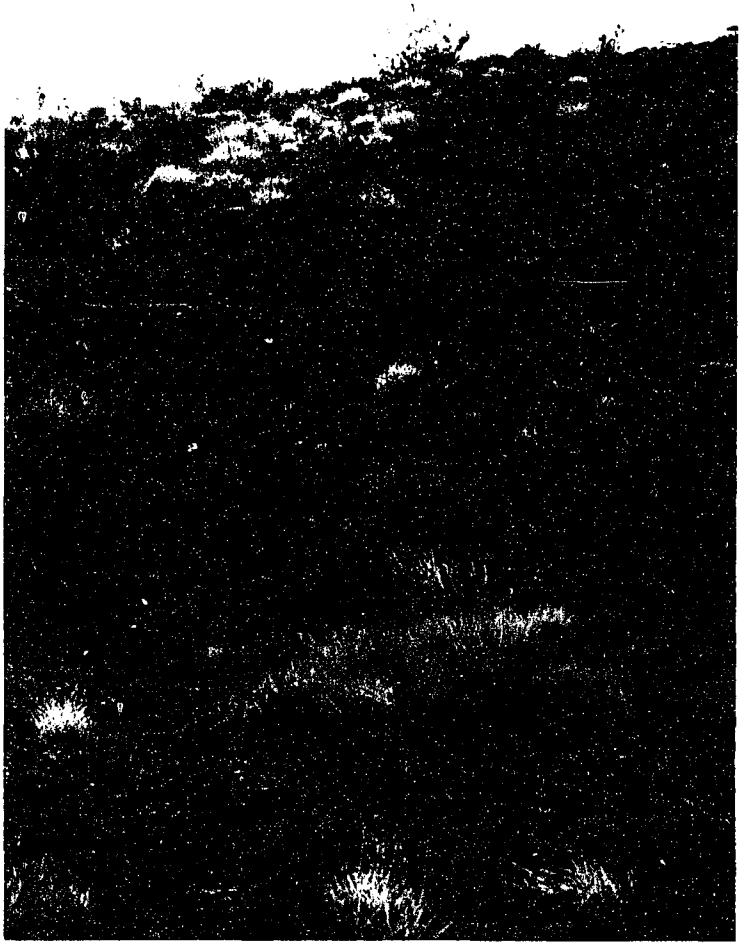

Figure 2.18. Photograph of uplifted and tilted late Quaternary alluvium along the Goldstone Lake fault zone (east branch). Thin black lines follow bedding contacts. Thick horizontal line near center of photograph is ~1.0 m long. View is to the northwest. The Goldstone Lake fault (east branch) is located several meters to the left.

just east of the main drainage (UTM: 511353E 3907096N), a splay of the Goldstone Lake fault (west branch) cuts a basalt-boulder strewn alluvial fan surface. The western side of this fault is apparently upthrown and stranded from continued sedimentation sourced from the basalt escarpment to the east. The northernmost exposure of the Goldstone Lake fault (west branch) first occurs near the south shore of Goldstone Lake (Plate 1); the fault possibly continues north beneath the lake bed and merges with the east branch of the Goldstone Lake fault zone.

Goldstone Lake has the form of a classic "releasing bend, pull-apart basin", analogous to Death Valley (Dokka, 1993)(Plates 1 and 2). Dokka (1993) proposed that Goldstone Lake is the consequence of extension formed due to a change in geometry of the Goldstone Lake fault zone. To the south, the west branch follows the main drainage passing through or near the MOJAVE facility (Plate 1) and continues southeast to near the VENUS site where motion along the fault has juxtaposed Cretaceous garnet-muscovite granite (on the east) against Jurassic quartz diorite and tonalite (on the west) (Plates 1 and 3).

The east and west branches of the Goldstone Lake fault zone become subparallel near the latitude of the VENUS facility. These faults are separated 4-6 km perpendicular to strike and likely continue southeast past Barstow Road, eventually intersecting with the Coyote Lake-Quinones Creek fault zone (Plate 1). The nature of this intersection is unclear.

Paradise Fault

The Paradise fault apparently merges with the west branch of the Goldstone Lake fault zone near MOJAVE (Plate 1). The Paradise fault can be traced or inferred to continue ~24 km to the south, through Superior Valley, continuing through the Paradise Range and south along the west side of the Coyote Lake basin (Plate 1). The fault is named for the Paradise Range where it is well exposed. The fault was

originally located by mappers of Southern Pacific Co. (Danehy, 1958b); the fault is not shown on subsequent compiled maps of the California Division of Mines and Geology (Jennings et al., 1992).

Evidence for this fault includes offset rock bodies that vary in age from Ordovician to Quaternary, the alignment of fault and fault-line scarps and the spatial association of the trace of the fault with seismic events (Plate 1). Pre-Tertiary structures and rocks in the pass between the southern Goldstone Lake area and Superior Valley are displaced ~1-3 km along the Paradise fault with apparent right-lateral offset (Plate 1, UTM: 510613E 3902484N). In Superior Valley, the Paradise fault is marked by topographic lineaments in basement exposures across a broad, gently inclined pediment surface (Plate 1, Fig. 2.19). Farther south in the Paradise Range, offset Mesozoic plutonic rocks and Paleozoic metasedimentary rocks suggest <2 km of right-lateral displacement. Earthquake epicenters occur along the projection between the north and south branches, suggesting that the fault is continuous across the intervening valley (Plate 1).

East Paradise Fault

The East Paradise fault is a heretofore unrecognized northwest striking fault that was initially detected as an alignment of earthquake epicenters (Plate 1). Imagery analysis led to the identification of subtle spectral contrasts that represented truncated lithologic units (Fig. 2.20). Field investigations confirmed the nature of this feature. Paradise Spring is located along the main southern fault segment and may be a consequence of groundwater upwelling at a right step between the two main strands of the East Paradise fault (Fig. 2.20, Plate 1 UTM: 517250E 38888820N). Although no piercing points or fault plane features have been identified that could be used to determine the sense of slip, right-lateral motion is likely based on fault orientation and

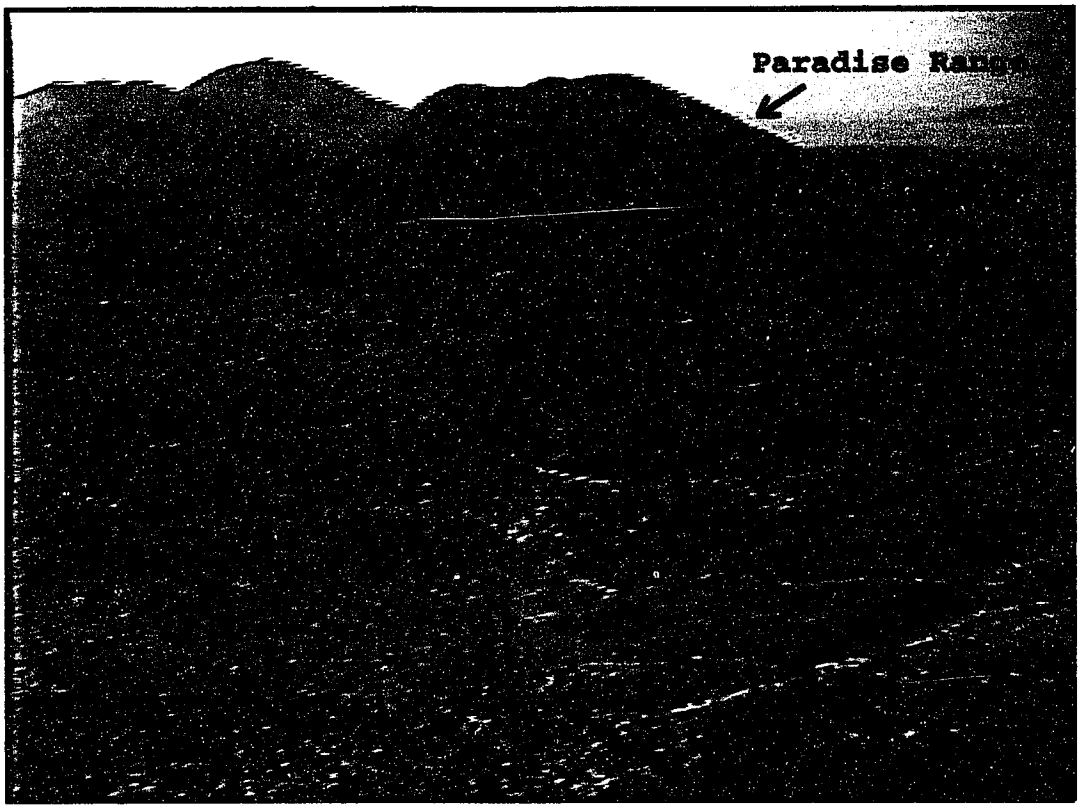

Figure 2.19. Oblique-view video image of the Paradise fault. View to the south-southeast. Paradise Range in background.

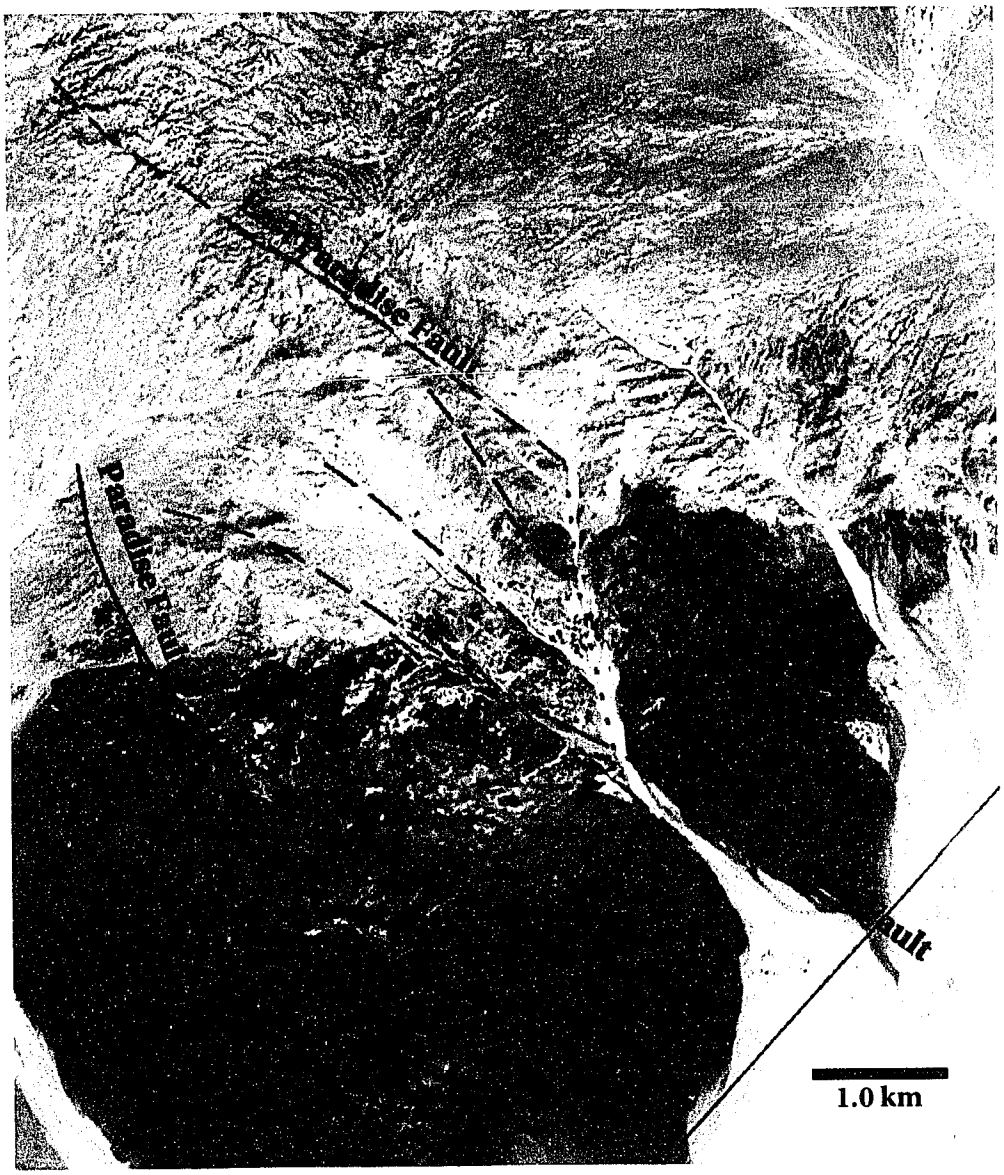

Figure 2.20. Landsat TM-SPOT merged image of the Paradise Range.

the regional strain pattern. Both the Paradise fault zone and East Paradise fault should be considered active based on their present level of seismic activity.

Coyote Lake-Alvord Mountain-Cronese Mountain

Coyote Lake-Quinones Creek Fault System

The Coyote Lake fault and the newly recognized Quinones Creek fault are grouped together as a single fault system in order to more accurately convey their genetic relationship and regional significance (Plate 1). Based on seismicity, the Quinones Creek fault together with the eastern segment of the Coyote Lake fault constitute the currently active strand. The Coyote Lake-Quinones Creek fault system serves as a major tectonic boundary within the Eastern California shear zone, separating domains that have experienced different strain and rotational histories (Dokka and Travis, 1990a)(Fig. 2.1). The following discussion describes the western segment of the Coyote Lake fault and the Quinones Creek fault separately and then characterizes the Coyote Lake-Quinones Creek fault system as a whole.

Coyote Lake Fault

The E-W striking Coyote Lake fault was first recognized by McCulloh (1952) from surface mapping in the hills north of Coyote Lake (Plate 1). The occurrence of springs along its trace suggests that the fault serves as a local barrier to shallow groundwater flow. Byers (1960) mapped the eastward continuation of the fault along the northern flank of Alvord Mountain. Although much of the fault is concealed by recent alluvium, exposures of highly sheared rocks and deformed Quaternary deposits can be found along its trace (Byers, 1960). Byers (1960) noted that west of Alvord Mountain, the southern block was down; this is in marked contrast to the segment to the east where the north side is down. Although the kinematic observations by Byers (1960) emphasize that the motions were dip-slip, he speculated on the basis of

similarity of geometry that the fault was genetically related to the Garlock fault and, thus fundamentally a left-lateral fault. He emphasized that this notion was unproven.

Quinones Creek Fault

The Quinones Creek fault is a previously unrecognized ~E-W to ENE striking fault that can be traced east from near the northwest shore of Coyote Lake to just northeast of Alvord Mountain where it likely merges with the Coyote Lake fault (Plate 1, UTM: 534660E 3888670N). The fault is named for a prominent stream canyon locally known as Quinones Creek. The Quinones Creek fault forms the northern edge of the Coyote Lake basin and displays evidence for sinistral as well as down-to-the-south relative motion. Previous workers considered the prominent break in slope associated with part of the fault to be a wave-cut bench formed in Pleistocene time by Coyote Lake (McCulloh, 1960).

The Quinones Creek fault was initially detected using enhanced Landsat Thematic Mapper imagery (Fig. 2.21). Examination of seismicity data revealed that the mapped trace of the fault is coextensive with a line of earthquakes that occurred following the Landers event (Plate 1). The trace of the fault is coincident with a pronounced topographic break in slope and with a zone of disrupted and sheared rock. Uplifted older Quaternary alluvial fans to the north end abruptly along the fault; the relief on this scarp is 3-7 m. Although these fans generally dip gently (5-10°) to the south, horizontal to slightly north dipping strata (<6°) occur near the fault (R. Dokka, 1993, unpublished mapping). North of the fault, Quinones Creek consists of a single main channel that drains much of the region north of Coyote Lake. Upon intersection with the fault, the channel abruptly widens (Fig 2.21). Field relations suggest that south of the fault the creek consists of an active channel to the west and two abandoned channels to the east. These channels were apparently continuations of the main channel that were abandoned as the southern block translated to the east.

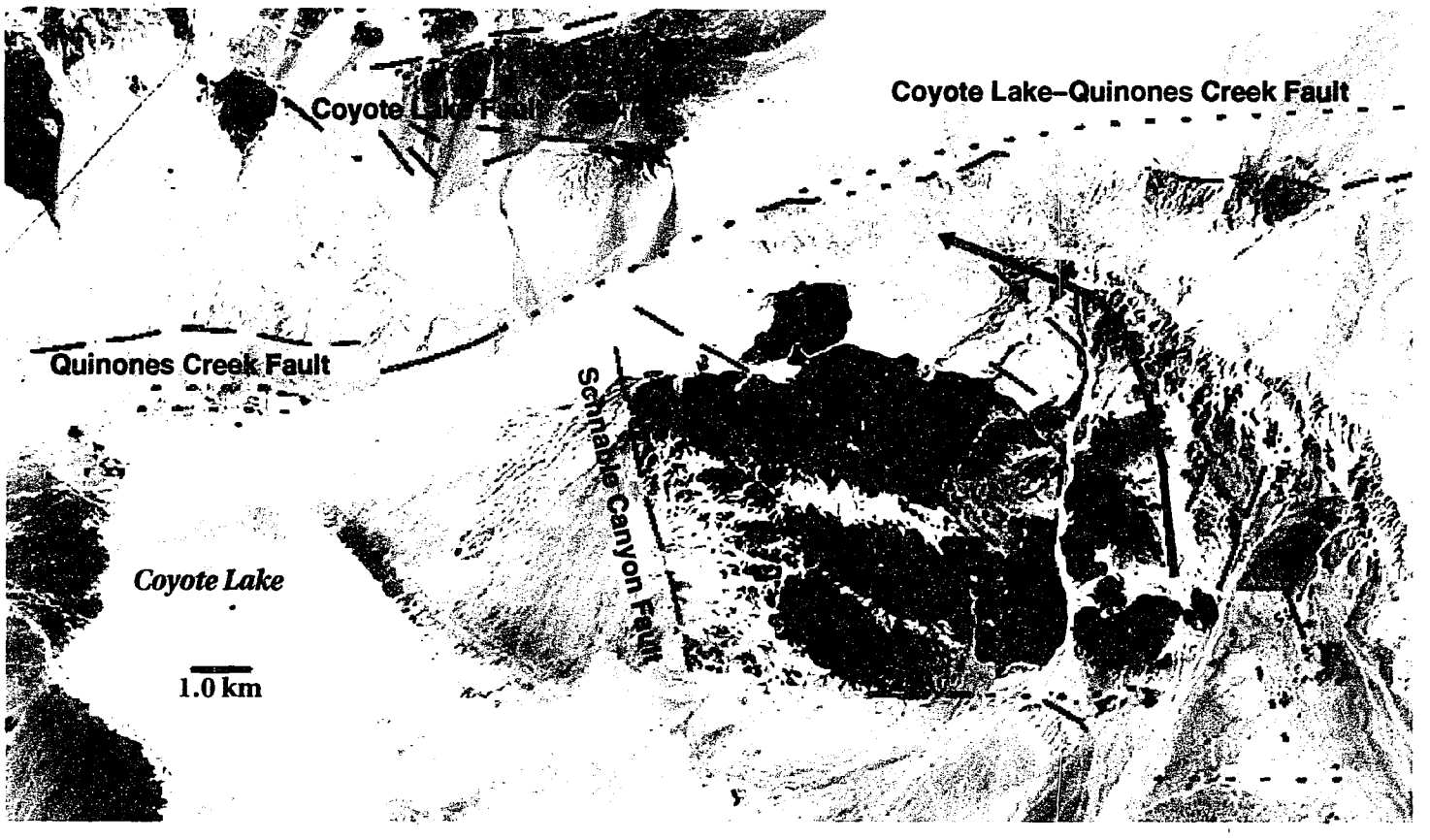

Figure 2.21. Landsat TM image of Coyote Lake and the Alvord Mountains: Showing the Coyote Lake-Quinones Creek fault system and Schnable Canyon fault. Note prominent fold in Alvord Mountains. North is toward page binding. Refer to Plate 1 for location index.

The spatial distribution and arrangement of faults and strain elements associated with the Coyote Lake-Quinones Creek fault zone are indicative of left shear. Folds to the north and east of Alvord Mountain affect all rock units ranging in age from pre-Tertiary to Quaternary but are particularly well expressed in Tertiary strata and slightly lithified late Quaternary fanglomerate (Fig. 2.21). Overall, the folds trend N-S but become ~NW-SE near the Coyote Lake-Quinones Creek fault system apparently in response to left-lateral movement along the Coyote Lake-Quinones Creek fault system. The folds are shallowly plunging, open, and upright to slightly asymmetrical near the fault.

Seismicity along the Coyote Lake-Quinones Creek fault system was sparse prior to the June 28, 1992 Landers earthquake and limited to the western end of the Quinones Creek fault; there are no events associated with the Coyote Lake fault. Following the Landers event, however, several events (M=2-4) occurred along the Quinones Creek fault as well as along the eastern segment of the Coyote Lake fault (Plate 1). Hafner and Hauksson (1994) determined a focal mechanism along the Quinones Creek fault that is consistent with left slip along a vertical, E-W striking fault. Field studies in December 1993 revealed several narrow (<1 cm), yet extensive (<~100 m) fractures that cut recent alluvium along the Coyote Lake fault . Some cracks contain the remains of annual grass that germinated during the last period of rain, suggesting that the cracks formed during or before Spring 1993. Similar cracks were observed in the hills north of Coyote Lake fault (D. Miller, written communication, 1993). We speculate that these fractures are sympathetic cracks related to earthquake(s) that occurred between September 2, 1992 and November 1993.

In summary, the spatial relations and geometric arrangement of folds and faults as well as the offset of stream courses along the Coyote Lake-Quinones Creek fault system are consistent with formation along a left slip fault. A focal mechanism on the

Quinones Creek fault is also consistent with left slip. The overall drainage and major physiographic features of the area are apparently a manifestation of the Coyote Lake-Quinones Creek fault system. Recency of movement is expressed by the faults' youthful geomorphic expression and the apparent interaction with and disruption of active streams.

The regional geometric-kinematic model of Dokka and Travis (1990a)(Fig. 2.1) predicts that the Coyote Lake fault is dominantly a left slip fault with ~13 km of net slip. They reckoned that eastward translation of the block to the south of the Coyote Lake fault (Alvord Mountain) created an extensional basin beneath Coyote Lake.

Schnable Canyon Fault

The Schnable Canyon fault is a north-striking, high-angle fault that occurs along the west side of Alvord Mountain (Fig. 2.21). It was first recognized but not named or studied in detail by mappers of the Southern Pacific Co. (Danehy, 1958a). The fault is named for Schnable Canyon, a local prominent stream channel that intersects the fault near 529400E 3883775N UTM (Plate 1). The fault separates pre-Tertiary high grade metamorphic rocks to the east from partially lithified Quaternary as well as recent deposits to the west and is marked by well developed, linear contact that corresponds to a pronounced break in slope (Fig.2.21). Mapping suggests that the Schnable Canyon fault does not extend north of the Quinones Creek fault nor can it be traced on the ground further to the south (Danehy, 1958a). Although the sense of motion on the Schnable Canyon fault is not known, its west side is apparently down; previous modelling predicts that it is a normal fault (Dokka and Travis, 1990a). Recent activity along the Schnable Canyon fault is implied by its youthful geomorphic character and association with several earthquakes (Plate 1).

Granite Mountains-Drinkwater Lake

Garlock Fault Zone

This study did not target the Garlock fault for detailed analysis but it is included in this compilation because it provides a useful northern boundary along which the geometry, timing, magnitude and sense of slip are relatively well constrained. The Garlock fault is a ~260 km long, E-W striking, sub-vertical sinistral fault that accommodates differential extension between the Basin and Range to the north and the Mojave Desert Block to the south (Davis and Burchfiel, 1973)(Fig. 1.1, Plate 1). Loomis and Burbank (1988) reasoned that the Garlock fault was initiated at ~10 Ma based on the timing of counter-clockwise vertical axis rotation of rocks in the El Paso Mountains. Approximately 65 km of left-lateral displacement has occurred along this fault since late Miocene time in the vicinity of the northeastern Mojave Desert region (Smith, 1962; Smith and Ketner, 1970; Davis and Burchfiel, 1973).

Desert King Spring Fault

The Desert King Spring fault, named for a prominent waterhole, is a NW strike-slip fault that forms the boundary between the Granite Mountains and the Leach Lake basin (Plate 1)(Dokka and Travis, 1990a). The fault displays strong, linear topographic and compositional contrasts on the ground as well as on Landsat TM imagery over a distance of >13 km. Exposures near 529630E 3929890N UTM show that the fault juxtaposes probable Mesozoic granitic basement against older Quaternary (12,000 yrs - 1.8 million years), moderately lithified, alluvial fanglomerate along a subvertical, sheared contact. This contact is overlain by younger, weakly lithified Quaternary alluvium which is in turn crosscut by active streams. Fault plane kinematic indicators show shallowly inclined grooves and slickenside striations, consistent with dominantly strike-slip displacement; small scale folds suggest that the sense of displacement was dextral. The inactive state of this fault is corroborated by a lack of seismicity.

East McLean Lake Fault

The East McLean Lake fault is a ~N80°E striking, subvertical fault that occurs in the Alpine Valley in the central Granite Mountains (Plate 1, Fig. 2.22). At its eastern end, the fault changes strike to ~E-W as it approaches the Desert King Spring fault zone at the western margin of Drinkwater Lake valley (UTM: 532100E 3928050N). Evidence for the fault trace is lost beneath alluvium at its western end in the McLean lake area. Exposures of the fault occur in ravines at the east end of Alpine valley. Mesozoic-age dikes are abundant north of the fault but are sparse to the south. A N-S striking dike occurs south of the fault at 533200E 3928110N UTM. This dike curves to the west near its intersection with the fault, a relation which suggests left shear (Fig. 2.23). A smaller fault, possibly related to the East McLean Lake fault, occurs ~2.5 km to the south-southeast and is marked by well developed scarps and vegetation lineaments. The kinematics of the East McLean Lake fault are unknown. No earthquakes are associated with the East McLean Lake fault nor are younger Quaternary deposits obviously disturbed along its trace. Based on the data presented above, it is concluded that the East McLean Lake fault is presently inactive.

Fort Irwin Fault Zone

The Fort Irwin fault zone is marked by an E-W trending alignment of fault scarps and fault-line scarps. The fault can be traced >50 km from south of Myrick Spring to a location 15 km north of Red Pass Lake (Plate 1). The most prominent exposures of the Fort Irwin fault zone occur along its eastern half in the area between Barstow Road at Granite Pass (UTM: 542575E 3920685N) to near No Name Lake (Plate 1). The eastern segment of the Fort Irwin fault zone exhibits triangular faceted ridges, truncated alluvial fans, and uplifted and truncated alluvial deposits. Offset of the Tertiary-basement unconformity suggest ~3.0-3.5 km of left separation (Fig. 2.24). The fault to the west, through Nelson Lake Valley to south of Myrick Spring, is poorly

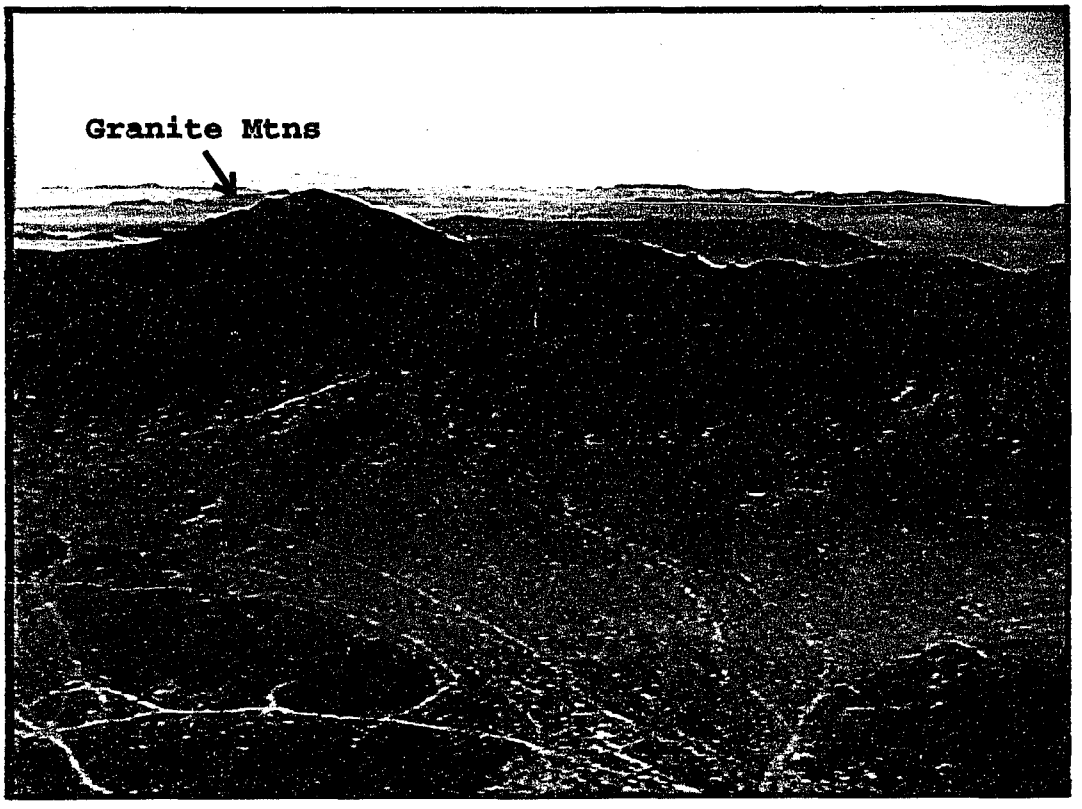

Figure 2.22. Oblique-view video image of the East McLean Lake fault. View to the north. Bajada dips to the north. Fault line indicated by black arrows.

Figure 2.23. Landsat TM (7,4,2)-SPOT merged image showing folded dikes near the East McLean Lake fault. Arrows point toward dikes showing apparent folding. Direction of deflection of dikes on both sides of the fault is consistent with left shear. North is toward page binding. Refer to Plate 1 for location index.

Figure 2.24. Landsat TM image of eastern segment of the Fort Irwin fault zone. Note offset of the Tertiary nonconformity; separation is ~3-3.5 km. Refer to Plate 1 for location index.

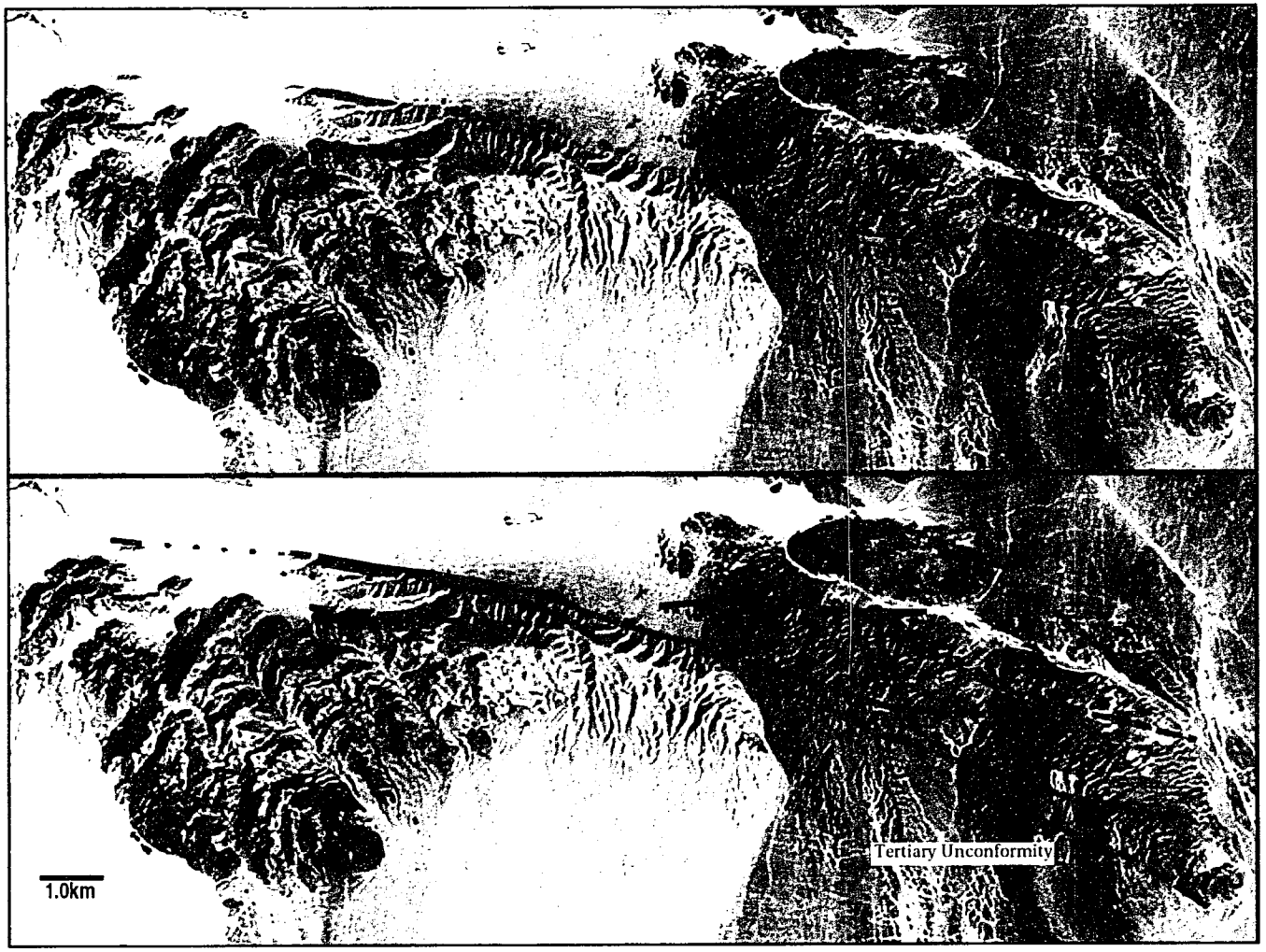
Tertiary Unconformity
1.0km

exposed and the location uncertain. Its position in this area is marked by an alignment of subtle topographic lineaments, and small scarps west of Barstow Road in Granite Mountains (Plate 1).

Trenching of shears along the western portion of the Fort Irwin fault zone by Santo et al. (1989, 1992) at the Goldstone Deep Space Communications Complex also provides evidence supporting a Quaternary age for faulting. This study, conducted in support of antenna construction at the MARS and URANUS sites, focused on fault detection and fault dating within a small site (1.7 km x 4.2 km). Faults initially observed on aerial photographs were trenched and dated using geomorphic and soil stratigraphic techniques. Their analysis indicates that the last displacement of two of the four faults that cut the area occurred between 12,000 and 35,000 years. Faults identified by Santo et al. (1992) typically consist of E-W striking, subvertical zones of shear several feet wide that exhibit up-to-the-north incremental offsets. The maximum displacement is unknown because the measurable offset was larger than the depth of the trenches (2-3 m). The amount of horizontal motion along these faults is unknown.

We conclude that the Fort Irwin fault is likely active based on the observation that late Quaternary deposits are obviously disturbed along its trace. More work is clearly needed to verify or dismiss this hypothesis.

West McLean Lake Fault

The West McLean Lake fault is an E-W striking family of subvertical faults, ~10 km in length, and occurs west of McLean Lake to near Myrick Spring (Plate 1). This fault system truncates Neogene volcanic and volcaniclastic rocks as well as partially lithified Quaternary deposits. Faults cut through uplifted and dissected alluvial fans, apparently affecting the progress of headward erosion of some gullies resulting in the alignment of knick points. Offsets in stream courses along fault traces are not systematic in sense. The geometry and timing of the West McLean Lake fault is similar to the

adjacent Fort Irwin fault zone which suggests that the two may be related and may connect south of McLean Lake.

Central Fort Irwin

Coyote Canyon Fault

The Coyote Canyon fault is an ~E-W striking, high-angle, left-slip fault that can be traced from the east branch of the Goldstone Lake fault zone at Pink Canyon east to 5 km north of Bicycle Lake; the fault may continue east across the northern reaches of Bicycle Lake and connect with the Tiefort Mountain fault (Plate 1). The fault is named for Coyote Canyon (UTM: 528888E 3907027N). Fault scarps and fault plane features can be observed all along its western trace. Almost all fault plane kinematic indicators (slickenside striations, grooves, fibrous mineral growths) are consistent with horizontal slip; these features are especially well developed near the mouth of Pink Canyon (Fig. 2.25) and at a location ~1 km north of Coyote Canyon (Fig. 2.26ab). Offsets in alluvial fans and diversion of active stream courses around shutter ridges and across alluvial fan surfaces consistently indicate recent sinistral displacement of at least 0.5-1.0 km (Fig. 2.27, Plate 1). A small pull apart (?) basin (UTM: 528947E 3908607N) is partially filled with gently dipping to horizontal Pliocene and younger sediments (Plate 3). The remains of a new world sloth was considered to be less than 4 My old (R. Reynolds, 1992, personal communication). The north side of the fault is upthrown from the Pink Canyon area (UTM: 518252E 3909805N) to north of Coyote Canyon. In the Pink Canyon area strata are folded into a NNE plunging antiform (Plate 2). Strata directly south of the fault dip steeply to the south and southwest in the Coyote Canyon area (Plate 2). The northeast trending Coyote Hills range is located south of the Coyote Canyon fault. This range dips homoclinally to the northwest forming the southeastern margin of a small triangular basin bounded to the north by faults and fault line scarps associated with the Coyote Canyon fault (Plate 2). It is

proposed that translation and horizontal-axis rotation of the Coyote Hills block has resulted in the lowering of the basin floor northwest of the Coyote Hills and is likely responsible for the down to the south character of the Coyote Canyon fault in this area (Plate 2). A similar half-graben style basin architecture is inferred to exist to the southeast of the Coyote Hills range. Yount et al. (1994) reports that the depth of basin fill increases from 30 m southeast of Fort Irwin to ~210 m on the northwest side. Total late Cenozoic left slip along the Coyote Canyon fault is likely to be <5 km based on the geographic distribution of Tertiary volcanic rocks on both sides of the fault in the Goldstone Lake region.

Tiefort Mountain Fault

The Tiefort Mountain fault zone is a generally E-W striking, high-angle fault zone that occurs along the north side of Tiefort Mountain (Plate 1). It can be traced from north of Bicycle Lake to near Red Pass Lake. The fault is subdivided into a main northern branch and a southern branch. The north branch of the Tiefort Mountain fault forms the northern, abrupt boundary of the range. The south side of the north branch is apparently upthrown. Left-lateral displacement along southern branch is evidenced by offset marble layers in basement rocks at 544600E 3906565N UTM. Although there are few earthquakes associated with the Tiefort Mountain fault zone, its youthful appearance suggests that it may be currently active.

Bicycle Lake Fault

The Bicycle Lake fault is an ~E-W striking, subvertical, left-slip fault that occurs south of Tiefort Mountain (Plate 1). The fault can be traced west of Bitter Springs to the hills east of Fort Irwin; the western part of the fault splays into several smaller faults that apparently terminate into the basin occupied by Fort Irwin. The fault displays ~3.5 km of left separation as revealed by the displacement of a distinctive pre-Tertiary marble unit (Byers, 1960)(Fig. 2.28). The fault consists of a <0.5 km zone

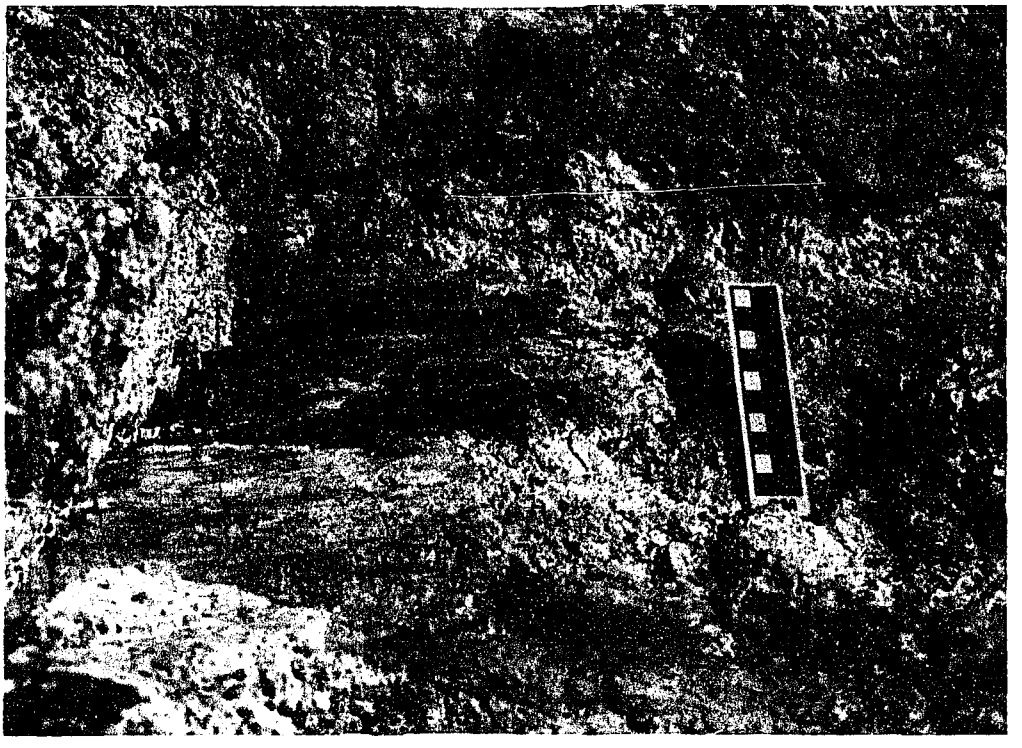

Figure 2.25. Slickensides with subhorizontal striae on the Coyote Canyon fault near Pink Canyon. Scale is in centimeters.

a)

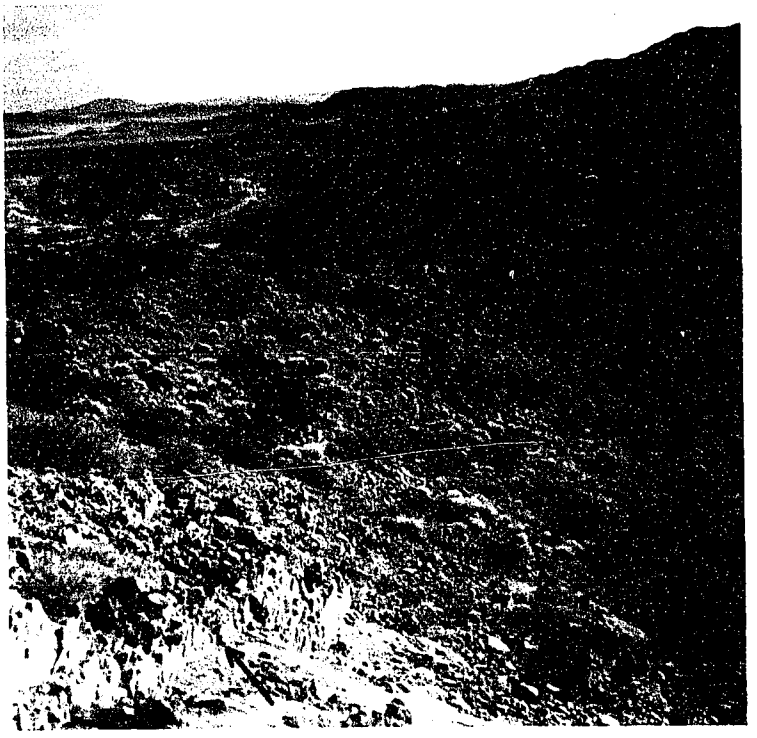

b)

Figure 2.26. Coyote Canyon fault: a) Arrows point to fault scarp on the Coyote Canyon fault north of Coyote Canyon; and b) Striae on same fault surface, pencil is ~15 cm long.

Figure 2.27. 3D image of the Coyote Canyon fault: Landsat TM (band-ratio)-SPOT merge draped over high resolution digital elevation data. DEM data derived from U.S.G.S. 7.5 minute topographic quadrangles. View is to the west. The E-W striking Coyote Canyon fault is centered on page. Note fault scarps and offset alluvial fans and stream courses. Approximately 1-2 km of left-lateral separation is observed on late Quaternary alluvial fans. The Coyote Canyon fault curves to the north (just west of page center) near its intersection with the Goldstone Lake fault zone (east branch). The Central Mesa area defines the horizon at page center.

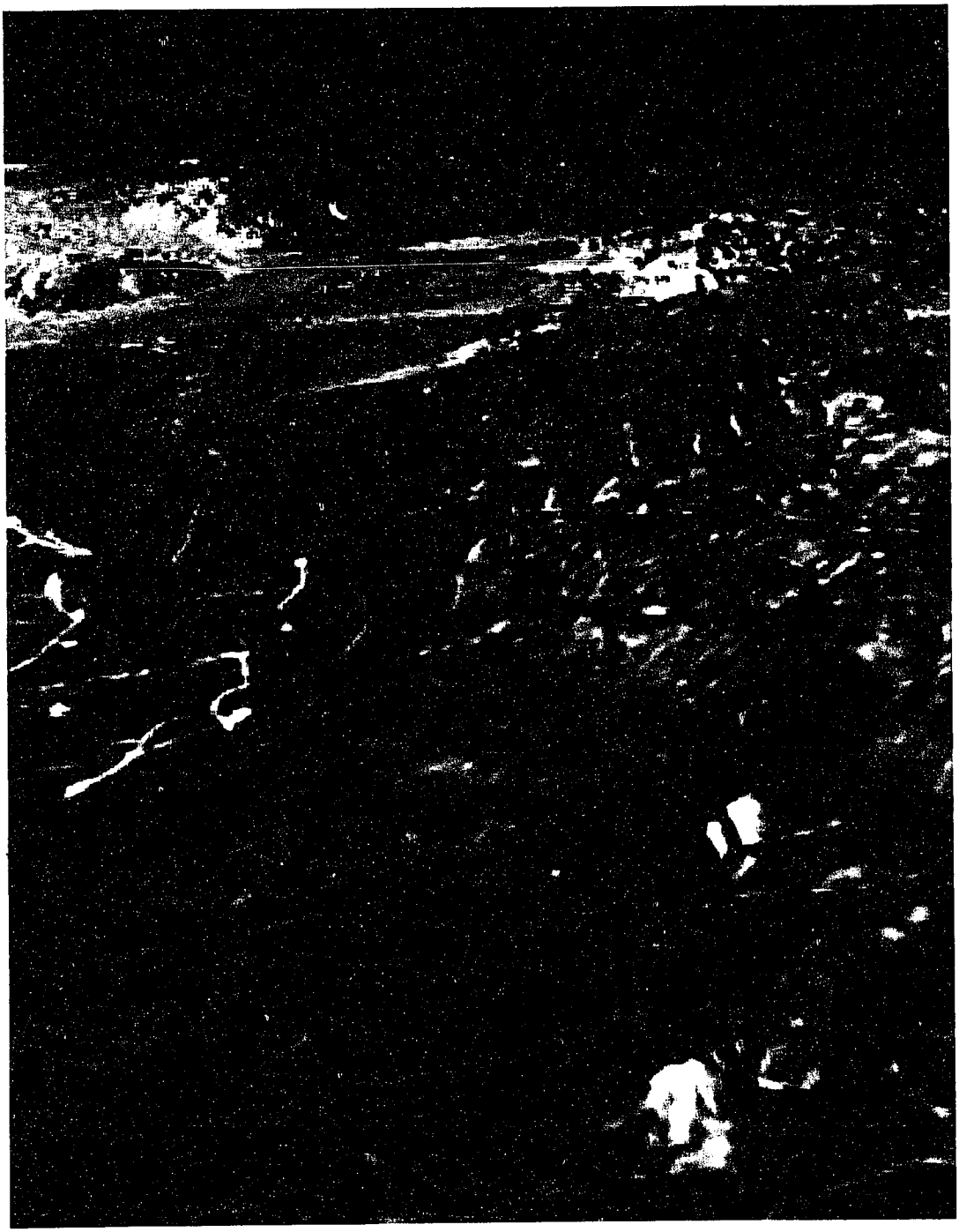

of anastomosing shears with locally intense brittle deformation. A young ~5.6 Ma (Yount et al, 1994) basalt unit south of Bicycle Lake is also truncated and displaced in a similar manner as the pre-Tertiary marble suggesting that movement is younger than the formation of the basalts (<5.6 Ma)(Fig. 2.28). A large (300m x 50 m), tabular pod composed mainly of calcium carbonate oriented ~E-W cuts upper Miocene-Pliocene (?) conglomerate and sandstones at a location 540100E 3899435N UTM. This deposit is interpreted to have formed as an extensional gash along the left-slip Bicycle Lake fault and is similar to young auriferous bodies of eastern California and western Nevada. Yount et al. (1994) propose that the age of the Bicycle Lake fault is at least as young as mid- to late Pliocene based on displacements occurred in alluvium. Recent activity along this fault is also suggested by the youthful morphology of the fault. This study identified only one seismic event along the Bicycle Lake fault.

Garlic Spring Fault

The Garlic Spring fault was first mapped by Byers (1960)(Plate 1). It is a NW striking, probably subvertical, shear named for a spring located at 532736E 3898325N UTM. The fault can be traced from just southeast of Fort Irwin ~8 km to near Langford Well Lake. Byers (1960) observed low angle (~25°) slickensides striations on the outcrops along the main fault segment. Yount et al. (1994) noted that parallel faults cut intermediate age alluvium and aligned spring deposits and estimated that faulting occurred in mid-Pleistocene time. Striae on these faults is reportedly horizontal and minor shear planes and fractures yield right-lateral sense of offset (Yount et al., 1994). However, the net sense of slip on this fault system has yet to be well defined (Yount et al., 1994).

Avawatz Mountains-Mesquite Valley Disturbed Zone

This subregion is a north-south trending zone delimiting the eastern margin of the study area (Figs. 1.1, 2.2, Plate 1). This area was not targeted for intensive analysis

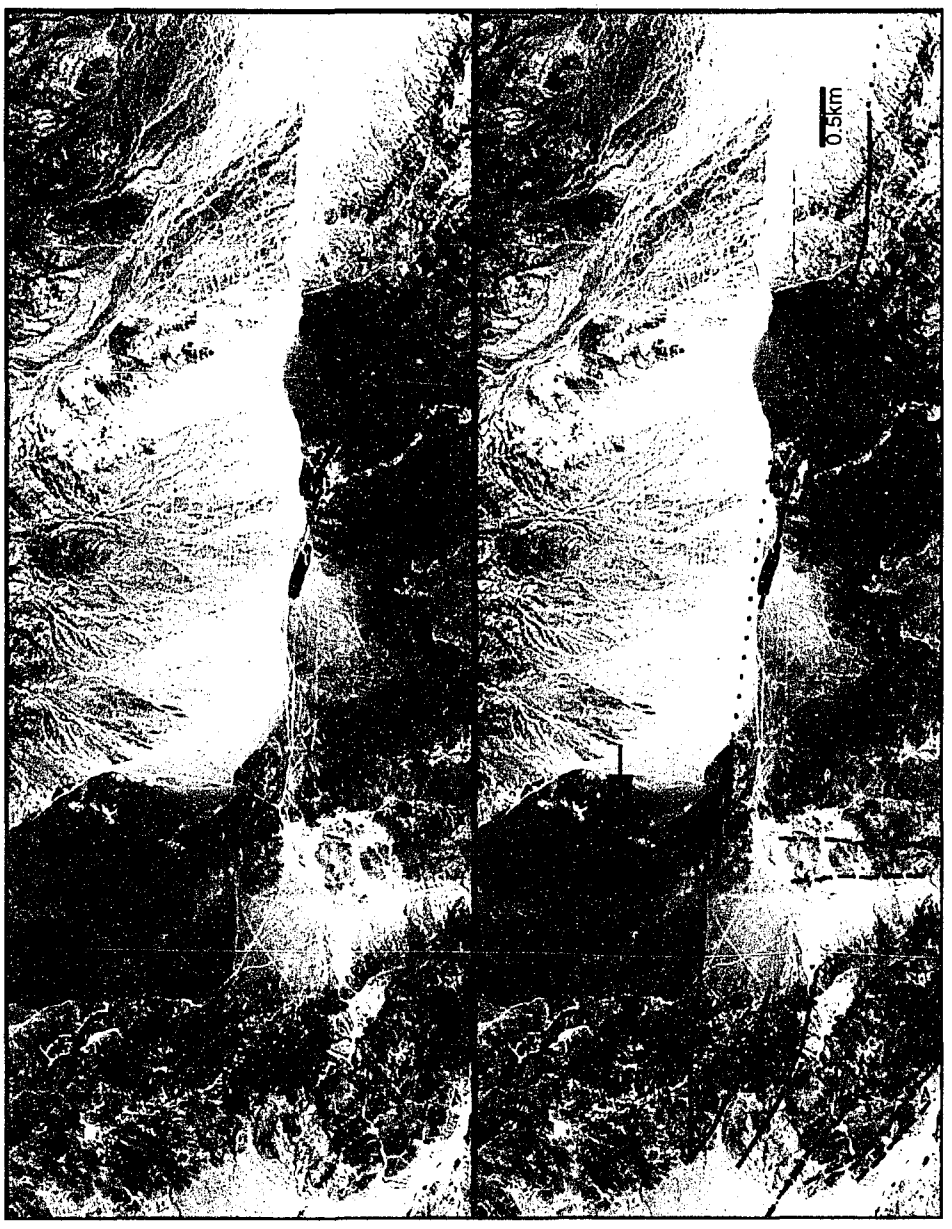

Figure 2.28. Landsat TM-SPOT merged image of the Bicycle Lake fault: Note offset marble and basalt units, separation is ~3.5 km. North is toward page binding. Refer to Plate 1 for location index.

in this study but is nevertheless important because modes of deformation here are thought to have significant impact on the region lying to the west, especially the northeastern Mojave Desert (Dokka and Travis, 1990a). Although tectonic studies in the Avawatz-Mesquite Valley disturbed zone subregion have recognized the major structural elements, the geometry, kinematics and interactions of fault-blocks are still disputed (Hewett, 1954; Troxel, 1970; Davis and Burchfiel, 1973; Spencer, 1981,1990; Brady, 1984; Brady and Verosub, 1984, Butler et al., 1988; Dokka and Travis, 1990a). The rather enigmatic nature of the tectonics in this region is a direct reflection of the complexity of the tectonic environment as well as the fact that late Cenozoic sedimentation in this region has buried important structural relations beneath modern sediments.

Topography of the Mojave Desert has its greatest relief in the Avawatz Mountains-Mesquite Valley disturbed zone subregion (Dokka and Travis, 1990a). The Avawatz Mountains rise up above the desert floor to an elevation of over 1300 meters; the adjacent Mesquite Valley disturbed zone contains areas as low as 300 m. The Avawatz Mountains and vicinity are at the intersection of two of the most prominent structural features in the western U.S., the ~NNW striking Death Valley fault zone (right shear) and the ~E-W striking Garlock Fault (left shear)(Fig. 1.1, Plate 1). Here, the Garlock and Death Valley faults merge and mutually deflect each other (Jahns and Wright, 1960). Right-lateral displacement on the Death Valley fault zone is likely ~20-35 km in the vicinity of the Avawatz Mountains (Brady and Verosub, 1984; Butler et al., 1988). Brady and Verosub (1984) proposed that the Garlock fault flattens southward beneath the Avawatz Mountains and terminates against the Death Valley fault zone as an east-vergent reverse fault which uplifted the range at least 2000 m since the Miocene. The Death Valley fault zone and the Garlock fault are currently active and seismogenic.

The Mesquite Valley disturbed zone (Fig. 2.2)(Dokka and Travis, 1990a) is a complex belt of late Neogene faulting that occurs between Ludlow and Soda Lake. Dokka and Travis (1990a) proposed that the Mesquite Valley disturbed zone had an extensional or transtensional origin based on palinspastic reconstructions, the presence of a shallow Moho, a regional physiographic depression, and the occurrence of east to NE striking normal faults.

Thus, the Avawatz-Mesquite Valley disturbed zone subregion appears to be evolving in response to three tectonic mechanisms: right shear associated with the southern extension of the Death Valley fault zone, left shear in response to differential extension across the Garlock fault, and transtension associated with southeastward translation of the terrane east of the northeastern Mojave Desert region.

Summary

Most faults of the northeastern Mojave Desert region have moved in late Quaternary time with many currently active and seismogenic (Table 2.1). Faults of the northeastern Mojave Desert can be divided into two major groups based on their orientation and sense of slip. As a general rule, major faults are predominantly strike-slip, dextral faults are oriented NW to NNW and sinistral faults are oriented ~E-W. Presently, the most prominent zone of seismicity is a NNW trending belt that extends from Yermo north through the Goldstone area and continuing to near the Garlock fault (Fig. 1.1). This zone is dominated by the Goldstone Lake fault zone. Other active faults include the Coyote Lake, Quinones Creek, and Schnable Canyon faults (Plate 1). Several faults lying to the east of the Goldstone Lake fault zone are also suspected of recent activity based on their youthful geomorphic expression and in some cases spatial association with small earthquakes; these include the West McLean Lake fault, Fort Irwin fault zone, Tiefort Mountain fault, Bicycle Lake fault, Coyote Canyon fault, Garlic Springs fault (Plate 1). The topographic expression of the Desert King Spring

fault zone and nearby East McLean Lake fault have been subdued by erosion, they do not cut active stream deposits, and are historically aseismic (Plate 1). On this basis, both of these faults are considered inactive. Throughout the northeastern Mojave Desert, minor amounts of crustal extension associated with Quaternary strike-slip faulting have led to the development of internally drained inter-range basins (e.g., Goldstone Lake basin, Fort Irwin basin, Leach Lake basin). In contrast, local convergence of fault blocks has led to the development of physiographic highs (e.g., the Avawatz Mountains, the Pink Canyon area, and the unnamed mountain just north of VENUS; Plate 1).

The integrated net left slip inferred to occur between the Garlock and Coyote Canyon faults is <15 km (Table 2.1). Relations presented here suggest that the net right slip across the Goldstone Lake fault zone is ~10 km. This amount of displacement represents a significant portion of the total right-shear, ~57 km, proposed to have occurred across the northeastern Mojave Desert since ~6-10 Ma (Dokka and Travis, 1990a).

CHAPTER 3: PALEOMAGNETISM STUDIES IN THE GOLDSTONE LAKE REGION

INTRODUCTION

This chapter focuses on paleomagnetism studies that were conducted in order to provide critical data regarding vertical-axis crustal rotations in the northeastern Mojave Desert. Paleomagnetic directions or poles from local crustal blocks can be compared to a reference direction or pole in order to determine relative motion between terranes; inclination anomalies indicate latitudinal translations (Hillhouse, 1977), whereas declination anomalies indicate vertical-axis rotations (Kamerling and Luyendyk, 1979; Luyendyk et al., 1985). Longitudinal translations cannot be detected using the paleomagnetic method because geocentric axial dipole nature of the geomagnetic field. In this study, inclination anomalies are small or absent; and, when present, they are thought to represent errors in method (i.e., inadequate sampling of the paleomagnetic field) rather than latitudinal movement. Thus, the focus of this paper is on declination anomalies and inferred vertical-axis crustal rotations; inclination anomalies are used to test the reliability of the data.

Three distinct styles of tectonism have been proposed to have had a profound influence on the geology of the Mojave Desert region since early Miocene time: 1) early Miocene detachment-style extensional tectonics (~24-20 Ma)(Dokka, 1986, 1989ab; Glazner et al., 1989), 2) early Miocene, E-W striking, regional dextral shear (~20-18 Ma)(Ross, 1994; Dokka and Ross, 1995), and 3) the present-day wrench tectonic regime. The Goldstone Lake region lies northeast of major early Miocene extension (Dokka, 1989ab; Martin and Walker, 1992). Thus the following discussion will be restricted to a review of early Miocene regional dextral shear and the late Cenozoic to present Eastern California shear zone.

Northern Extent of Early Miocene Rotations

This report provides constraints on the northern extent of early Miocene (~20 - 18 Ma) regional vertical-axis tectonic rotations in the Mojave Desert. Dokka and Ross (1995) propose an integrative model that relates early Miocene plate interactions to the development of extensional terranes in the Mojave Desert, California and Arizona, to oroclinal folding in the southern Sierra Nevada-central Mojave Desert region and to the San Andreas fault system. Dokka and Ross (1995) presents structural and paleomagnetic evidence for a major ~E-W striking zone of deformation, the Trans Mojave-Sierran shear zone (TMSSZ), which transferred strain from extensional terranes in Arizona to the North American plate margin in southern California. A key element in this model is the interpretation of early Miocene regional rotations determined from paleomagnetic studies (Golombek and Brown, 1988; Ross et al., 1989; Ross, 1994; Valentine et al., 1993; Ross, 1995). Paleomagnetism studies presented in this chapter suggest that the TMSSZ did not rotate rocks in the Goldstone Lake region. Furthermore, because there is no evidence of significant early Miocene ~E-W striking dextral faults or related structures in the Goldstone Lake region, it is likely that all deformation associated with the TMSSZ occurred south of the Goldstone Lake region.

Late Cenozoic Deformation in the Northeastern Mojave Desert

Over the course of the last two decades three classes of models have been proposed to explain the late Cenozoic deformation in the northeastern Mojave Desert. The fundamental differences between these models center on: 1) the causative mechanism of regional deformation 2) the structures thought to facilitate deformation, and 3) the predicted amounts and geographic extent of vertical axis rotation.

Based on generalized fault orientations and displacements, Garfunkel (1974) proposed that uniform stresses acting over the entire Mojave Desert region resulted in a homogeneous, E-W trending, simple sinistral shear system linked to extension in the

Basin and Range province (Fig. 3.1a). Areas where the faults are predominantly E-W striking, as Garfunkel (1974) envisaged for the northeastern Mojave Desert, would not have been subject to tectonic rotation as left slip alone would have accommodated the strain. However, Garfunkel (1974) proposed that the northeastern Mojave Desert had undergone clockwise rotation resulting from a deviation in homogeneous shear expressed in the bending of the Garlock fault (a quantitative estimate of this rotation was not proposed).

Luyendyk et al. (1980), Luyendyk et al. (1985), and Carter et al. (1987) (Fig. 3.1b) proposed that all deformation was linked to dextral shear caused by Pacific-North American plate interactions. These models, based on paleomagnetic data from limited areas outside the northeastern Mojave Desert, predict between ~40° (Carter et al., 1987) and ~80° (Luyendyk et al., 1980; Luyendyk et al, 1985) of clockwise rotation of the northeastern Mojave Desert region.

Dokka and Travis (1990a) and most recently, Dokka (1993) proposed that deformation of the northeastern Mojave Desert was intimately linked to deformation in adjacent parts of the Eastern California Shear zone and caused by dextral shear associated with Pacific-North American plate interactions. In contrast to the previous models, Dokka and Travis (1990a) and Dokka (1993) proposed that deformation of the region was facilitated by a combination of NW striking, right slip faults as well as east striking, left slip faults; this resulted in an overall strain pattern of ~N-S shortening and ~E-W extension. It was reasoned that oblique extension along the Mesquite Valley disturbed zone created new space that has now been partially filled by fault blocks translated from the north and west (Fig. 3.1c). Left slip motions along generally east striking faults such as the Fort Irwin and Bicycle Lake fault zones are thought to be associated with fault blocks that "escaped" eastward toward the extensional Mesquite

Figure 3.1. Models for the late Cenozoic tectonic evolution of the Mojave Desert region. Modified from a) Garfunkel, 1974 b) Carter et al., 1987 c) Dokka, 1990a GF = Garlock fault, GLR = Goldstone Lake region, PMF = Pinto Mountain fault, SAF = San Andreas fault. Area within thick outline is the northeastern Mojave Desert region. Scale is approximate.

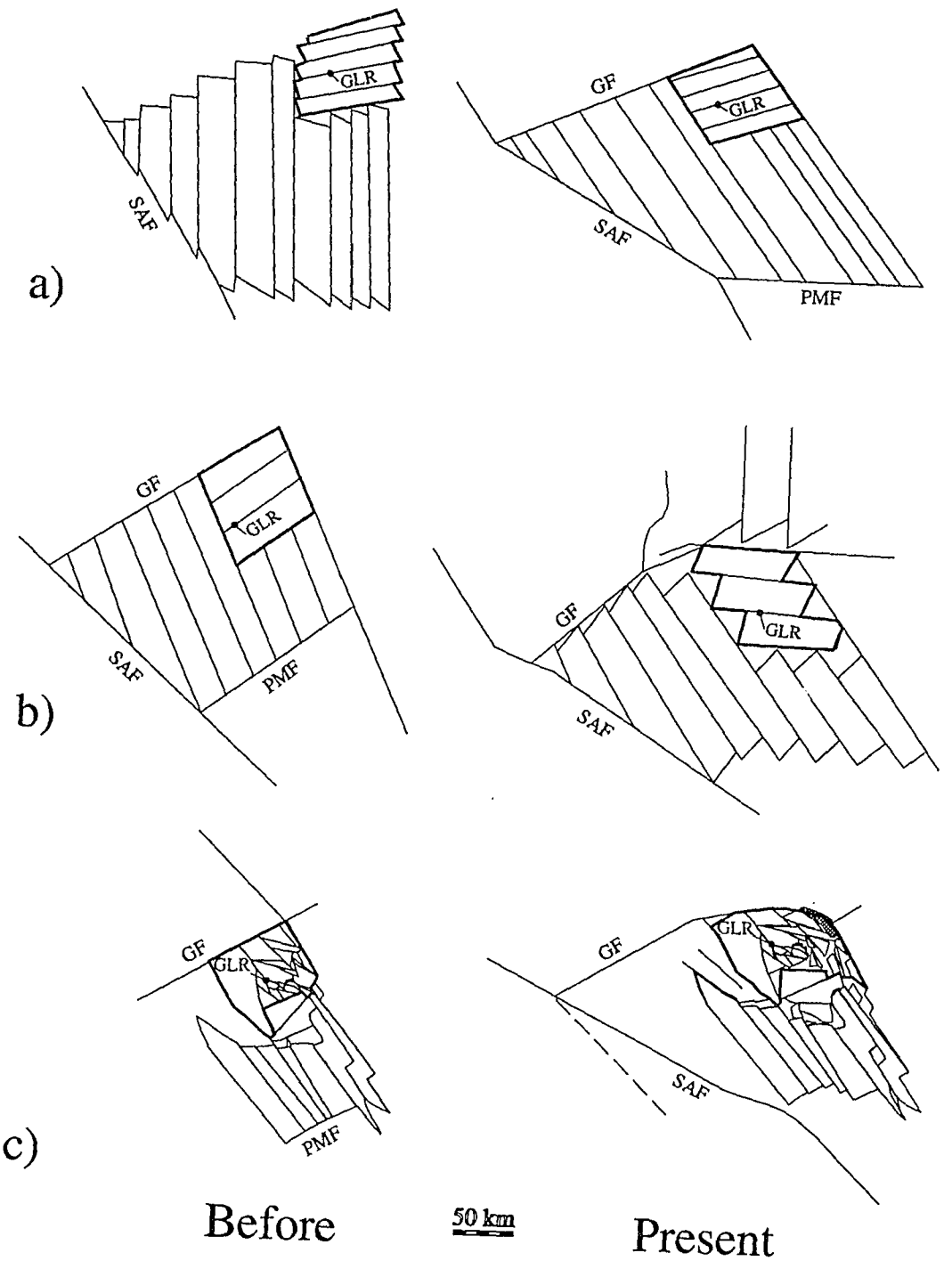
a)
GLR
SAF
GF
GLR
SAF
PMF
b)
GF
GLR
SAF
PMF
GF
GLR
SAF
c)
GF
GLR
PMF
GF
GLR
SAF
Before
50 km
Present

Valley disturbed zone (Fig. 3.1c). Both of these later models predicted that the northeastern Mojave Desert has not been affected by significant regional vertical-axis rotation. The Dokka and Travis (1990a) model predicted that only those fault blocks south of the Fort Irwin fault zone and east of the Goldstone Lake fault (Fig. 3.1c) would show local vertical-axis rotation (0°-40° clockwise).

Geologic Setting of the Goldstone Lake Region

The general geology and stratigraphy of the study area are described in Chapter 2. To review, rocks of the area include Mesozoic plutonic and metamorphic basement (Miller and Sutter, 1982), Tertiary volcanic rocks and epiclastic strata, and basin-filling Quaternary fanglomerate, lacustrine and alluvial sediments. $^{40}Ar/^{39}Ar$ age-spectrum dating of Tertiary strata yielded an age of 18.4 ± 0.2 Ma (whole rock, stepwise) on a formation capping basalt and an age of 22.3 ± 1.5 Ma (hornblende, total fusion) taken from underlying rhyolite air-fall pumice deposits (A.K. Baksi, as reported in MacConnell et al., 1994).

Two major faults occur in the study area, the NW striking, right slip Goldstone Lake fault zone and the ~E-W striking, left slip Coyote Canyon fault (Plate 2); both faults cut unconsolidated Quaternary alluvium and have a component of dip-slip movement. Faults show little variation in strike through topographically irregular terrane, and have subvertical dips where exposed; thus, these faults have near vertical attitudes at least in the shallow subsurface. The sense of slip on both of these faults is inferred from kinematic indicators such as slickenside striations, oriented mineral growths, and lithologic offsets, as well as offsets of abandoned alluvial fans and drainage systems (more detailed descriptions of these and other faults of the northeastern Mojave Desert are presented in Chapter 2). These faults intersect immediately southwest of the Pink Canyon area, and dissect the terrain into three major fault blocks: the Pink Canyon block, the Central Mesa block, and the Coyote Hills-Corral Hills block (Plate 2). The

rocks of the Pink Canyon block are folded into a broad, gently NNE plunging antiform, as reflected in the physiography of the area (Plate 2). The rocks in the Central Mesa block are very gently folded and dip at low angles to the north and west (Plate 2). The Coyote Hills-Corral Hills block is cut by a minor splay of the Goldstone Lake fault (east branch) into two ranges and have been sampled and analyzed separately. The Coyote Hills-Corral Hills block is tilted homoclinally to the northwest on both sides of the splay with some folding in the Corral Hills. The strike of the Goldstone Lake fault (east branch) is apparently unaffected at its juncture with the Coyote Canyon fault. In contrast, the Coyote Canyon fault is apparently folded about a subvertical axis, curving toward the north, near the Goldstone Lake fault (east branch); the change in strike is ~25°.

PALEOMAGNETISM STUDIES

Sample Collection

Oriented samples for paleomagnetic analysis were collected in the field using a portable drill fitted with a 1" coring bit, or oriented blocks sampled by hand and cored in the laboratory with a drill press. All orientations were made with a magnetic compass and clinometer. Site localities were chosen where the structure and stratigraphy were well known from detailed geological mapping performed by the author. Samples were collected from 30 sites (Plate 3): eleven from the Central Mesa block, eight from the Pink Canyon block, six from the Corral Hills and five from the Coyote Hills. Samples were taken from basalt and rhyolite flows, a rhyolite dike, a basaltic pyroclastic fall deposit and volcaniclastic rocks. Table 3.1 gives the paleomagnetic data and pertinent statistics.

Lab Analysis

Natural remanent magnetization (NRM) directions were measured at Louisiana State University for all specimens using a CTF three-axis super-conducting cryogenic

Table 3.1. Site Mean Paleomagnetic Directions of the Characteristic Magnetization

Map Index	Site Name	Rock Type	UTM (easting-northing)	N/N_0	Bedding (S/D)	In Situ (D/I) deg	Fold Corrected (D/I) deg	Plunge Corrected # (D/I) deg	a_{95}	k
					Pink Canyon					
PC1	PCR1	rhyolite	518410-3909780	14/15	274/15	029.6/67.5	020.1/53.4	000.5/52.7	3.4	139.4
PC2	PCS1	sandstone	518560-3909970	19/19	289/13	016.1/50.1	016.7/37.1	351.8/37.1	2.4	191.7
PC3	PCR2	rhyolite	518560-3910150	21/21	219/22	024.2/42.2	008.2/33.5	346.0/33.5	4.4	53.6
PC4	PCS3	sandstone	517830-3910830	5/5	257/23	036.4/61.3	017.0/43.3	353.9/43.3	4.3	315.0
PC5	PCS2	air-fall tuff	517780-3910950	8/10	237/33	031.7/58.0	003.3/36.0	342.0/36.0	6.5	72.5
PC6	PCB3	basalt	519300-3910270	8/8	329/24	358.9/70.0	030.8/52.7	004.0/52.7	5.0	125.9
PC7	PCB2	basalt	519370-3910320	8/8	329/24	010.1/65.9	032.5/46.4	005.7/46.4	2.9	366.2
PC8	PCB1	basalt	519370-3910430	4/4	329/24	332.0/70.5	019.1/58.7	352.4/58.7	6.1	228.6
					Central Mesa					
CM1*	EV1	conglomerate	513710-3907150	6/6	194/16	N/A	N/A	N/A	120.8	1.3
CM2	BU1-6	basalt	515300-3908400	18/18	218/03	009.1/61.8	004.5/60.2	N/A	2.2	240.9
CM3	BU7-8	basalt	515200-3908400	6/6	218/03	356.1/58.8	352.7/56.7	N/A	4.6	209.7
CM4	CC1-2	basalt	514000-3908000	6/6	183/03	005.6/63.3	359.6/63.3	N/A	3.5	360.7
CM5	CC4	basalt	514000-3908000	3/3	183/03	354.9/58.6	350.1/58.0	N/A	4.3	812.1
CM6	CC5	basalt	514000-3908000	3/3	183/03	348.1/55.8	344.0/54.9	N/A	4.0	933.7
CM7	CC6	basalt	514000-3908000	3/3	183/03	358.8/51.9	355.0/51.6	N/A	4.4	800.6
CM8	SM1	basalt	513800-3907150	8/9	194/16	020.0/51.5	000.1/50.4	N/A	3.6	240.3
CM9	SM2	sandstone	513800-3907150	8/9	194/16	021.9/51.5	001.5/48.5	N/A	3.1	315.3
CM10	SM3	sandstone	513800-3907150	6/6	194/16	009.0/47.3	353.0/43.6	N/A	4.8	192.5
CM11	SM4	basalt	513800-3907150	8/8	194/16	007.6/47.4	351.7/43.4	N/A	1.7	1038.4
					Corral Hills					
CR1	ADH1	sandstone	524620-3900070	4/5	237/18	003.8/59.3	352.0/43.7	N/A	19.4	23.3
CR2	ADH4	basalt	524620-3900230	9/9	237/18	344.3/73.0	335.8/55.5	N/A	3.0	288.8
CR3	TW1	sandstone	526300-3901400	10/10	237/18	060.3/75.0	009.3/67.4	N/A	2.8	294.4
CR4	TW2	sandstone	526300-3901400	7/7	237/18	017.9/60.6	001.0/47.1	N/A	5.0	146.1
CR5	TW3	basalt	526300-3901400	11/11	237/18	053.0/74.3	007.5/65.5	N/A	2.6	320.5
CR6	TW4	basalt	526300-3901400	7/9	237/18	042.2/64.9	014.0/55.8	N/A	3.7	271.1
					Coyote Hills					
CH1	CH1	sandstone	527780-3904870	6/6	206/27	02.7/35.4	349.7/21.7	N/A	12.0	32.2
CH2	CH2	sandstone	527780-3904870	12/12	206/27	18.9/37.2	001.4/29.5	N/A	12.0	950.9
CH3	CH3	basalt	527780-3904870	4/4	206/27	23.8/38.3	004.5/32.6	N/A	11.2	67.8
CH4	CH4	basalt	527770-3904900	4/4	206/27	29.2/33.8	011.7/31.1	N/A	11.8	61.9
CH5	CH7	basalt	524700-3904850	7/7	224/07	08.6/51.6	002.2/47.2	N/A	10.2	36.0

corrected for tilt on fold limbs, plunge of fold axis (D/I = 24/15) and local vertical-axis folding as per MacConnell et al., 1994;
* Conglomerate test site, R=2.11, not used in determination of mean direction.

magnetometer. Alternating field (AF) and thermal demagnetization analyses on a few pilot specimens showed similar results. Thermal demagnetization was conducted by heating specimens in a three-zone furnace powered by Lindberg components and protected from the earth's magnetic field by three mu-metal shields. Samples were AF treated using a tuned solenoid driven by a Behlman AC power supply. The rest of the specimens were analyzed using standard partial thermal demagnetization techniques. All specimens were demagnetized in nine or more steps. Orthogonal vector endpoint diagrams (e.g., Zijderveld, 1967) were constructed for each specimen to evaluate the magnetic components present and to define the characteristic remanent magnetization (ChRM). Many samples showed one or more low unblocking temperature component(s). A higher unblocking temperature component which showed nearly univectorial decay toward the origin of the diagrams was selected as representative of the ChRM direction. Representative orthogonal vector endpoint diagrams are shown in Figure 3.2.

With the exception of one site, PCB1 (Fig.3.2), all site directions exhibit normal polarity. Most samples were strongly demagnetized by ~580°C suggesting that the ChRM component primarily resides in magnetite; however, almost all specimens had a small high unblocking temperature component that remained after heating to this level. This remaining component is generally in the ChRM direction as can be seen by the inspection of orthogonal vector endpoint diagrams (Fig. 3.2) and indicates the presence of a minor early acquired magnetization residing in hematite. The ChRM is taken to be the primary magnetization. In the case of the igneous rocks, the ChRM is most likely a thermal remanent magnetization (TRM) acquired when the rocks cooled through the unblocking temperature of the magnetic mineral grains. For volcaniclastic rocks, the ChRM likely represents detrital remanent magnetization (DRM) acquired when the sediments were deposited.

Figure 3.2. Orthogonal end-point diagrams showing examples of basalts (BU 4.2, PCB 1.2a), volcaniclastic rocks (PCS 3d, PCS 1.9a), and rhyolites (PCR 2.4a2, PCR 1.7). Solid circles indicate vector end-points projected onto a horizontal plane; open circles indicate vector end-points projected onto a vertical plane.

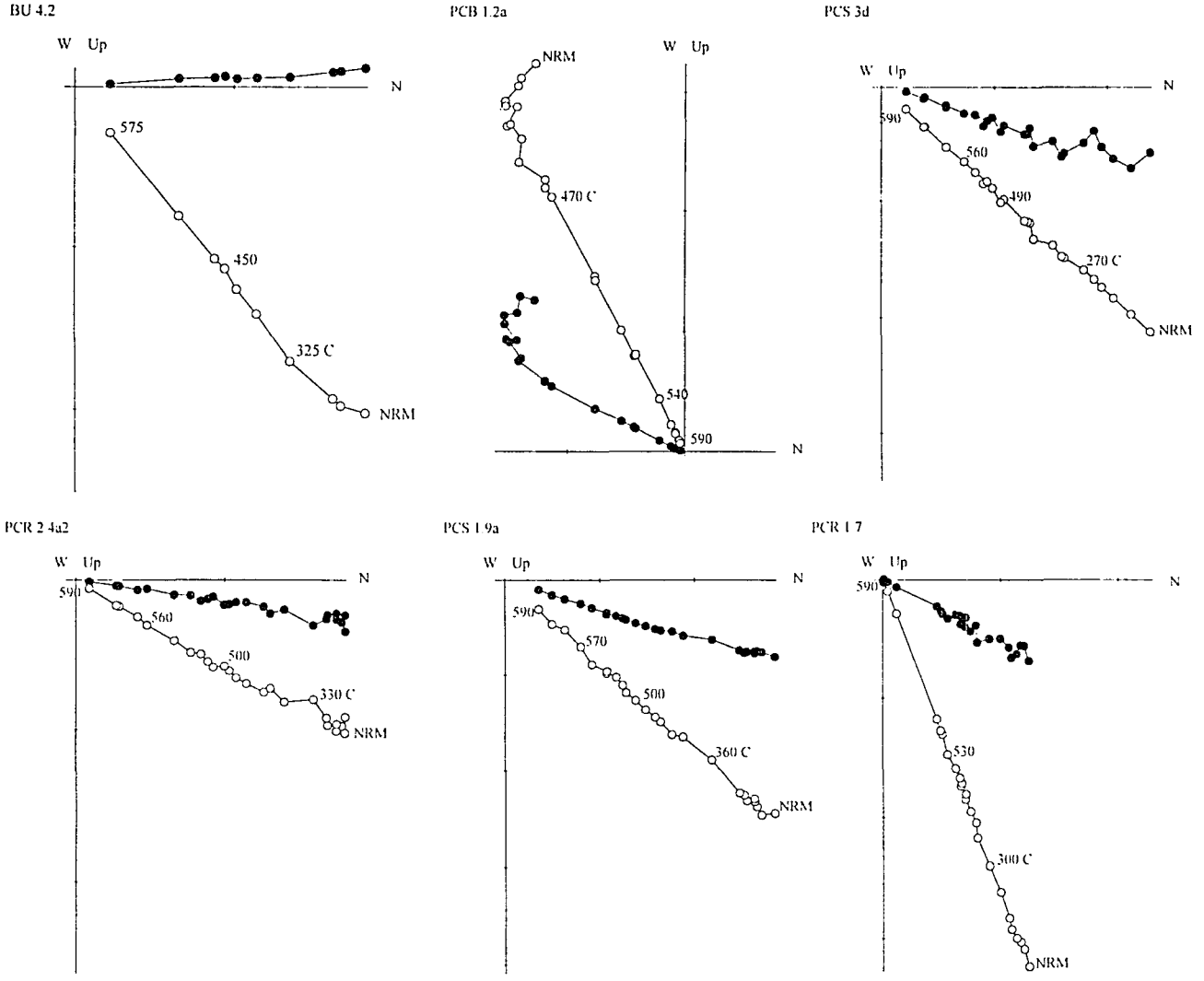
BU 4.2
W Up
N
575
450
325 C
NRM
PCB 1.2a
NRM
W Up
470 C
540
590
N
PCS 3d
W Up
N
590
560
490
270 C
NRM
PCR 2 4a2
W Up
N
590
560
500
330 C
NRM
PCS 1 9a
W Up
N
590
570
500
360 C
NRM
PCR 1 7
W Up
N
590
530
300 C
NRM

Fold Test

Application of the correlation fold test (McFadden, 1990) on all sites from the Pink Canyon block showed no correlation for in situ directions and significant correlation (i.e, decreased dispersion of site-mean directions about the overall mean direction) for structurally corrected directions, indicating passage of the fold test at the 99% confidence level. The optimal test statistic was found at 56% unfolding. The inclinations of site mean directions are statistically indistinguishable from the expected inclination for the site before structural correction (in situ = 61.9° ± 9.3° , vs. 53.5°), but marginally shallower after structural correction (45.3° ± 7.5°). This may be the result of a small component of primary dip. Unaccounted for primary dips on these units may also explain the unexpected prediction by the optimal test statistic of synfolding remagnetization. Synfolding remagnetization is unlikely given the lack of evidence for deep burial or hot fluid migration through these rocks. Moreover, the strike of bedding is such that the mean declination for the Pink Canyon area is not significantly affected by the structural correction (before correction D = 18.1°; after correction D = 18.8°).

Conglomerate Test

At site EV1 (map index=CM1) six individual pumice clasts were sampled from an outcrop of massive "tuff breccia" and were analyzed using partial thermal demagnetization techniques. The Watson (1956) test for randomness of directions was applied to the resulting specimen mean data. The EV1 samples passed the test for randomness at the 95% confidence level. This suggests that these pumice clasts were deposited as a matrix-supported volcaniclastic conglomerate (possibly of laharic origin) and that this unit has not been strongly remagnetized since deposition. This conclusion is corroborated by the small scale, basin filling, onlap geometry of the deposit. The interpretation that EV1 has not been remagnetized implies that none of the sites have

been substantially remagnetized by a regional chemical/thermal event, and that the ChRM directions of all sites have likely remained stable since deposition.

Directional Independence Tests

Directional independence tests were performed on basalt-flow sites, BU1-8 and CC1-6, from the Central Mesa block to define "cooling units" as described by Calderone et al. (1990). The mean direction for each site/flow was compared to the stratigraphically adjacent site/flow using the statistical test derived by McFadden and Lowes (1981) for two populations having unequal precision parameters. Six distinct "cooling units" were identified at the 99% confidence level. Thus, 14 individual sites were sampled, but were then reduced to six distinct "cooling units" referred to as BU1-6, BU7-8, CC1-2, CC4, CC5, and CC6 (see Table 3.1 for map indices). This method should result in a mean direction (and associated statistical parameters) that more closely approximates an independent sampling of the paleofield (Calderone et al., 1990).

Tectonic Corrections

Tectonic corrections were applied to all sites assuming an original horizontality of bedded units. This assumption is supported by the wide-spread distribution and lateral continuity of small-scale "flood" type basalts as well as the parallel-bedded nature and lateral continuity of volcaniclastic and pyroclastic rocks. After bedding and fold corrections were applied to the Pink Canyon sites a declination anomaly of 28.4° ± 9.0° clockwise was present (Fig 3.3). The magnitude and sense of this anomaly is similar to the measured angle of deflection (~25° clockwise) of the westernmost segment of the Coyote Canyon fault near its juncture with the Goldstone Lake fault (east branch) (Plate 3). It is proposed that both the clockwise tectonic rotation of the rocks in the Pink Canyon block and the northward folding of the western segment of the Coyote Canyon fault are the result of localized fault drag along the right slip Goldstone Lake fault (east branch). In accordance with this model, an additional structural correction of 25°

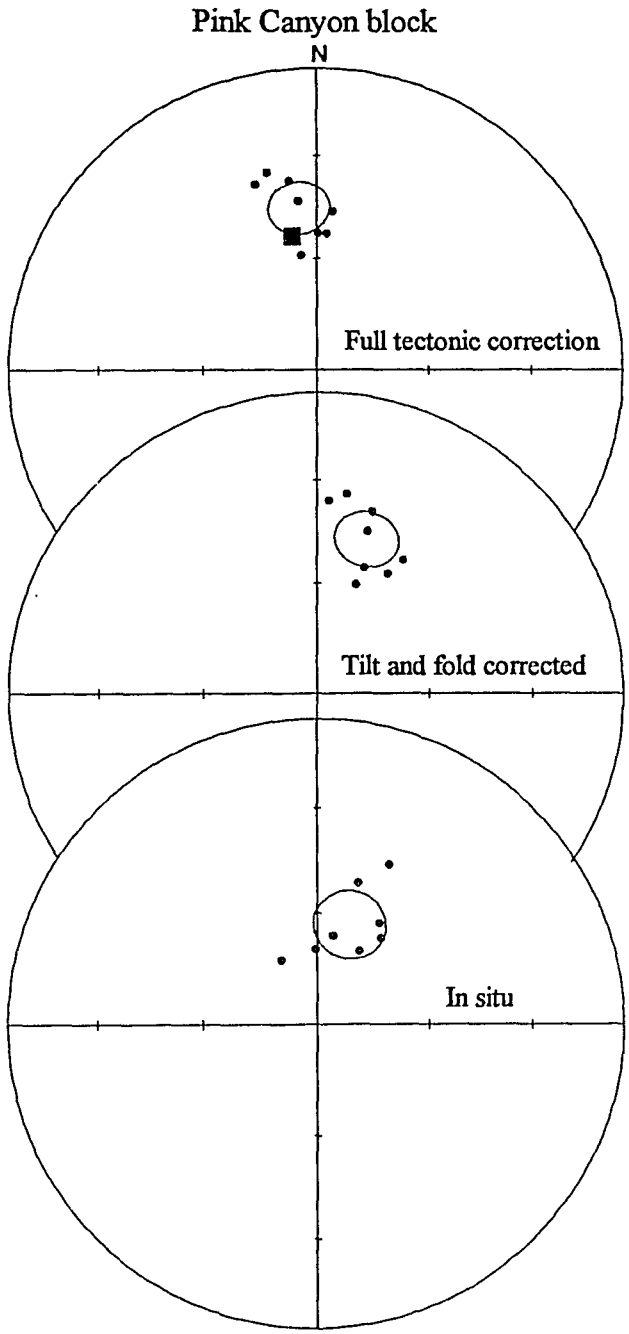

Figure 3.3. Equal-area projections showing in situ, tilt and fold corrected, and local vertical-axis fold corrected paleomagnetic directions from the Pink Canyon block. Directions shown as solid circles, 95% confidence limits of mean directions shown as open circles, and Miocene reference direction (recalculated from Diehl et al., 1988) shown as solid square.

clockwise has been applied to the sites in the Pink Canyon block eliminating the effects of this local vertical-axis rotation (Fig. 3.3).

Results

In situ and structurally corrected paleomagnetic directions for all fault blocks are compared to the expected direction for stable Miocene North America (recalculated from Diehl et al., 1988) in Figure 3.4. Mean directions were determined independently for the sites of the Pink Canyon, the Central Mesa, the Corral Hills, and the Coyote Hills fault blocks. After structural correction, the means show a Declination / Inclination of 353.8° / 45.3° (a_{95} = 7.5°) (Fig. 3.3), 355.0° / 53.2° (a_{95} = 4.5°) (Fig. 3.5), 358.8° / 56.5° (a_{95} = 10.2) (Fig. 3.6) and 1.7° / 32.6° (a_{95} = 11.0) (Fig. 3.7) for the Pink Canyon, Central Mesa, Corral Hills, and Coyote Hills blocks, respectively, using the statistical methods of Fisher (1953). Rotation and flattening statistics of Demarest (1983) yield a rotation, R = 3.4° ± 9.0° and a flattening, F = 8.2° ± 6.5° for the Pink Canyon area, R = 4.6° ± 6.6°, F = 0.3° ± 4.3° for the Central Mesa area, R = 8.4° ± 15.2°, F = -3.0° ± 8.5° for the Corral Hills sub-block, and R = 11.3° ± 10.8° , F = 20.9° ± 9.1° for the Coyote Hills sub-block (see Table 3.2). As there are no flow or "cooling" units that can be uniquely correlated across the faults, the rotation and flattening statistics are given with respect to the Miocene reference field rather than between the fault blocks. The inclinations of the paleomagnetic directions for the Central Mesa block and the Corral Hills sub-block are statistically indistinguishable from the Miocene reference direction. The somewhat anomalous inclination in the Pink Canyon mean direction (F = 8.2° ± 6.5°) is interpreted to be due to unaccounted primary dips of volcaniclastic rocks and rhyolite flows (see above discussion on tectonic corrections). The inclination anomaly present in the Coyote Hills sub-block is more enigmatic (F = 20.9° ± 9.1°). Most sites in the Coyote Hills area exhibited anomalously low inclinations prior to structural correction. All structural corrections imposed on these

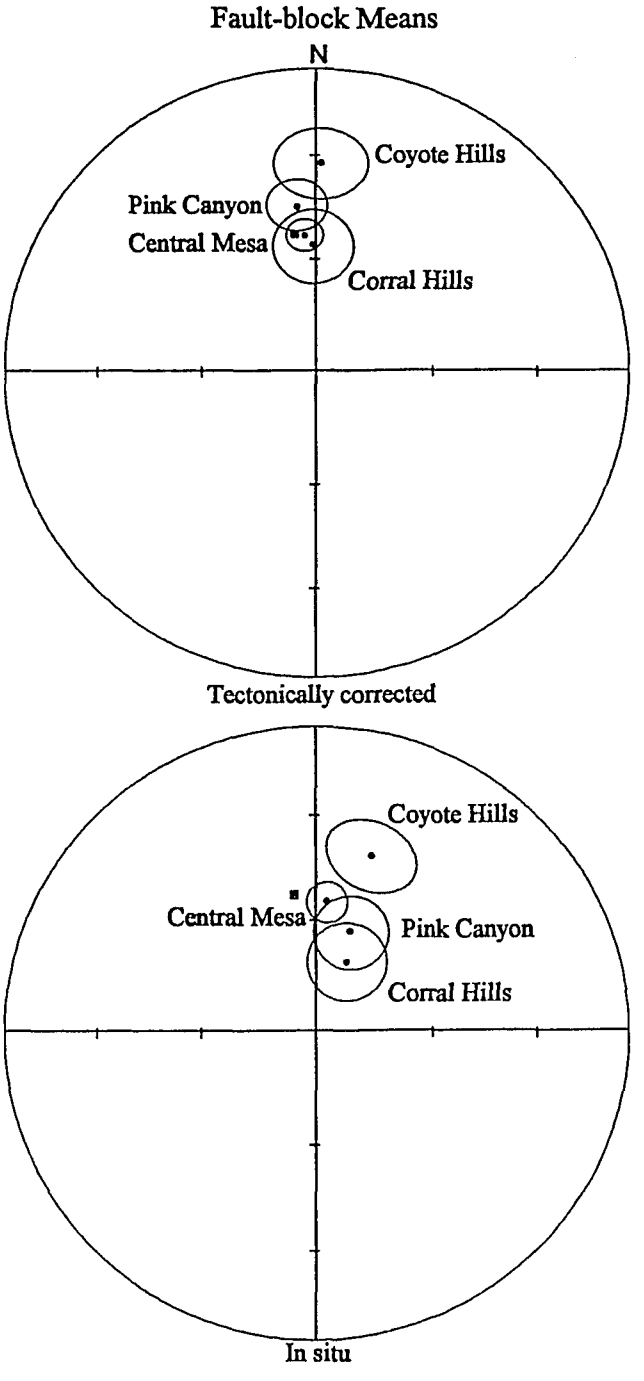

Figure 3.4. Equal-area projections showing in situ and tectonically corrected fault-block mean paleomagnetic directions from the Goldstone Lake region. Mean directions shown as solid circles, 95% confidence limits shown as open circles, and Miocene reference direction (recalculated from Diehl et al., 1988) shown as solid square.

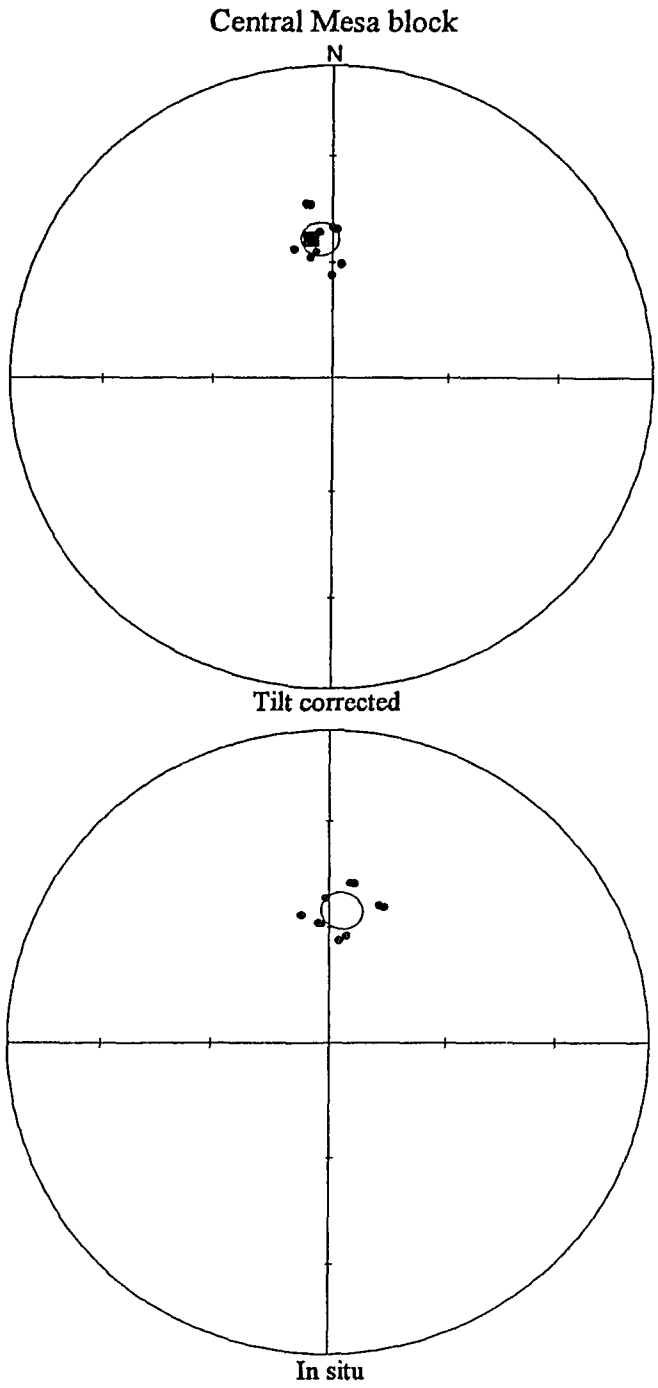

Figure 3.5. Equal-area projections showing in situ and structurally corrected paleomagnetic directions from the Central Mesa block. Directions shown as solid circles, 95% confidence limits of mean directions shown as open circles, and Miocene reference direction (recalculated from Diehl et al., 1988) shown as solid square.

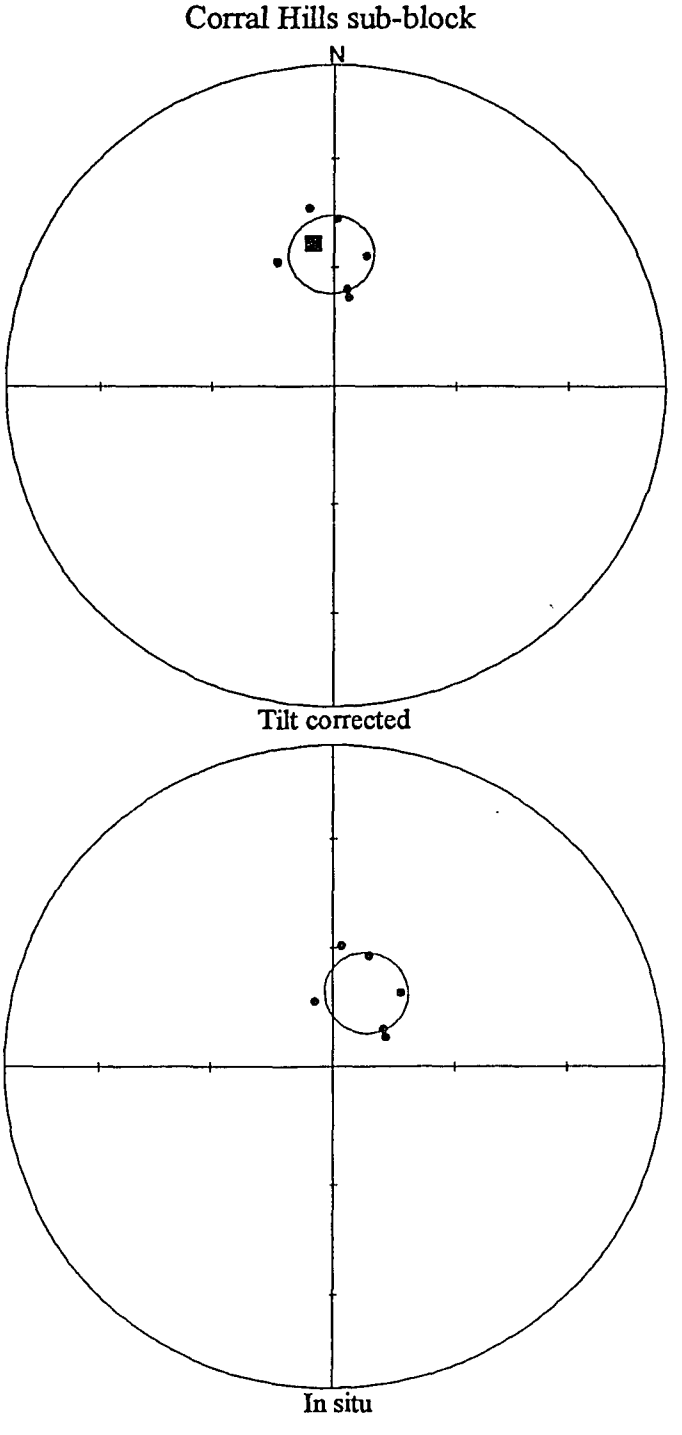

Figure 3.6. Equal-area projections showing in situ and structurally corrected paleomagnetic directions from the Corral Hills sub-block. Directions shown as solid circles, 95% confidence limits of mean directions shown as open circles, and Miocene reference direction (recalculated from Diehl et al., 1988) shown as solid square.

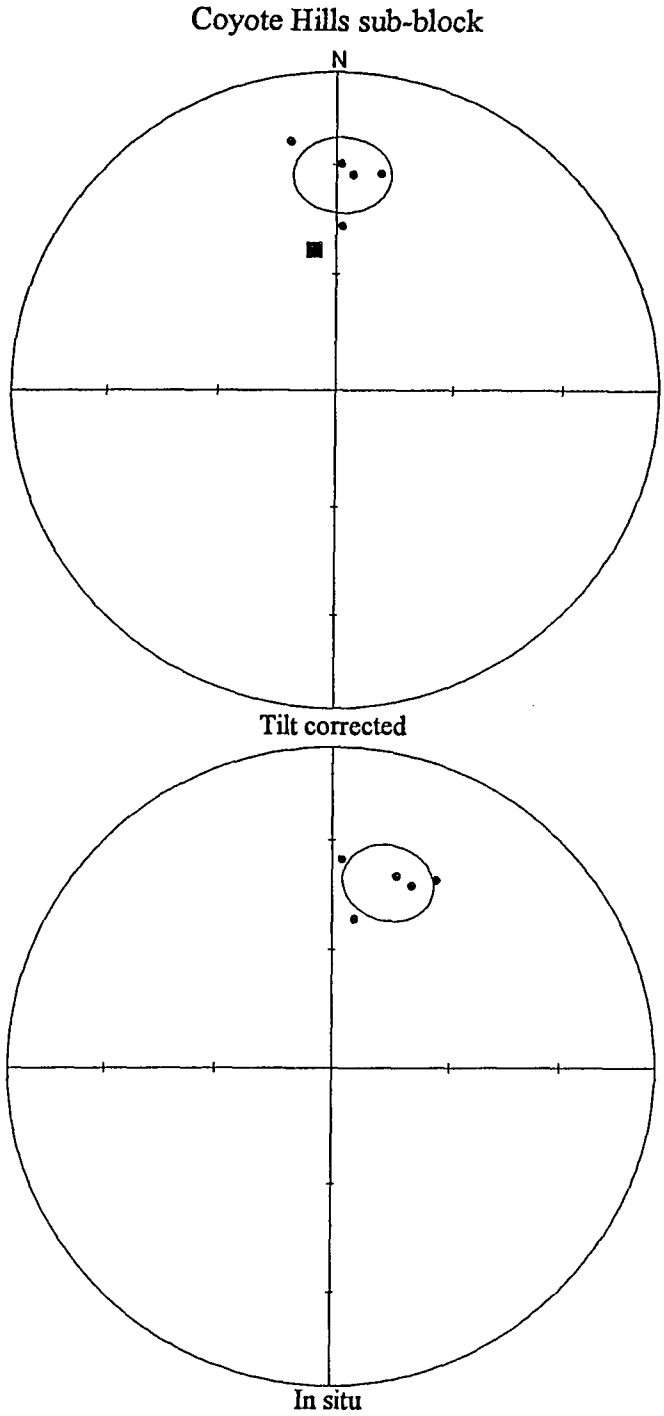

Figure 3.7. Equal-area projections showing in situ and structurally corrected paleomagnetic directions from the Coyote Hills sub-block. Directions shown as solid circles, 95% confidence limits of mean directions shown as open circles, and Miocene reference direction (recalculated from Diehl et al., 1988) shown as solid square.

Table 3.2. Local Mean Paleomagnetic Directions of the Characteristic Magnetization

Means	n	In Situ	$a_{95(In\ Situ)}$	k(In Situ)	Corrected	$a_{95(corrected)}$	k(corrected)	R^	F^
Pink Canyon	8	18.1/61.9	9.3	36.1	353.8/45.3	7.5	55.1	3.4 ± 9.0	8.2 ± 6.5
Central Mesa	10	05.6/55.2	5.1	91.5	355.0/53.2	4.5	115.9	4.6 ± 6.6	0.3 ± 4.3
Corral Hills	6	24.0/69.7	10.2	44.1	358.8/56.5	10.2	44.1	8.4 ± 15.2	-3.0 ± 8.5
Coyote Hills	5	17.0/39.7	10.5	53.7	001.7/32.6	11.0	49.3	11.3 ± 10.8	20.9 ± 9.1
Goldstone Lake Region	29	6.5/53.3	5.3	26.7	356.8/48.3	4.3	39.4	6.4 ± 5.9	5.2 ± 4.2

^ R and F calculated as per Demarest (1983); reference direction calculated from the Miocene reference pole of Diehl et al. (1988) (pole lat = 82.0N, long = 146.9E, A-95 = 2.9).

rocks had the effect of decreasing the resulting vector inclination. It is geologically untenable to visage primary dips on these strata that were larger than those existing today, nor can the present dips be ignored in the calculation of paleomagnetic directions. This being the case, a simple tectonic correction was made, untilting the in situ directions perpendicular to the strike of bedding. The most plausible explanation for the anomalously low inclinations from the Coyote Hills sub-block is that secular variation has not been averaged adequately by the five sites. The fault-block mean directions for the Pink Canyon block, Central Mesa block, and the Corral Hills sub-block show declinations that are indistinguishable from the Miocene reference direction. The paleomagnetic declination for the Coyote Hills sub-block is marginally distinguishable from the Miocene reference direction (R = 11.3° ± 10.8°); this anomaly, just as was likely the case for the inclination anomaly associated with this sub-block, may be due to inadequate time-average sampling of the paleomagnetic field.

The above results strongly suggest that none of these fault blocks have been rotated significantly since early Miocene time. If we accept this conclusion, we can group the data from all sites to better define a regional paleomagnetic direction. Figure 3.8 shows all site mean directions, the regional a_{95}, and the Miocene reference direction. The rotation and flattening statistics of Demarest (1983) yield a rotation, R = 6.4 ± 5.9 and a flattening, F = 5.2 ± 4.2 for the Goldstone Lake Region (Table 3.2).

The angular dispersion of site mean directions, the presence of a reversed-polarity site, and the age range of the volcanic sequence suggest that the secular variation of the geomagnetic field has been averaged, or at least partially averaged in this study. Based on this foundation, we feel justified in applying the geocentric axial dipole field hypothesis to our results in the following discussion.

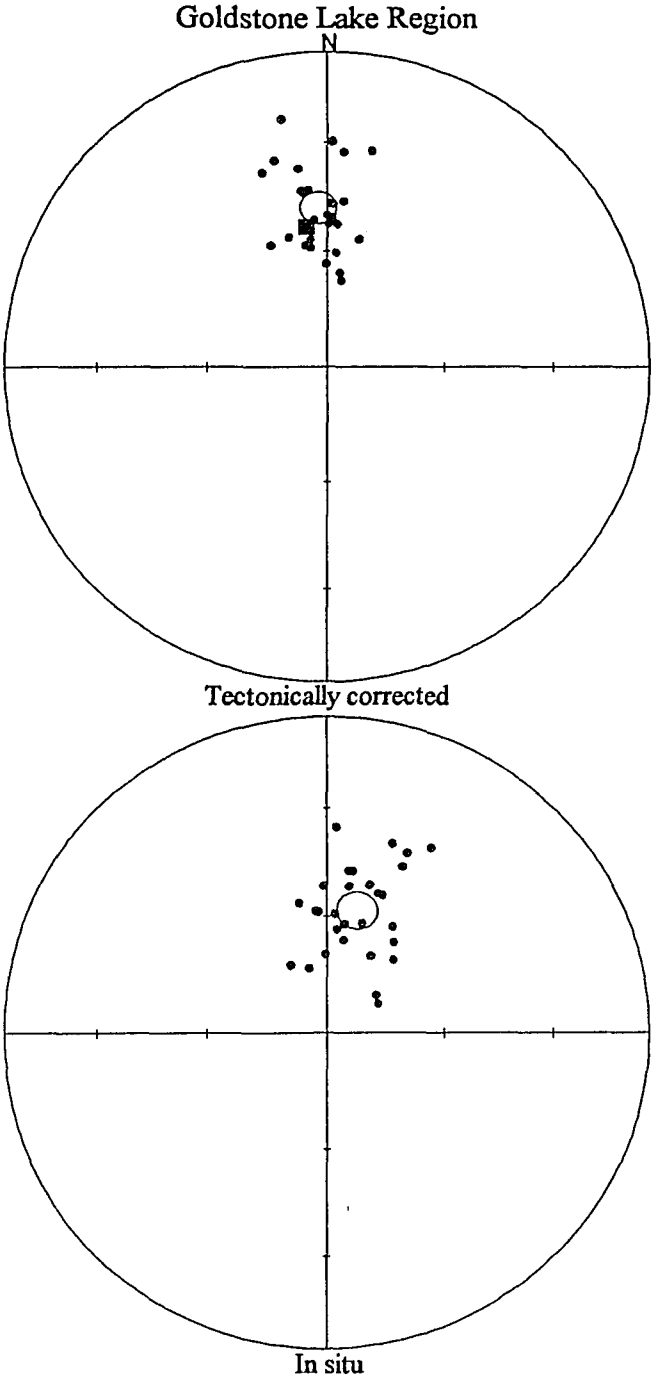

Figure 3.8. Equal-area projections showing in situ and tectonically corrected paleomagnetic directions from the Goldstone Lake region. Directions shown as solid circles, 95% confidence limits of mean directions shown as open circles, and Miocene reference direction (recalculated from Diehl et al., 1988) shown as solid square.

CONCLUSIONS

The major conclusion of this study is that there has been little to no regional vertical-axis rotation of the Goldstone Lake region since ~22 Ma. This result constrains the northern limit of the region of extensive early Miocene vertical-axis rotations that formed as a consequence of right shear along the Trans Mojave-Sierran shear zone TMSSZ (Dokka and Ross, 1995). Furthermore, given that there is no evidence in the study area for 20-18 Ma faults which would accommodate E-W trending dextral shear it appears likely that all deformation associated with the TMSSZ occurred south of the Goldstone Lake region.

The results of this study are consistent with the models of Dokka and Travis (1990a) and Dokka (1993) that predict that post-18 Ma vertical axis rotations in the northeastern Mojave Desert are local rather than regional in extent and associated with strike-slip faulting. The data do not support the models of Garfunkel (1974), Luyendyk et al. (1980, 1985), and Carter et al. (1987) that predict regional homogeneous vertical-axis rotations in the northeastern Mojave Desert.

A third outcome of this study is the demonstration that local vertical-axis rotations can develop along the margins of fault blocks and can be measured using paleomagnetic techniques as was the case in this study at the juncture of the Coyote Canyon fault and the Goldstone Lake fault (east branch) in the Pink Canyon block. Thus, a potential pitfall in the use of the paleomagnetic method for studies of tectonic rotations is that local rotations can be misinterpreted as being regional in nature. This pitfall can be avoided if the local geologic context from which the samples are taken is well understood, and if the sampling program covers a geographic region large enough to distinguish local declination anomalies (caused by fault block margin effects, or small-scale block rotations) from the regional mean paleomagnetic direction.

CHAPTER 4: ACTIVE TECTONICS OF THE NORTHEASTERN MOJAVE DESERT

OVERVIEW

This study of active tectonics was designed to investigate several aspects of late Cenozoic tectonics in the northeastern Mojave Desert . The major questions to be resolved include: 1) What is the structural architecture of the northeastern Mojave Desert? 2) What is the late Cenozoic tectonic history of the northeastern Mojave Desert region and how does it relate tectonically to the rest of the Mojave Desert Block? 3) Which faults have been active in the Quaternary and what is the likelihood of future activity?

In order to realize this goal, an integrative study was conducted to define the spatial and temporal distribution of Neogene strata as well as the geometry, timing, and kinematics of late Cenozoic faults and associated fault blocks. Field studies, coupled with analyses of earthquake data, satellite imagery, and paleomagnetic data have resulted in an improved understanding of the active tectonics and seismic hazards of the northeastern Mojave Desert region and have provided a means with which to assess regional strain models proposed by previous workers (Garfunkel, 1974; Luyendyk et al., 1980,1985; Carter et al., 1987; Dokka and Travis, 1990; Dokka, 1993; Ross, 1994, Dokka and Ross, 1995).

STRUCTURAL ARCHITECTURE

All major faults of the northeastern Mojave Desert exhibit features characteristic of strike-slip faults: the traces of all major faults are markedly straight; and, the sense of vertical uplift alternates from one side of the fault to the other along strike (e.g., Wilcox, 1973; Crowell, 1974; Cristie-Blick and Biddle, 1985). Focal mechanisms on the Paradise and Quinones Creek faults show horizontal motion consistent with a NNW

striking, right-slip rupture surface and an E-W striking, left-slip rupture surface, respectively (Hafner and Hauksson, 1994). Fault-plane kinematic indicators and map-scale offsets in rock units consistently indicate right slip along NNW striking faults and left slip along E-W striking faults. Thus, major faults are predominantly strike-slip; dextral faults are oriented NW to NNW and sinistral faults are oriented ~E-W (Table 1). Throughout the northeastern Mojave Desert, minor amounts of crustal extension associated with Quaternary strike-slip faulting has led to the development of internally drained inter-range basins such as Goldstone Lake basin, Fort Irwin basin, and Leach Lake basin (Plate 1). In contrast, contraction along faults has created local physiographic highs (e.g., the Avawatz Mountains, the Pink Canyon area, and the unnamed mountain just north of VENUS; Plate 1).

The minimum integrated net left slip determined from major E-W trending faults between the Coyote Canyon fault and the Garlock fault is likely <15 km (Table 1). It is proposed that the net right slip across the Goldstone Lake fault zone is ~10 km. This amount of displacement represents ~18% of the total right-shear, ~57 km, considered to have occurred across the northeastern Mojave Desert since ~6-10 Ma (Dokka and Travis, 1990a).

LATE CENOZOIC TECTONIC HISTORY

Early Miocene Extensional Tectonics

In early Miocene time the central Mojave Desert underwent a profound change in physiography, tectonics, magmatism, and sedimentation patterns as a result of detachment-style extensional tectonics (~24-20 Ma)(Dokka, 1986, 1989ab; Dokka and Woodburne, 1986; Glazner et al., 1989; Walker et al., 1995). This detachment-dominated extensional orogen was a locus of pre-, syn- and post-kinematic volcanic activity from ~24 to 18 Ma (Dokka et al., 1988, 1991; Walker et al., 1995). The northeastern Mojave Desert region lies to the north and east of the Mojave Extensional

Belt (Dokka, 1989) in the unextended "highlands." There are no known occurrences of Tertiary age "deep-rooted" detachment-faults in the study area, nor is there a regular pattern of normal faulting and tilting of Tertiary strata or other evidence that would suggest that the northeastern Mojave Desert was the site of early Miocene detachment-dominated extensional tectonics. The above discussion suggests that the mechanism responsible for early Miocene (~22 - 18 Ma, a probable minimum range, MacConnell et al, 1994) volcanism in the northeastern Mojave Desert was not directly related to detachment-dominated regional extension. Based on regional gravity data, physiography, and the spatial and temporal distribution of rock types, the early to middle Miocene volcanic rocks of the northeastern Mojave Desert likely represent an ancient caldera system (MacConnell, this paper; Sabin et al., 1994).

Northern Extent of Early Miocene Regional Tectonic Rotations

This report provides constraints on the northern extent of early Miocene (~20 - 18 Ma) regional vertical-axis tectonic rotations in the Mojave Desert. Dokka and Ross (1995) propose an integrative model that relates early Miocene plate interactions to the development of extensional terranes in southeastern California and Arizona, to oroclinal folding in the southern Sierra Nevada-central Mojave Desert region and to the San Andreas fault system. Their paper presents structural and paleomagnetic evidence for a major ~E-W striking zone of deformation, the Trans Mojave-Sierran shear zone (TMSSZ), which transferred strain from extensional terranes in Arizona to the North American plate margin in southern California. A key element in this model is the interpretation of early Miocene regional rotations determined from paleomagnetic studies (Ross et al., 1989; Ross, 1994; Ross, 1995). Paleomagnetism studies (Chapter 3; MacConnell et al., 1994) confirm the notion that the northeastern Mojave Desert lay well beyond the zone affected by the TMSSZ in early Miocene time. Furthermore, because there is no evidence of significant early Miocene ~E-W striking dextral faults or related

structures in the Goldstone Lake region, it is likely that all deformation associated with the TMSSZ occurred south of the Goldstone Lake region.

Assessment of Geometric/Kinematic Models of the Late Cenozoic Tectonic Evolution of the Northeastern Mojave Desert

Over the course of the last two decades three classes of models have been proposed to explain the late Cenozoic deformation in the northeastern Mojave Desert. The fundamental differences between these models center on: 1) the causative mechanism of regional deformation 2) the structures thought to facilitate deformation, and 3) the predicted amounts and geographic extent of vertical axis rotation. Based on generalized fault orientations and displacements, Garfunkel (1974) proposed that uniform stresses acting over the entire Mojave Desert region resulted in a homogeneous, E-W trending, simple sinistral shear system linked to extension in the Basin and Range province (Fig. 3.1a). Areas where the faults are predominantly E-W striking, as Garfunkel (1974) envisaged for the northeastern Mojave Desert, would not have been subject to tectonic rotation as left slip alone would have accommodated the strain. However, Garfunkel (1974) proposed that the northeastern Mojave Desert had undergone clockwise rotation resulting from a deviation in homogeneous shear expressed in the bending of the Garlock fault (a quantitative estimate of this rotation was not proposed).

Luyendyk et al. (1980), Luyendyk et al. (1985), and Carter et al. (1987) (Fig. 3.1b) proposed that all deformation was linked to dextral shear caused by Pacific-North American plate interactions. These models, based on paleomagnetic data from limited areas outside the northeastern Mojave Desert, predict between ~40° (Carter et al., 1987) and ~80° (Luyendyk et al., 1980, 1985) clockwise rotation of the northeastern Mojave Desert region.

Dokka and Travis (1990a) and, most recently, Dokka (1993) proposed that deformation of the northeastern Mojave Desert was intimately linked to deformation in

adjacent parts of the Eastern California shear zone and caused by dextral shear associated with Pacific-North American plate interactions. In contrast to the previous models, Dokka and Travis (1990a) and Dokka (1993) proposed that deformation of the region was facilitated by a combination of NW striking, right slip faults as well as east striking, left slip faults; this resulted in an overall strain pattern of ~N-S shortening and ~E-W extension. It was reasoned that oblique extension along the Mesquite Valley disturbed zone created new space that has now been partially filled by fault blocks translated from the north and west (Fig. 3.1c). Left slip motions along generally east striking faults such as the Fort Irwin and Bicycle Lake fault zones are thought to be associated with fault blocks that "escaped" eastward toward the extensional Mesquite Valley disturbed zone (Fig. 3.1c).

Mapping of the late Cenozoic faults of the region (Plate 1) indicates that regional strain has been facilitated by both dextral and sinistral shears and, thus, do not support the models of Garfunkel (1974), Luyendyk et al. (1980, 1985), and Carter et al. (1987). Furthermore, the models of Garfunkel (1974), Luyendyk et al. (1980, 1985), and Carter et al. (1987) assume homogeneous simple shear across the entire northeastern Mojave Desert. Such models do not account for the common occurrence of irregularly shaped basins in the area. These models all require substantial region-wide vertical-axis rotations of major E-W trending fault blocks. The results of paleomagnetic studies presented in this paper and in MacConnell et al. (1994) indicate clearly that rocks in the Goldstone Lake region have not been affected by regionally homogeneous tectonic rotations. Finally, although the above models are too generalized to accurately depict the position or the number of major faults in the northeastern Mojave Desert, analysis of these models shows that they require that all major E-W trending faults have uniform displacements on the order of three to five times larger than observed in this study. Given the above evidence that the models proposed by Garfunkel (1974), Luyendyk et

al. (1980, 1985), and Carter et al. (1987) consistently fail to predict the nature of deformation in the northeastern Mojave Desert, they are categorically dismissed from further consideration.

Recent models genetically linked to Dokka and Travis (1990a) show varying degrees of success in accounting for this new data set. The "highly speculative" model presented in Dokka and Travis (1990a) is conceptually consistent with first order tectonic relations observed in this study in that it correctly predicts the styles of faulting, the local nature of vertical axis rotations (where present), the overall geometry of strain, and the kinematics of most individual faults. However, the Dokka and Travis (1990a) model predicts the presence of faults that do not exist, and does not account for all known faults. The most recent model of Dokka (1993), however, provides a more realistic depiction of the overall strain, as well as the motions and magnitude of displacement on most faults. This model's major failing is that it does not account for several second order details reported here, such as the Quinones Creek and Schnabel Canyon faults, and the crustal extension south of the Coyote Canyon fault, nor does it account for the relatively large amount of offset (~10 km) on the Goldstone Lake fault as proposed in this study.

Westward Shift of Tectonism

Although Dokka and Travis (1990a) documented the timing, magnitude and sense of shear strain in the southern Mojave Desert, they lacked the requisite data to determine how strain was transferred through the northern Mojave Desert and into the fault systems of the Basin and Range (i.e., Death Valley fault zone, Panamint Valley fault zone, Owens Valley fault zone). Dokka and Travis (1990a) proposed that the locus of activity in the ECSZ migrated west from the eastern Mojave in Quaternary time (between 1.5 and 0.7 Ma) and resulted in the formation of new faults in the south-central Mojave. The geodetic analysis of Savage et al. (1990) showed that present-day strain through the

Mojave Desert-southwestern Basin and Range province is concentrated along a NNW trending belt 50-100 km wide. This belt is coincident with the western ECSZ and contains the Goldstone Lake fault zone. Savage et al. (1990) proposed that the main locus of faulting in the southwestern Basin and Range province may also have shifted westward from the Death Valley fault to the Owens Valley fault system in a similar manner to that proposed by Dokka and Travis (1990a) for faults of the southern Mojave desert.

Timing relations of faults in the northeastern Mojave Desert and present-day seismicity patterns are also consistent with this interpretation. All active NW to NNW striking faults in the northeastern Mojave Desert are aligned with the Goldstone Lake fault zone; to the east of this zone only one major NW striking fault has been observed, the Desert King Spring fault (Table 1). The Desert King Spring fault is aseismic and is locally buried under young (Holocene) alluvial deposits. Furthermore, to the east of the Goldstone Lake fault zone seismic events are scarce, and of the few that exist, almost all are associated with E-W striking fault systems.

If tectonism did migrate westward in the northeastern Mojave Desert in a similar fashion to the migration proposed to the south and north (Dokka and Travis, 1990a; Savage et al., 1990), then the age of inception of the Goldstone Lake fault zone would be ~1.5-0.7 Ma. Given that the total right-lateral displacement is ~10 km then the slip rate would be ~1 mm / year. This rate is similar to other well documented faults in the eastern and southern Mojave Desert (Dokka, 1983; Dokka and Travis, 1990a).

ACTIVITY

Although our efforts have not been expressly directed at seismic hazard analysis, the data compiled in this study provide a first order assessment of potential seismic activity. Most major faults of the northeastern Mojave Desert region have been active in late Quaternary time with many faults being currently active and seismogenic (Table 1).

Presently, the most prominent zone of seismicity is a NNW trending belt that extends from Yermo north through the Goldstone area (Fig.1.1). This zone is dominated by the Goldstone Lake fault zone including the Paradise fault. Other seismogenic faults include the Coyote Lake, Quinones Creek, and Schnable Canyon faults (Plate 1). Several faults lying to the east of the Goldstone Lake fault zone are also suspected of recent activity based on their youthful geomorphic expression and in some cases spatial association with small earthquakes; these include the West McLean Lake fault, Fort Irwin fault zone, Tiefort Mountain fault (north and south branches), Bicycle Lake fault, Coyote Canyon fault, and Garlic Springs fault (Plate 1). The topographic expression of the Desert King Spring fault zone and nearby East McLean Lake fault have been subdued by erosion, they do not cut active stream deposits, and are historically aseismic (Plate 1). On this basis, both of these faults are considered inactive.

Data also suggest that the assessment of activity of a particular fault based exclusively on the occurrence of historic earthquakes is problematic given the punctuated history of seismicity on several faults of the area. For example, the Quinones Creek fault of the northern Coyote Lake basin was virtually aseismic prior to the 1992 Landers earthquake. Following this event, many earthquakes have occurred, one being associated with the development of a local ground rupture. Clearly, the historical record of seismicity may be too short to be used to correctly characterize the activity of a fault. Other long, sinistral faults such as the Bicycle Lake, Tiefort Mountain, and Fort Irwin faults are predicted to be active based on their young geomorphic expression and tectonic models yet they show little to no seismicity (Table 1). Given the overall length of these faults and the likelihood of future activity, these faults may pose a greater threat of significant seismicity than previously thought.

Importance of North-Northwest Striking Faults in the Present-day Tectonic Environment

Seismicity patterns, surface ruptures, and focal mechanisms suggest that there may have been a recent change in the mechanically favored direction of faults in the Mojave Desert region. Almost all major dextral faults in the Mojave Desert strike ~NW (Fig 1.1)(Dibblee, 1960; Dokka, 1983). On the basis of fault plane solutions determined on six of the largest (M=5.2 to 7.3) earthquakes to have occurred in the Mojave Desert since 1947, and the orientation of their associated surface ruptures, Nur et al. (1989, 1993) proposed that NW trending faults were no longer oriented in the mechanically preferred direction required by the present-day stress field. Although recent paleomagnetism studies (Ross, 1994; Dokka and Ross, 1995) do not support Nur et al. (1993) as to the causative mechanism of this phenomena, the concept of a change in the preferred orientation of faulting is supported by the evidence presented below.

The earthquakes and surface ruptures that occurred during and after the Landers event, define two prominent NNW trending zones of intense seismicity (Fig. 1.1). The southern zone of seismicity includes the Landers earthquake (M=7.3). This zone of seismicity, and its associated faults, changes orientation to a more westward trend near the zone's northern terminus (Fig. 1.1). Here, the pattern of seismicity and surface ruptures becomes more complex. Two E-W trending zones of seismicity branch off from the main zone and step sharply to the east (Fig. 1.1). The spatial association of the westward change in orientation of the main zone of seismicity and faulting, the right step, and the termination of activity suggests that the change in orientation was mechanically unfavorable with respect to the present-day stress field. This phenomenon is repeated on a smaller scale. The Landers epicenter is located on a NNW trending segment of the Johnson Valley fault (Sieh et al. 1993). During the Landers event, ground ruptures propagated ~NNW along the Johnson Valley fault for ~13 km at which point strike changed direction to ~NW (Fig. 4.1). Near the location of change in strike,

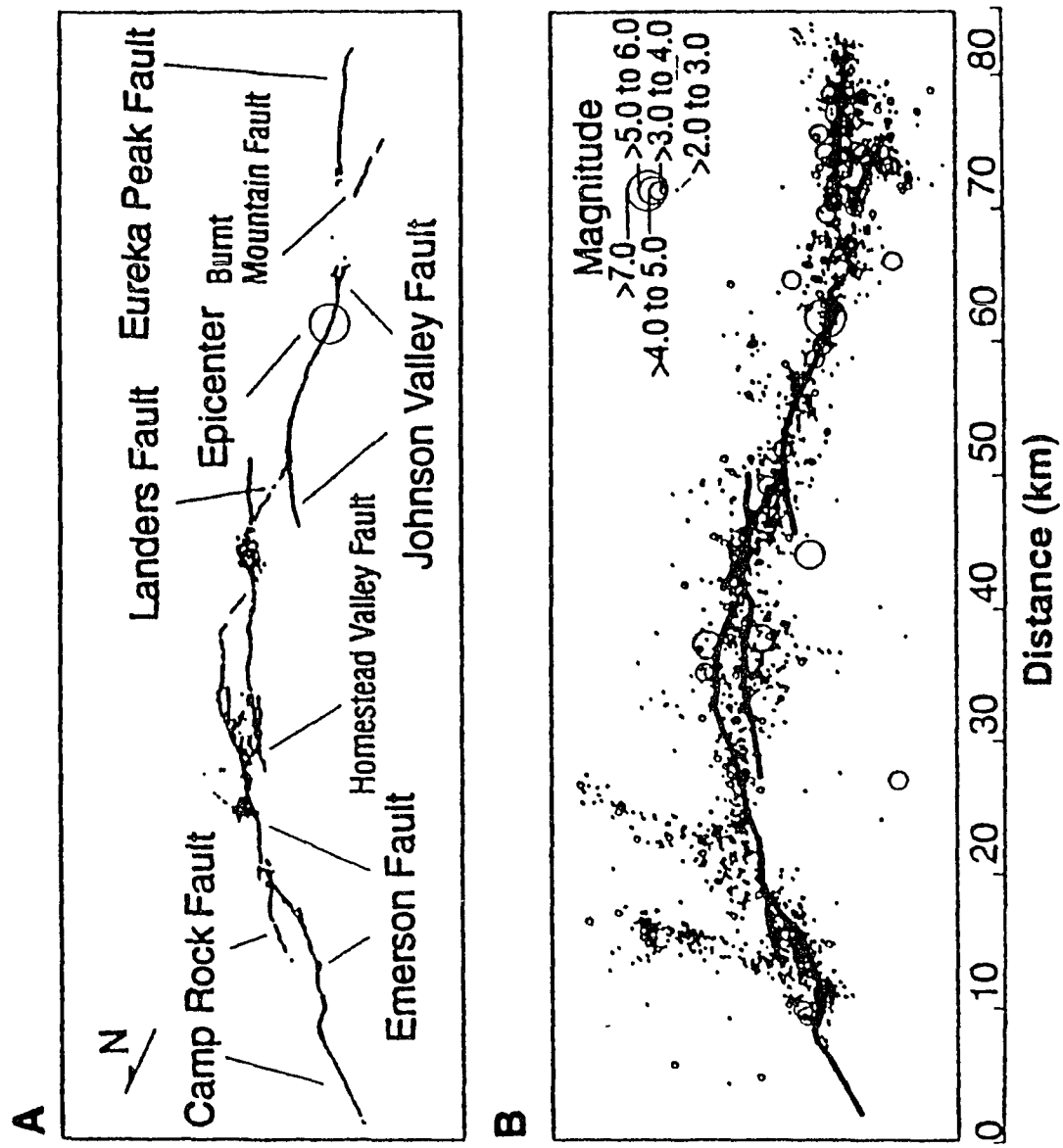

Figure 4.1. Fault ruptures and seismicity associated with the Landers Earthquake, June 28, 1992: a) Map view of surficial fault ruptures of the Landers earthquake; and b) Map view of the seismicity recorded by the Southern California Seismographic Network from June 28, 1992 to August 18, 1992. Modified from Sieh et al., 1993.

a new fault, the "Landers fault", cut across the valley floor striking ~N-S (Sieh et al., 1993). Sieh et al. (1993) noted that few aftershocks occurred along the NW striking surface rupture of the Johnson Valley fault, whereas many occurred along the NNW segment and along the Landers fault. Hauksson et al. (1993) suggested that a likely explanation for the lack of aftershocks at the ends of such faults was due to the change in strike of the rupture. Furthermore, near the intersection of the Landers and Homestead Valley faults, the fault block west of the Landers fault has apparently overridden the Homestead Valley fault along thrust faults (Sieh et al., 1993) as would be predicted at the location of a westward step along a ~N-S striking dextral fault (Crowell, 1974). Thrust faults would not be expected here if the NW trending faults were in the preferred orientation for accommodating dextral slip.

The northern zone of seismicity occurs west and northwest of Yermo (Fig. 1.1). This belt of earthquakes trends ~NNW and is not in close alignment with important NW striking Quaternary faults of the area; rather, it intersects the Calico-Blackwater fault system at an angle of 10°-20° (Hauksson et al., 1993). Most focal mechanisms in the northern zone of seismicity show right-lateral strike-slip motion on NNW striking planes. These relations suggest that none of the major faults of the area are favorably oriented for failure (Hauksson et al., 1993).

The Goldstone Lake fault zone is the only major, active NNW striking fault zone in the entire northern Mojave Desert (Fig. 1.1). The Goldstone Lake fault zone is also nearly coaxial with the strike of the mainshock rupture of the Landers event. Given the record of recent activity Goldstone Lake fault zone, it would be prudent to anticipate potentially hazardous activity. The overall length of the Goldstone Lake fault zone, 65+ km, is as large as the straight line length of the mainshock surface rupture associated with the Landers earthquake. Thus, the Goldstone Lake fault zone may be capable of producing earthquakes similar in magnitude to that of the Landers event.

REFERENCES

Armstrong, R. L. and Higgins, R. E.,K-Ar dating of the beginning of Tertiary volcanism in the Mojave Desert, California: *Geol. Soc. Am. Bull,*. 84, 3, 1095-1099, 1973.

Armstrong, R. L., and J. Suppe, Potasium-Argon geochronometry of Mesozoic igneous rocks in Nevada, Utah, and southern California, *Geol. Soc. Am. Bull,*. *84*, 1375-1392, 1973.

Armstrong, R. L. and P. Ward, Evolving geographic patterns of Cenozoic magmatism in the North American Cordillera: the temporal and spatial association of magmatism and matamorphic core complexes, *Jour. Geophys. Res., 96,* 13,201-13,224, 1991.

Atwater, T., Implications of plate tectonics for the Cenozoic tectonic evolution of western North America, *Geol. Soc. Am. Bull., 81*, 3513-3536, 1970.

Bailey, R. A., G. B. Dalrymple and M. A. Lanphere, Volcanism, Structure, and Geochonology of Long Valley caldera, Mono County, California, *Jour. Geophys. Res., 81*, 5, 725-744, 1976.

Bonnichson and Kauffman, Physical features of rhyolite lava flows in the Snake River Plain volcanic province, southwestern Idaho, in Fink, J. H. , ed., The Emplacement of silicic domes and Lava flows, *Spec. Pap. Geol. Soc. Am. , 212,* 119-145, 1987.

Brady, R. H., III, Neogene stratigraphy of the Avawatz Mountains between the Garlock and Death Valley fault zones, southern Death Valley, California: Implications as to the late Cenozoic tectonics, *Sediment. Geol., 38*, 127-157, 1984.

Brady, R. H., III, Southward continuation of the Southern Death Valley fault zone from the Avawatz Mountains to the Bristol Mountains, San Bernardino County, California, *Geol. Soc. Am. Abstr. Programs, 20*, 145, 1988.

Brady, R. H., III, and K. L. Verosub, Intersecting wrench faults, northeastern Mojave terrane, and symmetrical terminations of the Garlock fault, southern California, *Geol. Soc. Am. Abstr. Programs, 16*, 453, 1984.

Burchfiel, B. C., and G. A. Davis, Mojave Desert and environs, in Ernst, W. G., ed., The geotectonic development of California (Rubey volume 1), *Englewood Cliffs, New Jersey, Prentice-Hall, 217-252,* 1981.

Butler, P. R., B. W. Troxel, and K. L. Verosub, Late Cenozoic history and styles of deformation along the southern Death Valley fault zone, California, *Geol. Soc. Am. Bull., 100*, 402-410, 1988.

Byers, F. M., Jr., Geology of the Alvord Mountain Quadrangle San Berdardino County, California, *U. S. Geol. Surv. Bull. 1089-A*, 71 pp., 1960.

Calderone, G.J., R.F. Butler, and G.D. Acton, Paleomagnetism of Middle Miocene volcanic rocks in the Mojave-Sonora Desert region of western Arizona and southeastern California, *J. Geophys. Res., 95*, 625-647, 1990.

Carr, M. D., F. G. Poole, A. G. Harris, and R. L. Christiansen, Western facies Paleozoic rocks in the Mojave Desert, California, *U.S. Geol. Surv. Open File Rep., 81-503*, 15-17, 1981.

Carter, J. N., B. P. Luyendyk, and R. R. Terres, Neogene clockwise rotation of the eastern Transverse Ranges, California, suggested by paleomagnetic vectors, *Geol. Soc. Am. Bull., 98*, 199-206, 1987.

Cas, R. A. F., and J. V. Wright, Volcanic successions modern and ancient, *Unwin Hyman Publishers, Boston, MA*, 528 pp., 1988.

Christie-Blick, N. and K. T. Biddle, Deformation and basin formation along strike-slip faults, *in* Biddle, K. T. and N. Christie-Blick, eds., Strike-slip deformation, basin formation, and sedimentation, *Soc. Econ. Pal. Min. Spec. Pub. 37*, 1-34, 1985.

Crippen, R., Development of remote sensing techniques for the investigation of neotectonic activity, eastern Transverse Ranges and Vicinity, southern California, *Ph.D. dissertation, University of California, Santa Barbara*, 1989.

Cross, T. A., and R. H. Jr. Pilger, Constraints on absolute motion and plate interaction inferred from Cenozoic igneous activity in the western United States, *Amer. Jour. Sci., 278*, 865-902, 1978.

Crowell, J.C., Origin of late Cenozoic basins in southern California, *in* Dickinson, W.R., ed., Tectonics and sedimentation, *Soc. Econ. Pal. Min. Spec. Pub. 22*, 190-204, 1974.

Danehy, E. A., Regional geologic mapping program, unpublished map sheet 11 of 53, scale 1:24,000, *Southern Pacific Company, Land Dept.*, 1958a.

Danehy, E. A., Regional geologic mapping program, unpublished map sheet 12 of 19, scale 1:24,000, *Southern Pacific Company, Land Dept.*, 1958b.

Davis, G. A., and B. C. Burchfiel, Garlock fault, an intracontinental transform structure, southern California, *Geol. Soc. Am. Bull., 84*, 1407-1422, 1973.

Demarest, H.H., Error analysis for the determination of tectonic rotation from paleomagnetic data, *J. Geophys. Res.*, 88, 4321-4328, 1983.

Dibblee, T. W., Jr., Evidence of strike-slip faulting along northwest-trending faults in the Mojave Desert, U.S. Geol. Surv. Prof. Pap., 424-B, B197-B199, 1961.

Diehl, J.F., K.M. McClannahan, and T.J. Bornhorst, Paleomagnetic results from the Mogollon-Datil volcanic field, southwestern New Mexico, and a refined mid-Tertiary reference pole for North America, *J. Geophys. Res.*, 93, 4869-4879, 1988.

Dokka, R. K., Displacements on late Cenozoic strike-slip faults of the central Mojave Desert, California, *Geology, 11,* 305-308, 1983.

Dokka, R. K., Patterns and modes of early Miocene extension in the central Mojave Desert, California, *Spec. Pap. Geol. Soc. Am., 208,* 75-95, 1986.

Dokka, R. K., The Mojave Extensional Belt of southern California, *Tectonics, 8,* 363-390, 1989a.

Dokka, R. K., Correction to the Mojave Extensional Belt of Southern California, *Tectonics, 8,* 937, 1989b.

Dokka, R. K., The Eastern California Shear Zone and its role in the creation of young extensional zones in the Mojave Desert region, *in* Craig, S. E., ed., Structure, tectonics and mineralization of the Walker Lane, Geol. Surv. Nev., *Walker Lane Symposium Voume*, 161-187, 1993.

Dokka, R. K., H. J. Henry, T. M. Ross, A. K. Baksi, J. Lambert, C. J. Travis, S. M. Jones, C. Jacobson, M. M. McCurry, M. O. Woodburne, J. P. Ford, Aspects of the Mesozoic and Cenozoic Evolution of the Mojave Desert, *in* Walawender, M. J., and B. B. Hanan, eds., Geological excursions in southern California and Mexico, *Geol. Soc. Am., Annual Meeting Field Trip Guidebook,* 1-43, 1991.

Dokka, R. K., and T. M. Ross, Collapse of southwestern North America and the evolution of early Miocene detachment faults, metamorphic core complexes, the Sierra Nevada orocline, and the San Andreas fault system, *Geology, 23,* 1075-1078, 1995

Dokka, R. K., and C.J. Travis, Late Cenozoic strike-slip faulting in the Mojave Desert, California, *Tectonics*, 9, 311-340, 1990a.

Dokka, R. K., and C.J. Travis, Role of the Eastern California shear zonein accommodating Pacific-North American plate motion, *Geophys. Res. Lett.*, 19, 1323-1326, 1990b.

Dokka, R. K., and M. O. Woodburne, Mid-Tertiary extensional tectonics and sedimentation, central Mojave Desert, California, *LSU Publ. Geol. Geophys., Tectonics and Sedimentation, 1,* 55 pp., Louisiana State University, Baton Rouge, 1986.

Fisher, R.A., Dispersion on a sphere, *Proc.R. Soc. London, 217,* 295-305, 1953.

Ford, J. P., R. K. Dokka, R. E. Crippen, and R. G. Blom, Faults in the Mojave Desert, California, as revealed on enhanced Landsat images, *Science, 248,* 1000-1003, 1990.

Garfunkel, Z., Model for the late Cenozoic tectonic history of the Mojave Desert and its relation to adjacent areas, *Geol. Soc. Am. Bull., 85,* 1931-1944, 1974.

Glazner, A. F., J. M. Bartley, and J.D. Walker, Magnitude and significance of Miocene crustal extension in the central Mojave Desert, California, *Geology, 17*, 50-54, 1989.

Glazner A. F. and D. P. Loomis, Effect of subduction on the Mendocino Fracture zone on Tertiary sedimentation in southern California, *Sedimentary Geology, 38*, 287-303, 1984.

Golombek, M. P., and L. L. Brown, Clockwise rotation of the western Mojave Desert, *Geology, 16*, 126-130, 1988

Hafner, K., and E. Hauksson, Aftershocks of the 1992 Mw 7.3 Landers earthquake sequence in the Barstow-Dagget-Fort Irwin area, in Reynolds, R. E., ed., Off limits in the Mojave Desert: field trip guidebook and volume for the 1994 Mojave Desert Quaternary Research Center field trip to Fort Irwin and surrounding areas, *San Bernadino County Museum Association, Spec. Pub. 94-1*, 38-40, 1994.

Hauksson, E, L. M. Jones, K. Hutton, and D. Eberhart-Phillips, The 1992 Landers earthquake sequence: seismological observations, *Jour. Geophys. Res, 98*, 19,835-19,858, 1993.

Hausback, B. P., An extensive, hot, vapor-charged rhyodacite flow, Baja California, Mexico, *in* Fink, J. H., ed., The Emplacement of silicic domes and lava flows, *Spec. Pap. Geol. Soc. Am. , 212*, 111-118, 1987.

Henry and Dokka, Metamorphic evolution of exhumed middle to lower crustal rocks in the Mojave Extentional Belt, southern California, USA, *J. Metamorphic Geol., 10*, 347-364, 1992.

Hewett, D. F., General geology of the Mojave Desert region, California, in R. Jahns, ed., Geology of Southern California, *Bull. Calif. Div. of Mines, 170,* 15-18, 1954.

Hildreth, W. and G. A. Mahood, Ring-fracture eruption of the Bishop Tuff, *Geol. Soc. Am. Bull., 97,* 396-403, 1986.

Hillhouse, J. W., Paleomagnetism of the Triassic Nikolai Greenstone, McCarthy Quadrangle, Alaska, *C. Jour. Earth Sci., 14,* 2578-2592, 1977.

Jahns, R. H., and L. A. Wright, Garlock and Death Valley fault zones in the Avawatz Mountains, California, *Geol. Soc. Am. Bull., 71,* 2063, 1960.

Jennings, C. W., J. L. Burnett, and B. W. Troxel, Geologic map of California, Trona sheet, 1:250,000 scale, California Division of Mines and Geology, 1962.

Jennings, C. W., J. L. Burnett, and B. W. Troxel, (unpublished) Geologic map of California, Trona sheet, 1:250,000 scale, California Division of Mines and Geology, 1992.

Kamerling, M. J. and B. P. Luyendyk, Tectonic rotations of the Santa Monica Mountains region, western Transverse Ranges, California, suggested by paleomagnetic vectors, *Geol. Soc. Am. Bull., 90*,.331-337, 1979.

Kane, M. F., D. R. Mabey and R. Brace, A gravity and magnetic investigation of the Long Valley caldera, Mono County, California, *Jour. Geophys. Res., 81*, 5, 754-762, 1976.

Lillesand, T. M. and R. W. Kiefer, Remote sensing and image interpretation, *John Wiley and Sons*, 721 pp., 1987.

Luyendyk, B. P., M. J. Kamerling, and R. Terres, Geometric model for Neogene tectonic rotations in southern California, *Geol. Soc. Am. Bull., 91*, 211-217, 1980.

Luyendyk, B.P., M.J. Kamerling, and R.R. Terres, and J.S. Hornafius, Simple shear of southern California during Neogene time suggested by paleomagnetic declinations, *J. Geophys. Res.*, 90, 12,454-12,466, 1985.

MacConnell, D. F., C. McCabe, R. K. Dokka, and M. Chu, Paleomagnetic and structural evidence for localized tectonic rotation associated with fault drag in the northeastern Mojave Desert: Implications for the late Cenozoic tectonic evolution of the Eastern California shear zone, *Earth Plan. Sci. Let., 126*, 207-216, 1994.

Martin, M. W., and J. D. Walker, Upper Precambrian to Paleozoic paleogeographic reconstruction of the Mojave Desert, California, *in* Cooper, J. D. and C. H. Stevens, eds., *Paleozoic paleogeography of the western United States-II: Pacific section SEPM, 67*, 167-192, 1991

Martin, M. W., and J. D. Walker, Extending the western North American Proterozoic and Paleozoic continental crust through the Mojave Desert, *Geology, 20*, 753-756, 1992.

McCulloh, T. H., Geology of the southern half of the Lane Mountain quadrangle, California, Ph.D. dissertation, 182 pp., Univ. of Calif., Los Angeles, 1952.

McCulloh, T. H., Geologic map of the lane Mountain quadrangle, California, scale 1:48,000, *U.S. Geol Surv. Open File Map*, 1960.

McFadden, P.L., A new fold test for paleomagnetic studies, *Geophys. J. Int.*, 109, 163-169, 1990.

McFadden, P.L. and F.J. Lowes, The discrimination of mean directions drawn from Fisher distributions, Geophys. *J. R. Astron. Soc.*, 67, 19-33, 1981.

Miller, E.L. and J.F. Sutter, Structural geology and ^{40}Ar-^{39}Ar geochronology of the Goldstone-Lane Mountain area, Mojave Desert, California, *Geol. Soc. Am. Bull.*, 93, 1191-1207, 1982.

Nilsen, T.H., and S. H. Clark, Sedimentation and tectonics in the early Tertiary continental boarderland of central California: *U.S. Geol. Suv.Prof. Pap. 925*, 1975.

Nur, A., H. Ron, and O. Scotti, Kinematics and mechanics of tectonic block rotations, *Amer. Geophys. Union. Monograph 49*, IUGG series 4, 31-46, 1989

Nur, A., R. Hagai, and G. Beroza, Landers-Mojave earthquake line: a new fault system?, *GSA Today, 3*, 10, 253-258, 1993.

Pakiser, L. C., M. F. Kane, and W. H. Jackson, Structural geology and volcanism of Owens Valley, California: a geophysical study, *U.S. Geol. Surv. Prof. Pap.438*, 1-68, 1964.

Ross, T. M., Neogene extension and regional rotation of the central Mojave Desert, California, *Ph.D. dissertation, Dept. Geol and Geophys., Louisiana State Univ., LA*, 156 pp., 1994.

Ross, T. M., North-south-directed extension, timing of extension, and vertical-axis rotation of the southwest Cady Mountains, Mojave Desert, California, *Geol. Soc. Am. Bull., 107*, 793-811, 1995.

Ross, T. M., B. P. Luyendyk, and R. B. Haston, Paleomagnetic evidence for Neogene clockwise tectonic rotations in the central Mojave Desert, California, *Geology, 17*, 470-473, 1989.

Sabin, A. E., Geology of the Eagle Crags volcanic field, northern Mojave Desert, China Lake Naval Air Weapons Station, California, *Ph.D dissertation, Colorado School of Mines, Dept. of Geol. and Geol. Eng., CO.*, 191 pp., 1994.

Sabin, A. E., F. C. Monestero and A. M. Katzenstien, Middle to late Miocene Age Stratovolcano on the South Ranges, Naval Air Weapons Station, San Bernadino County, California, *in* McGill, S. F., and T. M. Ross, eds., Geological investigations of an active margin, *Geol. Soc. Am., Cordilleran Section Field Trip Guidebook*, 293-301, 1994.

Santo, D. S., M. B. Schluter, H. A. Spellman, and T. C. Benson, Fault and seismic investigation, DDS 14 MARS station, JPL/Goldstone Deep Space Communications Compex, San Bernadino County, California, unpublished report, CCP Project No. 87-31-142-07, *Converse Consultants Pasadena, Pasadena, CA*, 1989.

Santo, D. S., M. B. Schluter, and R. J. Shlemon, Fault indentification using multidisiplinary techniques at the MARS/URANUS station antenna sites, unpublished report, TDA Progress Report 42-111, *Converse Consultants Pasadena, Pasadena, CA*, 1992.

Sauber, J., W. Thatcher, and S. Solomon, Geodetic measurement of deformation in the central Mojave Desert, California, *J. Geophys. Res., 91*, 12,683-12,694, 1986.

Savage, J., M. Lisowski, and W.H. Prescott, An apparent shear zone trending north-northwest across the Mojave Desert into Owens Valley, eastern California, *Geophys. Res. Lett., 17*, 2113-2116, 1990.

Sieh, K, and 19 others, Near-field investigations of the Landers earthquake sequence, April to July 1992, *Science, 260*, 171-176, 1993.

Silver, L. T., and T. H. Anderson, Possible left-lateral early to middle Mesozoic disruption of the southwestern North America craton margin, *Geol. Soc. Am. Abstr. Programs, 6*, 955-956, 1974.

Smith, G. I., Large lateral displacement on Garlock fault, California, as measured from offset dike swarms, *Am. Assoc. Pet. Geol. Bull., 46*, 85-104, 1962.

Smith, G. I., and K. B. Ketner, Lateral displacement on the Garlock fault, suggested by offset sections of similar metasedimentary rocks, *U.S. Geol. Surv. Prof. Pap., 700-D*, D1-D9, 1970.

Snow, J. K., Large-magnitude Permian shortening and continental-margin tectonics in the southern Cordillera, *Geol. Soc. Am. Bull., 104*, 80-105, 1992.

Spencer, J. E., Late Cenozoic extensional and compressional tectonics in the southern and western Avawatz Mountains, southeastern California, *in* B. Wernicke, ed., Basin and Range Extensional Tectonics near the Latitude of Las Vegas, Nevada, *Sp. Pap. Geol. Soc. Am.*, 1990.

Stewart, J. H., Extensional tectonics in the Death Valley area, California, Transport of the Panamint Range structural block 80 km northwest, *Geology, 11*, 153-157, 1983.

Stewart, J. H., J. P. Albers, and F. G. Poole, Summary of regional evidence for right-lateral displacement in the western Great Basin, *Geol. Soc. Am. Bull., 79*, 1407-1413, 1968.

Stewart, J. H., J. P. Albers, and F. G. Poole, Reply to discussion on summary of regional evidence for right-lateral displacement in the western Great Basin, *Geol. Soc. Am. Bull., 81*, 2175-2180, 1970.

Troxel, B. W., Anatomy of a fault zone, southern Death Valley, California, *Geol. Soc. Am. Abstr. Programs, 2*, 154, 1970.

Valentine, M. J., L. L. Brown, and M. P. Golombek, Cenozoic crustal rotations in the Mojave Desert from paleomagnetic studies around Barstow, California, *Tectonics, 12*, 666-677, 1993.

Walker, J. D., J. M. Bartley and A. F. Glazner, Large-magnitude Miocene extension in the central Mojave Desert: implications for Paleozoic to Tertiary paleogeography and tectonics, *Jour. Geophys. Res., 95*, 557-569, 1990.

Walker, J. D., J. M. Fletcher, R. P. Fillmore, M. W. Martin, W. J. Taylor, A. F Glazner, and J. M. Bartley, Connection between igneous activity and extension in the central Mojave metamorphic core complex, California, *Jour. Geophys. Res., 100*, 10,477-10,494, 1995.

Watson, A test for randomness of directions, *Geophys. J. R. Astron. Soc.*, 7, 160-161, 1956.

Williams, H. and A. R. McBirney, Volcanology, *Freeman, Cooper and Co., San Francisco, CA*, 397 pp., 1979.

Wilcox, R. E., T. P. Harding, and D. R. Seely, Basic wrench tectonics, *Am. Assoc. Pet. Geol. Bull., 57*, 74-96, 1973.

Wohletz, K. H. and M. F. Sheridan, A model pyroclastic surge, *in* Chapin, C. E. and W. E. Elston, eds., Ash-flow tuffs, *Spec. Pap. Geol. Soc. Am., 180*, 177-194, 1979.

Yokoyama, I., Structure of caldera and gravity anomaly, *Bull. Vol., 26*, 67-72, 1963.

Yount, J. C., E. R. Schermer, T. J. Felger, D. M. Miller, and K. A. Stephens, Preliminary geologic map of Fort Irwin basin, north-central Mojave Desert, California, *U.S. Geol. Surv. Open File Rep., 94-173*, 1994.

Zijderveld, J. D. A., A. C. demagnetization of rocks: analysis of results, *in* Collinson, D. W., and S. K. Runcorn, eds., Methods in paleomagnetism, Elsevier, Amsterdam, 245-286, 1967.

VITA

David MacConnell was born in Orange, California, on the 6th of June, 1964; he was the youngest of five children born to John and Barbara MacConnell. As a consequence of the divorce of his parents and his mother's second marriage, his immediate family grew to include a second father and an additional brother and sister in 1973. He attended public school through the 11th grade. In April of 1981, he passed the California State Proficiency Examination and graduated from high school. He spent the next two and one half years working as a self-employed carpenter as well as a heating and air conditioning technician with a small owner-operated company based in Norco, California. Mr. MacConnell attended Fullerton College in Fullerton, California, from 1983 to 1985. He attended San Diego State University from August 1985, to December 1988, where he earned a Bachelor of Science in applied arts and science with distinction in the geological sciences. Mr. MacConnell participated in the National Science Foundation funded 1987 Summer Research Program in Physical Sedimentology at the Massachusetts Institute of Technology. He began a doctor of philosophy program in geology at Louisiana State University in August of 1989. Mr. MacConnell's geology related work experience includes employment with Alton Geoscience, an environmental company in Irvine, California (1988), British Petroleum in Houston, Texas (1990), and Dorset, England (1994), and Amoco Oil Co. in Houston, Texas (1993). He will begin full-time employment with EXXON Exploration Company in December of 1995. He will obtain the doctor of philosophy degree in May, 1996.

DOCTORAL EXAMINATION AND DISSERTATION REPORT

Candidate: David F. MacConnell

Major Field: Geology

Title of Dissertation: Active Tectonics of the Northeastern Mojave Desert, California

Approved:

Major Professor and Chairman

Dean of the Graduate School

EXAMINING COMMITTEE:

Date of Examination:

December 15, 1995